

THE ROLE OF MAC-1 INTEGRIN CLUSTERING IN THE BIOGENESIS OF NEUTROPHILIC GRANULOCYTE-DERIVED ANTIBACTERIAL AND PRO-INFLAMMATORY EXTRACELLULAR VESICLES

Ph.D. thesis

Viktória Szeifert PharmD.

Molecular Medicine Doctoral School

Semmelweis University



Supervisor: Ákos Márton Lőrincz, M.D., Ph.D.

Official reviewers: Noémi Sándor, Ph.D.
Balázs Legeza, M.D., Ph.D.

Head of the Complex Examination Committee: Miklós Csala, M.D., D.Sc.

Members of the Complex Examination Committee:
László Cervenák, M.D., Ph.D.
András Szarka, D.Sc.

Budapest
2022

TABLE OF CONTENTS

TABLE OF CONTENTS	2
LIST OF ABBREVIATIONS	4
1. INTRODUCTION	8
1.1. EXTRACELLULAR VESICLES	8
1.1.1. Examination of extracellular vesicles.....	9
1.1.2. Examination of biological effects of extracellular vesicles: antibacterial effect	10
1.1.3. Effects of extracellular vesicles	12
1.2. NEUTROPHILIC GRANULOCYTES	13
1.2.1. Effector functions of neutrophilic granulocytes	15
1.2.2. Role of Mac-1 integrin in the effector functions of neutrophilic granulocytes.....	20
1.2.3. Neutrophil-derived extracellular vesicles	22
1.2.4. Effect of neutrophil-derived EVs on other cells	23
2. OBJECTIVES	29
3. METHODS	30
3.1. MATERIALS	30
3.2. ISOLATION OF HUMAN NEUTROPHILIC GRANULOCYTES	32
3.3. OPSONIZATION OF ZYMOSAN AND BACTERIA.....	32
3.4. ISOLATION OF EXTRACELLULAR VESICLES.....	32
3.4.1. Differential centrifugation and gravitational filtration	33
3.4.2. Size exclusion chromatography (SEC).....	33
3.5. EV QUANTIFICATION BY FLOW CYTOMETRY.....	34
3.6. WESTERN BLOT ANALYSIS OF EV SAMPLES	34
3.7. MEASUREMENT OF SIZE DISTRIBUTION OF EVS BY DYNAMIC LIGHT SCATTERING	35
3.8. MEASUREMENT OF SIZE DISTRIBUTION OF EVS BY NANOPARTICLE TRACKING ANALYSIS.....	35
3.9. BACTERIAL SURVIVAL ASSAY BASED ON OPTICAL DENSITY MEASUREMENT	35
3.10. BACTERIAL SURVIVAL ASSAY BASED ON FLOW CYTOMETRY MEASUREMENT ..	36

3.11.	MEASUREMENT OF CYTOKINE PRODUCTION OF NEUTROPHILS	39
3.12.	MEASUREMENT OF REACTIVE OXYGEN SPECIES PRODUCTION OF PMNs	39
3.13.	TIRF IMAGING OF CLUSTERING	39
3.14.	INDUCTION OF CLUSTER FORMATION WITH ANTIBODIES	41
3.15.	STATISTICS	41
4.	RESULTS	42
4.1.	VALIDATION OF THE NEW, FLOW CYTOMETRY-BASED BACTERIAL SURVIVAL ASSAY	42
4.2.	QUALITY CONTROL FOR THE DIFFERENTIAL CENTRIFUGATION, FILTRATION BASED PMN EV ISOLATION WITH SIZE EXCLUSION CHROMATOGRAPHY	44
4.3.	ROLE OF MAC-1 IN THE FORMATION OF NEUTROPHIL EVs	49
4.3.1.	Mac-1 ligand surface induces EV production from adherent PMNs.....	51
4.3.2.	Mac-1 receptor clustering on BSA and C3bi surface	54
4.3.3.	Mac-1 ligand surface- and antibody-induced clustering initiates antibacterial and pro-inflammatory PMN EV production.....	57
4.4.	ROLE OF Ca ²⁺ SIGNAL IN THE FORMATION OF NEUTROPHIL EVs	60
4.4.1.	Role of Ca ²⁺ supply in the PMNs' EV production	60
4.4.2.	Role of Ca ²⁺ supply in PMNs' antibacterial and pro-inflammatory EV production.....	62
5.	DISCUSSION	64
6.	CONCLUSIONS	67
7.	SUMMARY	68
8.	ÖSSZEFOGLALÁS	69
9.	REFERENCES	70
10.	BIBLIOGRAPHY OF CANDIDATE'S PUBLICATIONS	91
11.	DIVISION OF RESULTS BETWEEN CO-AUTHORS	93
12.	ACKNOWLEDGEMENTS	94

LIST OF ABBREVIATIONS

aEV	opsonized particle activation-induced neutrophil EV (own abbreviation)
ALIX	ALG-2(apoptosis-linked gene 2)-interacting protein X
ANOVA	analysis of variance
apoEV	apoptotic neutrophil EV (own abbreviation)
AU	arbitrary unit
ATCC	American Type Culture Collection
BCR	B-cell receptor
BPI	bacterial permeability-increasing protein
BSA	bovine serum albumin
C3bi	inactivated C3 complement fragment
CD	cluster of differentiation
CLEC-2	C-type lectin-like receptor 2
CR3	complement receptor 3, Mac-1, CD11b/CD18, integrin $\alpha_M\beta_2$
CR4	complement receptor 4, CD11c/CD18, integrin $\alpha_x\beta_2$
DAP-12	DNAX activating protein of 12 kilodalton
DC+F	differential centrifugation and filtration-based EV isolation method
DLS	dynamic light scattering
DMSO	dimethyl sulfoxide
DNA	deoxyribonucleic acid
DPI	diphenyleneiodonium chloride
ECL	enhanced chemiluminescence
EDTA	ethylenediaminetetraacetic acid
ELISA	enzyme-linked immunosorbent assay
ESCRT	endosomal sorting complexes required for transport
ESAM	endothelial cell-selective adhesion molecule
EV	extracellular vesicle
FC	flow cytometry
FcR γ	Fc receptor γ -chain
FH	factor H complement control protein
FITC	fluorescein isothiocyanate
fMLP	N-formylmethionyl-leucyl-phenylalanine

fMLP-R	N-formylmethionyl-leucyl-phenylalanine receptor
FSC	forward scatter
FH	factor H
GM-CSF	granulocyte macrophage-colony stimulating factor
G-CSF	granulocyte-colony stimulating factor
GFP	green fluorescent protein
GTPase	nucleotide guanosine triphosphate binding and hydrolyzing enzyme
ICAM-1	intercellular cell adhesion molecule 1
IFN- γ	interferon gamma
IL	interleukin
ITAM	immunoreceptor tyrosine-based activation motif
JAM	junctional adhesion molecule
HBSS	Hanks' Balanced Salt Solution
LB	lysogeny broth
LFA-1	lymphocyte function-associated antigen 1, CD11a/CD18, integrin $\alpha_L\beta_2$
LPS	lipopolysaccharide
LT β R	lymphotoxin β receptor
Mac-1	macrophage antigen 1, CR3, CD11b/CD18, integrin $\alpha_M\beta_2$
MALDI-TOF	matrix-assisted laser desorption/ionization time-of-flight
Mcl	macrophage C-type lectin
MDA5	melanoma differentiation-associated protein 5
MDL-1	myeloid DAP12-associating lectin
Mincle	macrophage-inducible C-type lectin
MISEV2018	Minimal information for studies of extracellular vesicles 2018, guideline
MCP-1	monocyte chemoattractant protein-1, chemokine (C-C) ligand 2, CCL2
MPO	myeloperoxidase
MSSA	methicillin-sensitive <i>Staphylococcus aureus</i>
N	sample size
NADPH	nicotinamide adenine dinucleotide phosphate
NE	neutrophil elastase
NET	neutrophil extracellular trap
NGAL	neutrophil gelatinase-associated lipocalin

NLRP	Nod-like receptor protein
NOD2	nucleotide-binding oligomerization domain-containing protein 2
NOX	NADPH oxidase
NRAMP-1	natural-resistance-associated macrophage protein 1
NTA	nanoparticle tracking analysis
OD	optical density
oZ-EV	opsonized zymosan activation-induced neutrophil EV (own abbreviation)
p	p-value, probability
PAFR	platelet-activating factor receptor
PBS	phosphate-buffered saline
PCR	polymerase chain reaction
PECAM	platelet endothelial cell adhesion molecule (CD31)
PI	propidium iodide
PLC γ 2	phospholipase C γ -2
PMA	phorbol12-myristate13-acetate
PMN	polymorphonuclear cells
PRR	pattern recognizing receptor
PS	phosphatidylserine
PSGL-1	P-selectin glycoprotein ligand 1
RANK	receptor activator of nuclear factor-kappaB
rcf	relative centrifugal force
RIG-I	retinoic acid-inducible gene-I-like receptor
RM	repeated measures
RNA	ribonucleic acid
ROS	reactive oxygen species
RPE	R(Rhodophyta)-phycoerythrin
rpm	revolutions per minute
SEC	size exclusion chromatography
SEM	standard error of the mean
SH2	Src Homology 2 domain
SLP-76	SH2 domain containing leukocyte protein of 76 kilodalton

SOD	superoxide dismutase
spEV	spontaneous neutrophil EV (own abbreviation)
SSC	side scatter
Syk	spleen tyrosine kinase
TCR	T-cell receptor
TGF- β	transforming growth factor beta
TIRF	total internal reflection fluorescence microscopy
TLR	Toll-like receptor
TNF α	tumor necrosis factor alpha
TRAIL	tumor necrosis factor-related apoptosis-inducing ligand
TSG101	tumor susceptibility gene 101 protein (ESCRT-I complex component)
USA300	GFP expressing, methicillin-resistant <i>Staphylococcus aureus</i> strain
VCAM-1	vascular cell-adhesion molecule 1
VEGF	vascular endothelial growth factor
VLA-4	very late antigen-4, CD49d/CD29, integrin $\alpha_4\beta_1$

1. INTRODUCTION

1.1. Extracellular vesicles

The extracellular vesicles (EVs) are phospholipid bilayered subcellular structures that cannot replicate (1). Both pro- and eukaryotic cells can release EVs and they carry biologically active molecules as a result of a well-regulated sorting process (2, 3). The EVs are reported to carry nucleic acids (DNA, RNA), lipids, proteins, and carbohydrates (4, 5). Due to their high surface-to-volume ratio, they are able to efficiently interact with cells and extracellular molecules (6). In this manner, EVs are a new route of intercellular communication and their potential role in diagnostics and therapeutics exponentially increased the scientific interest for them over the last 20 years.

EVs are very heterogeneous not only by their originating cell but also in the respect of their size and biogenesis (7) (*Figure 1*). The exosomes (30-100 nm) have an endosomal origin, they are released upon the fusion of multivesicular bodies with the plasma membrane (8). It is recommended to identify the exosomes by endosomal markers such as TSG101 or ALIX, CD63, CD9, and CD81 tetraspanins (9). Their biogenesis can be dependent or independent of the endosomal sorting complexes required for transport machinery (ESCRT) (10-13). The EVs that are shed from the plasma membrane of the cells (100-1000 nm) are called microvesicles (or microparticles or ectosomes). It is recommended to refer to them as medium-size EVs because of the way of their isolation (approx. 10 000 g pellet) until one can prove their plasma membrane-derived biogenesis by markers (9). The release of these EVs is associated most likely with the change of the membrane asymmetry. Phosphatidylserine (PS) is exposed in the outer leaflet that can be a result of a calcium-dependent activation of scramblases, floppases, and the inhibition of flippases (14). Another notable group of EVs are the apoptotic bodies. The apoptotic bodies are produced upon programmed cell death (apoptosis) and they contain specific markers such as DNA and histones (15). However, during apoptosis, the size of the EVs produced via apoptosis spread between 100 and 5000 nm (16, 17). The biogenesis of these EVs is similar to the microvesicles, but the specific condition of their generation justifies their distinction.

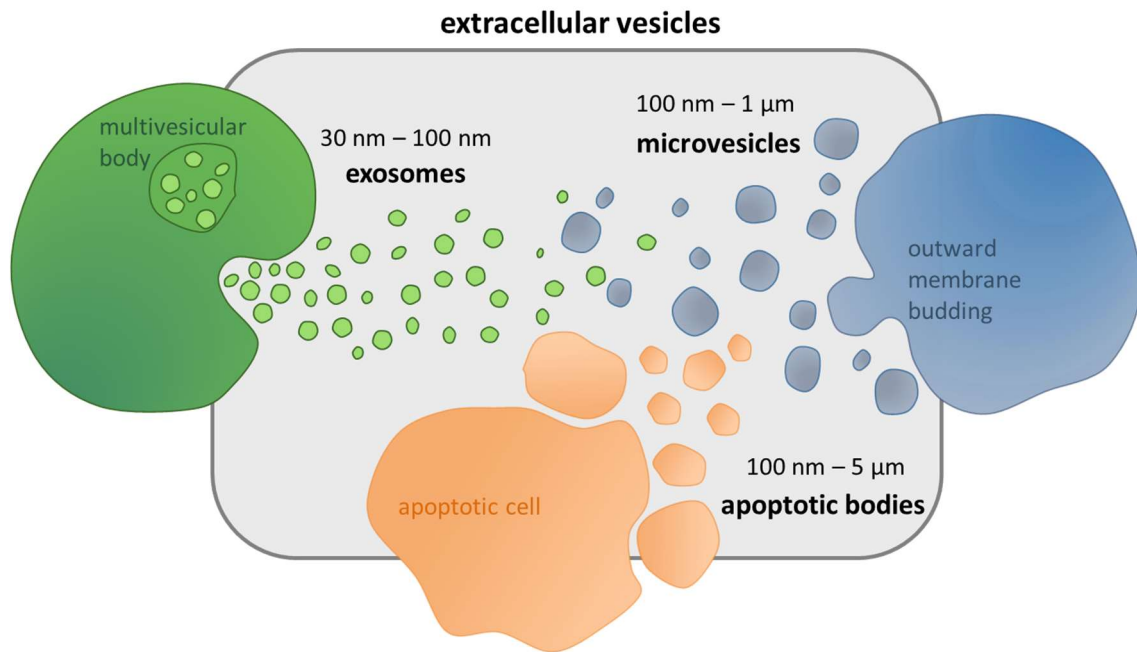


Figure 1. Classification of extracellular vesicles by their size and biogenesis

It is still challenging to determine the origin of the EVs without imaging the act of the EV generation of the cells. Therefore the latest recommendation for the nomenclature of the EVs defined by the “Minimal information for studies of extracellular vesicles” guideline reflects either on their physical characteristics (small EVs <100 nm, medium/large EVs >100 nm), or on their composition (e.g. CD63⁺CD86⁺ EVs, PS⁺ EVs), or on their cellular origin (1).

1.1.1. Examination of extracellular vesicles

The difficulties of EV research and the technical possibilities for EV research emerged hand in hand over the years. We have several EV-related modalities to examine, but we have to be really careful and combine several methods in order to get appropriate conclusions.

Based on the MISEV2018 recommendation, there is no one, gold standard optimal method neither for isolation nor for the characterization of the EVs. For the separation, one should consider the sample origin, and also the downstream applications (1). Differential centrifugation and density gradient centrifugation both has the drawback of possible lipoprotein contamination and aggregation of the EVs (9, 18). While, in the case of ultrafiltration the EVs can attach to the filtration membrane which can decrease the efficiency of the isolation (19, 20).

The precipitation- and affinity-based methods have issues with the applied reagents, buffers, and antibodies that can interfere with the downstream application, the EVs can get damaged upon separation from beads or the samples can contain non-EV contaminants in case of the precipitation techniques (21). The size exclusion chromatography (SEC) technique on the other hand can result in a quite diluted sample that may need re-concentration (18, 22).

One of the greatest difficulties in EV research is to separate EVs from protein aggregates, lipid particles, and DNA that often contaminate EV samples (23-25). According to a lately published paper, the proteins from blood plasma can form a corona around the EVs (26). The storage of vesicles also has a great impact on the properties and effects of EVs (27). Freezing-thawing cycles can induce aggregation in the samples (28). Another challenge is to prove the vesicular nature of the samples. The widely used method is the lysis of the EVs, but the different populations of EVs show differential sensitivity to detergent lysis (29). Considering the above-mentioned aspects, it is suggested to characterize and examine EVs in multiple modalities and with different methods.

As for the quantification of the EVs, the number of the EVs can be expressed in total particle number or total protein content, but the protein to particle, lipid to particle, or lipid to protein ratios are also recommended (1). Still, both single particle, and bulk measurements have drawbacks and limitations. Therefore it is highly recommended to perform quantification with different methods in parallel. For general EV population characterization, it is required to show at least three positive protein markers (at least one transmembrane or cytosolic) and one negative also. For single EV characterization, the application of at least two methods: a microscopic (e.g. electron, atomic force, super resolution microscopy) and a non-microscopic (e.g. nanoparticle tracking analysis, flow cytometry) technique are advised (1).

1.1.2. Examination of biological effects of extracellular vesicles: antibacterial effect

The above-mentioned aspects of EV isolation can influence and pose greater challenges to the investigation of functional properties of extracellular vesicles. In functional characterization experiments of the EVs, negative/background controls and soluble/non-EV macromolecular contaminants controls are inevitable as well as dose-response experiments (1).

In our investigations, we aimed to examine the antibacterial effect and the dose-dependency of neutrophilic granulocyte-derived EVs. However, we faced the drawbacks of the available methods (30). The classical counting of colony forming units (CFU) is the most widely used and easy technique which needs a lot of manual work (31). Therefore the throughput of CFU counting is low on top of the long incubation time (48 hours). Less widely used techniques are the enzyme reaction-based methods (32-34). Their general weak point is that the measured parameter is enzyme activity can be modified by several factors independent of the true bacterial count and this can easily falsify the data evaluation. The usage of PCR is not common to test the antibacterial effect, probably because of its high cost, also the conversion of the measured parameter, fluorescent signal to bacterial count is not always straightforward and the duplication or depletion of the tested gene during cultivation may falsify the results (35, 36). The fluorescence quenching-based method has a strong limiting factor: only phagocytosed quenchable fluorescent bacteria can be tested, therefore we cannot examine the effect of subcellular or soluble agents (37, 38). Our group has previously described one of the methods based on following the optical density (OD) changes, however, this technique measures bacterial growth during a long incubation time (16 hours) which depends not only on the initial bacterial count but also on the growth rate and there is a limitation in the number of parallel samples (39). The matrix-assisted laser desorption/ionization time-of-flight (MALDI-TOF) mass spectrometry seems to be a promising technique not only for bacteria identification but also for the assessment of antibacterial effect (40, 41). The drawback of this method is that it cannot provide adequate information about the number of bacteria as it is deduced from protein quantity and the presence of resistance factors. The demand for high throughput procedures inspired the previously introduced flow cytometry-based methods. These techniques follow the bacterial membrane potential or integrity changes to estimate indirectly the antibacterial effect with the application of expensive fluorescent dyes. However, there are alterations by different bacterial strains and staining protocols that can affect the results (42-44). Therefore one of our aims was to develop a new, high-throughput FC-based technique for our purposes to examine the effect of subcellular elements as EVs.

1.1.3. Effects of extracellular vesicles

EVs as carriers of biologically active molecules take part in intercellular communication. On the one hand, EVs are important for the maintenance of cellular homeostasis by removing cellular waste, and dangerous molecules from the cells, on the other hand, they also prompt pathological processes (45, 46). On this basis, there are several diagnostic and therapeutic applications of the vesicles under development, albeit the questions of biodistribution, clearance, handling, and storage of EV samples are still not clarified (47). EVs take part in the transfer of RNA, receptors and participate in antigen presentation (48-50). Focusing on their role in Immunology, we can say that basically all types of immune cells release EVs that affect the other participants of the immune response. Previous studies suggest that the EVs can be captured by the recipient cells by their surface receptors and after that, the EVs can be internalized by the recipient cell (49). In many cases, cytokines have been also reported to be associated with EVs (51). NK cell-derived EVs activated immune cells, but these EVs showed cytotoxic activity against tumor cells, moreover, the composition of these EVs depended on the surrounding environmental conditions (52, 53). Monocyte-derived EVs enhanced effector functions and the cytokine production of other immune cells: increased TNF- α , IL-6 release, and ROS production of monocytes/macrophages; increased IL-6 and MCP-1 production of podocytes; increased IL-8 release and up-regulated MCP-1 and ICAM-1 of airway epithelial cells (54-56). Mast cell-derived EVs can target other mast cells and transfer mRNA and miRNA to the recipient cell, but they can also activate B- and T-cells, induce dendritic cell maturation, and deliver antigens (50, 57). Even eosinophil granulocyte secreted EVs have been reported to influence the pathogenesis of asthma by modification of eosinophil functions (58).

On the other side, prokaryotic EVs can also modulate immune functions: some examples, *S. typhimurium*, *Yersinia pseudotuberculosis*, and *Y. pestis*-derived outer membrane vesicles can alter the inflammatory response of the host via Toll-like receptors; *Helicobacter pylori*-derived EVs induced the proliferation and IL-8 production of gastric epithelial cells; while *S. aureus*-derived EVs induced atopic dermatitis-like skin inflammation (59-61). These bacterial EVs can also deliver toxins to eukaryotic cells, and exchange protein and DNA between bacteria (62).

There are also, non-cellular effects of the EVs, they are able to interfere with the complement and coagulation system (63, 64). Several studies showed that platelet EVs promote coagulation by the PS exposure on their surface that can provide a catalytic surface for the assembly of the coagulation complexes (65). Other platelet- and erythrocyte-derived EVs have been observed to support thrombin generation in a FXII-dependent manner, while monocyte-derived EVs have been shown to initiate coagulation through tissue factor (66). Accordingly, the erythrocyte-derived EVs have been shown to activate the complement system through this thrombin-dependent process (67).

However, there are data showing anti-coagulant properties of platelet and erythrocyte EVs through the Protein S, and Protein C system that may counterbalance the pro-coagulant ability of these EVs (68, 69). EVs are able to modulate immune functions by expressing complement regulators (e.g. CD55, CD59), or providing a surface for complement activation (e.g. membrane attack complex formation) (70-72). EVs can also serve as a way of prevention against complement attack by the elimination of membrane attack complex (73). Increased levels of complement carrier EVs have been also reported in patients with autoimmune diseases (74-77).

The various effects of EVs are uncountable since up to our knowledge all kinds of cells produce vesicles and their effects can vary by the circumstances of their generation, the state of their mother cell, and the recipient cell. In my thesis, I focus on the biogenesis and effect of neutrophil granulocyte-derived vesicles.

1.2. Neutrophilic granulocytes

Neutrophilic granulocytes (neutrophils) form the most abundant leukocyte population in the human peripheral blood (50-65 % of the white blood cells). They fight in the first line by a wide range of effector tools with the pathogens (bacteria, fungi) that get through the physical barriers of the body (78). These fast-acting, professional phagocytes take part in acute inflammatory responses. Also, their inappropriate activation can lead to autoimmune and inflammatory diseases (79). In the past years, their role in cancer development is also revealed, as they can influence both metastasis formation and tumor growth (80).

They develop in the bone marrow from the common myeloid progenitor cells during granulopoiesis. At the end stages of this process, their nucleus becomes segmented (3-5 segments) and therefore they belong to the polymorphonuclear (PMN) cell family (along with eosinophilic and basophilic granulocytes). Approximately 10^{11} neutrophils are produced each day. They have a short lifespan, they spend approximately 10-12 hours in the bloodstream and at the end of their life cycle they die by apoptosis. Macrophages take up the apoptotic neutrophils, the primary site of neutrophil elimination is the liver (81). The numbers of the neutrophils follow a circadian rhythm that affect also the circulating cells' phenotype (82).

Apart from the neutrophil's segmented nucleus, the other characteristic morphological property is its granulated cytoplasm. There are four different types of granules, namely: azurophil (primary), specific (secondary), gelatinase (tertiary), and secretory granules. These granules differ in their composition (**Figure 2**) and also in their development. The azurophil granules appear first during the maturation of the cells and they are the largest, while the secretory granules are smaller and formed in mature, segmented cells (83). The secretory granules formed by endocytosis contain several cell membrane receptors (e.g. CR1, CR3). Therefore the secretory granules serve as stores of receptors and can enhance the extravasation, migration, and phagocytosis of the cells. When the cells eliminate the pathogens, the enzymes and toxic proteins from these granules are released to the extracellular space (degranulation) or to the phagosome (upon a fusion with the phagosomal membrane). The granules also differ by their tendency for exocytosis and their Ca^{2+} sensitivity (84, 85). At the lowest Ca^{2+} level the secretory granules are secreted in very large numbers, then the gelatinase and the specific granules are released. The azurophil granules show limited exocytosis, and they more likely fuse with the phagosome (86).

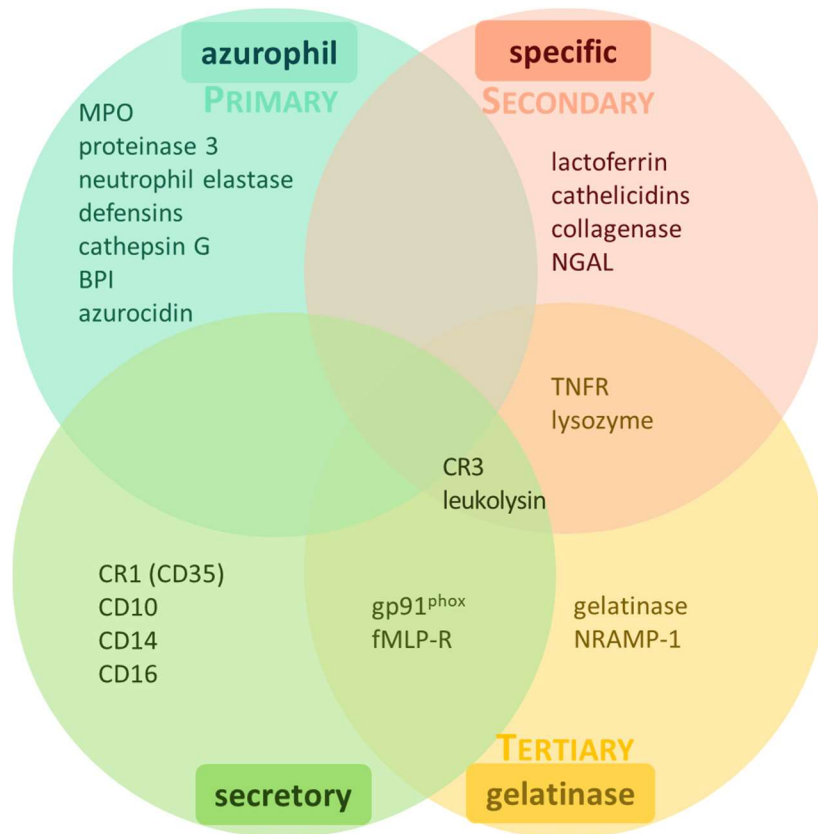


Figure 2. Composition of the granules of neutrophilic granulocytes, based on (87, 88)

Effector functions of neutrophilic granulocytes

When inflammation occurs, the fast-acting neutrophils respond to the local activation of the vascular endothelial cells, bind to the endothelial adhesion molecules, and start the multistep process of extravasation (see **Figure 3** at the end of the chapter). They leave the vessels and migrate through endothelial cells, pericytes, and basement membrane to the site of the infection. The cascade starts with selectin molecules (E-, P-, and L-selectins interacting with PSGL-1 and other glycosylated ligands) mediated rolling on the surface of the endothelial cells. Then chemokines and other chemoattractants trigger the arrest of the cells. The stronger adhesion, spreading, and crawling requires integrin activation (LFA-1, Mac-1) and their bind to the ICAM-1 and VCAM-1 molecules expressed on the surface of the endothelial cells. In the transmigration, apart from the integrins, PECAM-1, JAMs, ESAM, and CD99 also have important roles. When the cells reached the interstitium, they are guided by chemoattractant molecules (e.g. chemokines, complement anaphylatoxins, formyl peptides, leukotriene B₄) and they migrate towards the inflamed tissues (89, 90).

Whenever neutrophils reached the place of action and encounter the pathogens they recognize them with their opsonin receptors (Fc γ and complement receptors) and pattern recognizing receptors (PRRs) (see **Table 1**).

Table 1. Receptors of neutrophil granulocytes, based on (91)

adhesion receptors	integrins	LFA-1, Mac-1, VLA-4, CR4
	selectins and selectin ligands	L-selectin, PSGL-1
cytokine receptors	type I cytokine receptors	IL-4R, IL-6R, IL-12R, IL-15R, G-CSFR, GM-CSFR
	type II cytokine receptors	IFN receptors, IL-10R
	interleukin-1 receptor family	IL-1 receptors, IL-18R
	tumor necrosis factor receptor family	TNF receptors, Fas, LT β R, RANK, TRAIL receptors
Fc receptors	Fc α -receptors	Fc α RI
	Fc γ -receptors	Fc γ RI, Fc γ RIIA, Fc γ RIIB, Fc γ RIII, Fc γ RIIIB, Fc γ RIV
	Fc ϵ -receptors	Fc ϵ RI, Fc ϵ RII
G-protein coupled receptors	chemoattractant receptors	leukotriene B4 receptors, PAFR, C5aR
	chemokine receptors	CXCR1, CXCR2, CCR1, CCR2
	formyl-peptide receptors	FPR1, FPR2, FPR3
pattern recognizing receptors	C-type lectins	Dectin-1, Mincle, MDL-1, Mcl, CLEC-2
	NOD-like receptors	NOD2, NLRP3
	RIG-like receptors	RIG-I, MDA5
	Toll-like receptors	TLR1, TLR2, TLR4, TLR5, TLR6, TLR8, TLR9

As professional phagocytes, the activated neutrophils can phagocytose the invading bacteria or fungi and perform an intracellular killing in the phagosome, phagolysosome. Depending on the participation of the NADPH-oxidase we can distinguish oxidative and non-oxidative killing mechanisms. In the case of non-oxidative killing, the effectors are the antimicrobial components of the granules that are fused with the phagosomes. The importance of the different mechanisms and even the different molecules differ by the microorganism. Namely, the neutrophil elastase has a crucial role in the elimination of Gram-negative bacteria (e.g. *K. pneumoniae* and *E. coli*) and *Candida albicans*, but in the case of the Gram-positive *S. aureus* bacteria, it seemed to be not as important (92, 93). The key enzyme of oxidative killing is the superoxide-producing NADPH-oxidase enzyme complex (NOX) that is localized in the membrane of the phagosome. The NOX is responsible for the oxidative burst of the cells by the production of various reactive oxygen species (ROS). In resting conditions, three subunits (p40^{phox}, p47^{phox}, and p67^{phox}) are localized in the cytoplasm, and two subunits (p22^{phox} and gp91^{phox}) are localized in the membrane of the specific and secretory granules (94). The activation of the NADPH-oxidase is a complex, and intricately regulated process. At the beginning of the phagocytosis, these five subunits assemble to form the NOX. During the oxidation of the NADPH, the NADPH-oxidase transports the free electron through the membrane to the molecular oxygen, resulting in the formation of superoxide anion radical (O₂^{•-}) (39). This superoxide anion reacts with the enzymes of the granules (MPO - myeloperoxidase, SOD - superoxide dismutase) and as a result, many, different reactive oxygen species are produced. The SOD catalyzes the production of the hydrogen peroxide (H₂O₂) from the O₂^{•-} and the MPO catalyzes the reaction of the H₂O₂ and Cl⁻ ions and as a result hypochlorite (OCl⁻) is produced. Then, other free radicals such as hydroxyl (•OH), peroxy (RO₂^{•-}), alkoxy (RO^{•-}) radical, and also hypochlorous acid (HOCl), ozone (O₃), and singlet oxygen (¹O₂) are produced (94, 95). The efficiency and contribution of the ROS species depend on the type of the microbe. The divergences can be due to the different cell wall compositions (Gram-negative or positive bacteria) and the produced bacterial enzymes (e.g. bacterial catalase can decompose the H₂O₂) (96). To wit, the role of HOCl has a particular role in the killing of fungi, but it has a rather marginal role in the case of *E. coli* (97). All at once, in the phagolysosome the granules' antimicrobial proteins, the ROS, and the pH act together in order to eliminate the pathogen.

Upon activation of the cells, they also release granules to the extracellular space (degranulation) and inhibit bacterial growth with the antimicrobial content of the granules. The granules contain cleaving enzymes (e.g. elastase, metalloprotease), and proteins that can sequester essential ions for the pathogen survival (e.g. lactoferrin) (*Figure 2*). The neutrophils can also release cytokines to activate and recruit other immune cells to participate in the immune response. They produce a generally lower amount of cytokines per cell compared to other cytokine-producing immune cells, but since they are in large numbers in the circulation and at the site of the infection, they are definitely an important source of cytokines (98). Upon stimulation, they can produce both pro-, anti-inflammatory, and immunoregulatory cytokines (e.g. TNF α , IL-1 β , IL-6, IL-8, IL-1ra, IL-12), chemokines, colony-stimulating factors (e.g. G-CSF) and other angiogenic/fibrogenic factors (e.g. VEGF) (99, 100). The most studied chemokine produced by neutrophils is the IL-8 which also targets neutrophils and recruits them to the inflammatory foci and enhances several effector functions of the cells (101). Lately, neutrophils have been reported to release transforming growth factor beta (TGF- β) in pathological conditions (102, 103).

Classically, the neutrophils were considered intracellular executioner cells until 2004 when the neutrophil extracellular trap (NET) formation was described (104). The activated neutrophils release web-like structures containing DNA-histone complexes and granule proteins that can grab microorganisms (bacteria, fungi, and even viruses). NET is also considered a second way to eliminate small, virulent bacteria that can escape phagosomes or those that interfere with the maturation of the phagosomes (105). Three key players participating in the NET formation have been described in the literature so far. Both the peptidylarginine deiminase 4, a nuclear citrullinating enzyme, and two granule proteins: MPO and neutrophil elastase promote chromatin decondensation (105). Because the firstly described NET formation was accompanied by the death of the cells, the process was considered a form of death and termed as NETosis (106).

Today, we can even distinguish vital (non-lytic) and suicidal (lytic) NETosis. The vital is a rapid form of NETosis (<30 minutes) is distinguished when the cells remain viable after they exposed their chromatin to the extracellular space, they can maintain the membrane integrity, and they continue to migrate and even phagocytose (107). However, the uncontrolled or excessive release of the NETs can contribute to many autoimmune and other pathological conditions (105).

Once, the pathogenic microorganism is eliminated, the death and the clearance of the dead neutrophils by macrophages are critical for the resolution of the inflammation. The delay in the efferocytosis can lead to tissue damage and chronic inflammation. Apart from apoptosis, many forms of cell death (necrosis, necroptosis, pyroptosis) of neutrophils have been described during the last years (108).

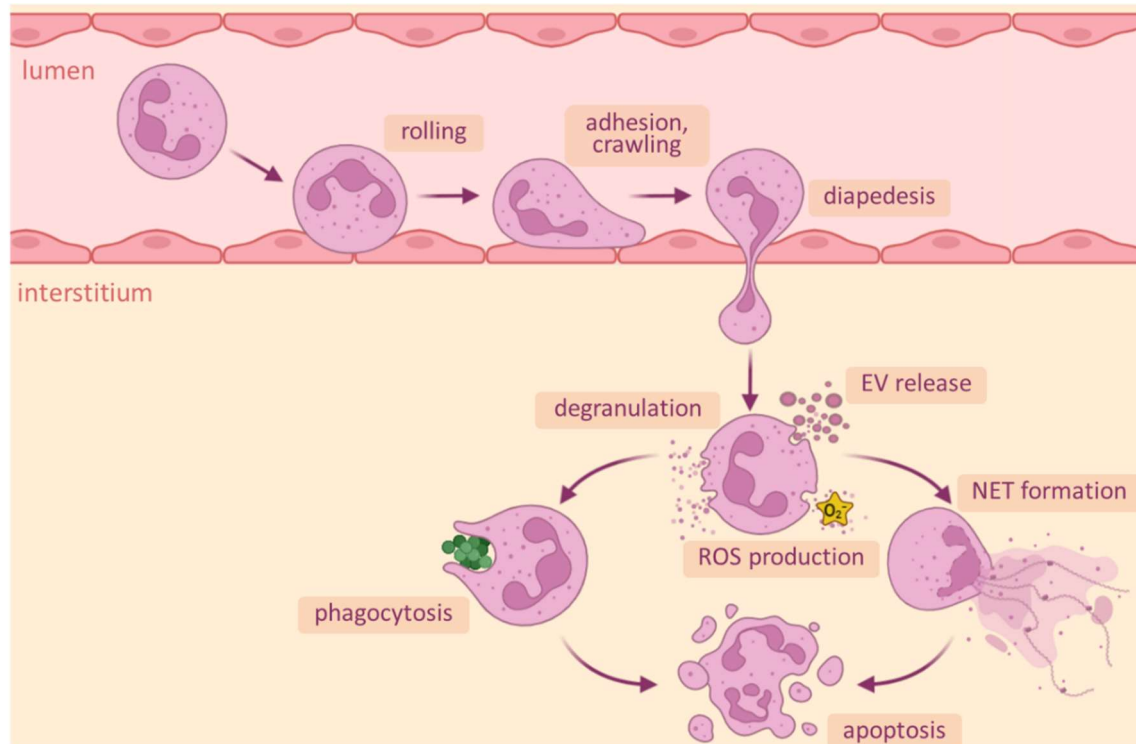


Figure 3. Extravasation and effector functions of neutrophil granulocytes in the interstitium

1.2.1. Role of Mac-1 integrin in the effector functions of neutrophilic granulocytes

Among complement receptors, the complement receptor 3 (CR3), or by another name macrophage-1 antigen (Mac-1) is the most abundant on neutrophilic granulocytes. The Mac-1 integrin complex has the capability to bind a broad range of ligands and to facilitate effector functions of the cells (109-111). Integrins in general are transmembrane heterodimeric glycoproteins that consist of α and β non-covalently associated subunits. In particular, Mac-1 is part of the β_2 subfamily of leukocyte integrins. In Mac-1 complex β_2 subunit (CD18) is associated with the α_M subunit (CD11b). Each subunit consists of a short cytoplasmic domain, a transmembrane domain, and a big extracellular domain (112).

The intracellular tail does not have enzymatic activity, but it can bind signaling and structure proteins. The integrin-ligand interaction depends on divalent cations as calcium and magnesium. Integrin signal is bidirectional that can be transmitted from inside the cells (inside-out signaling) and from outside the cells (outside-in signaling) (*Figure 4*). Like traditional signaling receptors, in the case of outside-in signaling, the binding to the extracellular ligand changes the conformation of the integrin and resulting activation. In the case of inside-out signaling, intracellular signals (e.g. initiated via E-selectin or PSGL-1 binding) lead to conformational changes and ligand binding (113). Three conformation/affinity states of integrins have been described: bent conformation/low affinity state, extended conformation with closed headpiece/intermediate affinity state, and extended conformation with open headpiece/high affinity state (112)(*Figure 4*).

In the case of Mac-1 and other β_2 integrins inserted domain (I domain) of the α -subunit is responsible for the recognition of a ligand. Mac-1 is a promiscuous integrin that has more than 40 known ligands (extracellular matrix elements as fibronectin and vitronectin; cell surface receptor ligands as CD16 or CD23; plasma protein ligands as C3bi, fibrinogen, or complement factor H; microbial ligands as LPS; counter receptors as E-selectin or ICAM, and other ligands as heparin or neutrophil inhibitory factor) (114). The binding sites of Mac-1 are overlapping with each other, but they are not identical (different amino acid residues within these structures may contact the ligands), and importantly, the ligands do not always activate all the available signaling pathways (115).

In outside-in signaling, the binding of the ligand leads to the activation of Src family kinases. Neutrophil activation via β_2 integrins also requires the activation of Syk tyrosine kinases by binding their SH2 domain to phosphorylated immunoreceptor tyrosine-based activation motives (ITAMs) (116). The adapter molecules FcR γ chain and DAP12 adapter molecules were shown to play a critical role in the Syk activation. Other participants of the downstream signaling are SLP-76 adapter protein, PLC γ 2 phospholipase, and Vav guanine exchange factor family members (113).

The Rap1 small GTPase is suggested to play a key role in the regulation of inside-out integrin activation by recruiting talin to integrin cytoplasmic tails. Talin-1 and kindlin-3 have been both important components of high-affinity conformation induction (**Figure 4**). While there is a direct linkage between talin and F actin, kindlin can only bind to the actin cytoskeleton through adapter molecules (117).

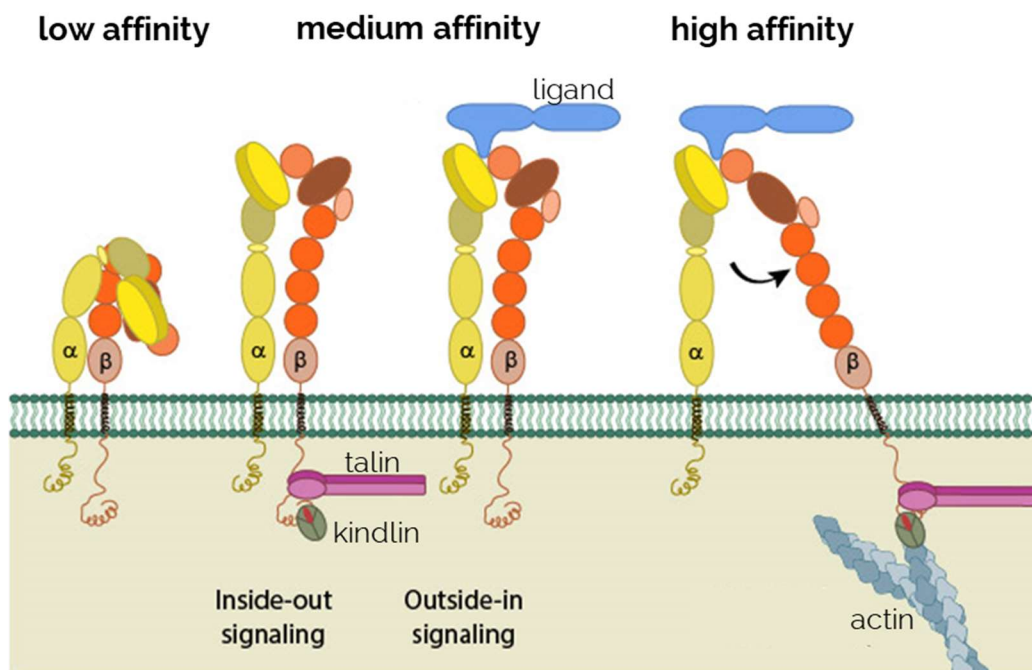


Figure 4. Conformations, inside-out and outside-in signaling of β_2 integrins. Modification of figure of mechanobio.info.

1.2.2. Neutrophil-derived extracellular vesicles

The observation of neutrophils releasing EVs in response to sublytic complement attack was first published in 1991 (118). Since then, several groups published data about neutrophil EVs formed with or without stimulation of the cells and upon apoptosis. This EV generation seems to be a constitutive process that cannot be inhibited so far neither with the application of inhibitors nor with genetic mutations of receptors or signaling molecules (119-121). The exact quantification of the neutrophil EVs is an unobtainable challenge due to the technical limitations that I mentioned earlier. Therefore, in most cases, the produced EV number is compared to control samples (e.g. without activator). The most prominent increase in the PMN EV number is initiated by encountering opsonized particles or due to apoptosis of the cells (47).

The majority of the studies show mostly medium size EVs in the case of the neutrophils: their size spreads between 100 and 700 nm, with a modus of 200-300 nm regardless of the applied stimulation (47). By microscopic image, they are heterogeneous in density. Explicitly, the apoptotic EVs show major differences compared to the other populations, since they have a less dense, rather empty appearance (16)(*Table 2*).

On the surface of the PMN EVs mother cell-specific CD11b, CD18, CD63, CD66b, and CD177 molecules, as well as general EV markers such as PS can be detected (119, 122, 123). Upon activation and degranulation other molecules, e.g. MPO, and NE can bind to the surface of the EVs, along with complement proteins from serum, e.g. C1q, C3b, C4b (26, 123, 124). The neutrophil vesicles contain proteins of the cytoskeleton, the granules, the mitochondria, and signal proteins (47, 119, 122, 125). We found that complement opsonized particle induces the enrichment of granule proteins in the produced EVs and these vesicles contain a higher proportion of proteins interacting with integrins and integrin-binding molecules (120, 126).

1.2.3. Effect of neutrophil-derived EVs on other cells

In spite of the similar physical characteristics, the biological effects of neutrophil EVs are very diverse, sometimes even controversial. The quality control of the neutrophils themselves and the isolated EVs are crucial for the accurate interpretation of the results of functional analysis. The neutrophils are sensitive cells and heterogeneous populations circulate in the bloodstream. Hence the determination of the viability of the parent cells is a crucial step. The separation method of choice and the storage of the EVs may affect greatly the observed effects, therefore the careful protocol setup with accurate control and parallel measurements is another essential aspect of neutrophil EV research in order to obtain reproducible data (1, 47).

Neutrophils proved to release EVs upon pharmacological stimulation as well. In the case of phorbol ester PMA activation, PMN released vesicles that inhibited monocyte-derived dendritic cell maturation and promoted Th2 polarization (127). Ca^{2+} ionophore activation resulted in EVs that caused MPO-dependent loss of membrane integrity of endothelial cells (128).

TNF- α induced PMN EVs could enhance the IL-6, IL-8, and superoxide production and ICAM-1 expression of endothelial cells (129). However, anti-inflammatory properties were also observed on macrophages and macrophage/fibroblast-like synoviocyte co-cultures (130). In one work, C5a triggered EVs featured a strong anti-inflammatory effect on macrophages by decreasing the secretion of pro-inflammatory cytokines and increasing the anti-inflammatory TGF- β secretion of zymosan-activated macrophages (131). While in another study the similarly induced EVs activated resting neutrophil's ROS and IL-6 production (132).

Other widely used neutrophil activators, bacterial products (e.g. N-formylmethionyl-leucyl-phenylalanine - fMLP, lipopolysaccharide - LPS) have been applied for the induction of EV release. The observed effects of these vesicles are quite disparate though. The fMLP-triggered EVs are thoroughly examined in several aspects. Schifferli's group found that the fMLP induced neutrophil EVs reduce the transcription of pro-inflammatory genes in zymosan-activated macrophages, increase the release of TGF- β , inhibit the C5a-mediated inflammasome activation of macrophages, and the maturation of monocyte-derived dendritic cells (131, 133-135).

Another group showed that the fMLP EVs inhibit the production of IFN- γ and TNF- α , and increase the TGF- β production of IL-2/IL-12 activated natural killer cells (136). There are various interesting data on the effect of fMLP-induced PMN EVs on endothelial cells. As an example, neutrophils attached to the endothelium produced EVs upon fMLP activation that inhibited the adhesion of resting neutrophils and IL-1 β induced leukocyte trafficking (137). Others found that endothelial cells increased their IL-8 and IL-6 release due to the fMLP-induced EV treatment (138, 139). These EVs have also been shown to increase the permeability and decrease the transendothelial electrical resistance of a monolayer of endothelial cells that can suggest that these EVs can interfere with the transmigration of the neutrophils (140). While the EVs produced after neutrophil extravasation enable the maintenance of the endothelial barrier function (141). The LPS treatment of the neutrophils resulted in EVs that induced airway smooth muscle cell proliferation (142). By LPS stimulation of splenocytes, they observed EVs that expressed pro-inflammatory, pro-coagulant, and pro-senescent responses in endothelial cells (143). The combination of the LPS and fMLP activation resulted in EVs with a clear pro-inflammatory effect, increasing the superoxide production of resting neutrophils and macrophages (144).

The most prominent stimulation of the neutrophils occurs via opsonized pathogen-derived complex activation of both PRRs and opsonin receptors. Our group found that opsonized bacteria or zymosan-induced, middle-sized EVs could impair the bacterial survival of *S. aureus* and *E. coli* strains compared to differently induced EV populations (119). In previous works, we labeled them as aEVs. The extent of the effect seems to be species-dependent, but we could observe dose-dependency in the case of *S. aureus* (30, 119). Besides, our group published that aEV population increases ROS and IL-8 production of neutrophils as well as endothelial cells' IL-8 release, VCAM-1, and E-selectin expression (47)(**Table 2**). In collaboration, we also found antifungal capacity of the aEVs as they could inhibit the growth of *Aspergillus fumigatus* hyphae (122). The background of the antibacterial effect remained elusive. However, our group revealed a phenomenon of the aEVs forming clumps with the bacteria, and the same EV-bacteria aggregates were observed in the plasma of septic patients (119). Based on this aggregate formation, an independent group published a sepsis diagnostic method (145).

Another group showed that *S. aureus*-PMN EV aggregates enhanced IL-6, IL-1 β production, and CD86, HLA-DR expression of macrophages (146). Similar observations were described on *Mycobacterium tuberculosis* infection-induced EVs with a pro-inflammatory profile: promoting the pro-inflammatory cytokine production, superoxide production, autophagy of macrophages, and consequently the bacterial clearance (147). In contrast, another work shows that upon *M. tuberculosis* infection the secreted PMN EVs diminished the antibacterial activity of macrophages (148). However, it is worth noting that in this particular case also the explanation can be found in the methodological differences between the two works (EV generation and isolation protocols, infection of neutrophils, etc.).

Meanwhile, neutrophils without activation have been reported to produce EVs that express a direct anti-inflammatory effect on macrophages by decreasing their antimycobacterial activity (148). Spontaneously formed PMN EVs reduce neutrophils' superoxide production and IL-8 production (126)(**Table 2**).

Several studies have shown that neutrophils undergoing apoptosis along with isolated apoptotic EVs can exert an anti-inflammatory effect on Th cells, decrease bacterial killing of macrophages, suppress neutrophil infiltration, and delay their ROS production (126, 149-151)(**Table 2**).

Based on these diverse observations of the literature, we outlined a continuous spectrum model of neutrophil EVs as the properties of the EVs depend on the prevailing activation state and extracellular environment of the parent cell (47)(**Figure 5**). The resting (without activation) and apoptotic cells produce EVs that convey rather an anti-inflammatory signal to surrounding cells (monocytes, other neutrophils) that can suggest local participation in inflammation resolution and inhibition of autoimmune processes. While, in case of infection, the stepwise activating PMNs start to release rather pro-inflammatory EVs to the neighboring cells, activating, recruiting them, and facilitating their own diapedesis.

To single activation with fMLP or TNF- α for instance the cells produce EVs that can exert even an anti-inflammatory effect on other neutrophils or monocytes, and inhibit them from activation, while these vesicles can stimulate endothelial cells and make them capable to anchor immune cells. However, when a second activation (e.g. LPS, GM-CSF) or complement activation (e.g. C3bi, C5a) occurs the neutrophil tends to release pro-inflammatory type EVs. Whenever they face an opsonized particle or pathogen, the cells start to secrete dominantly pro-inflammatory and antimicrobial EVs. In this sense, this secondary activation from other immune cells or the complement system endorses the neutrophils for the initiation of the inflammatory response (47).

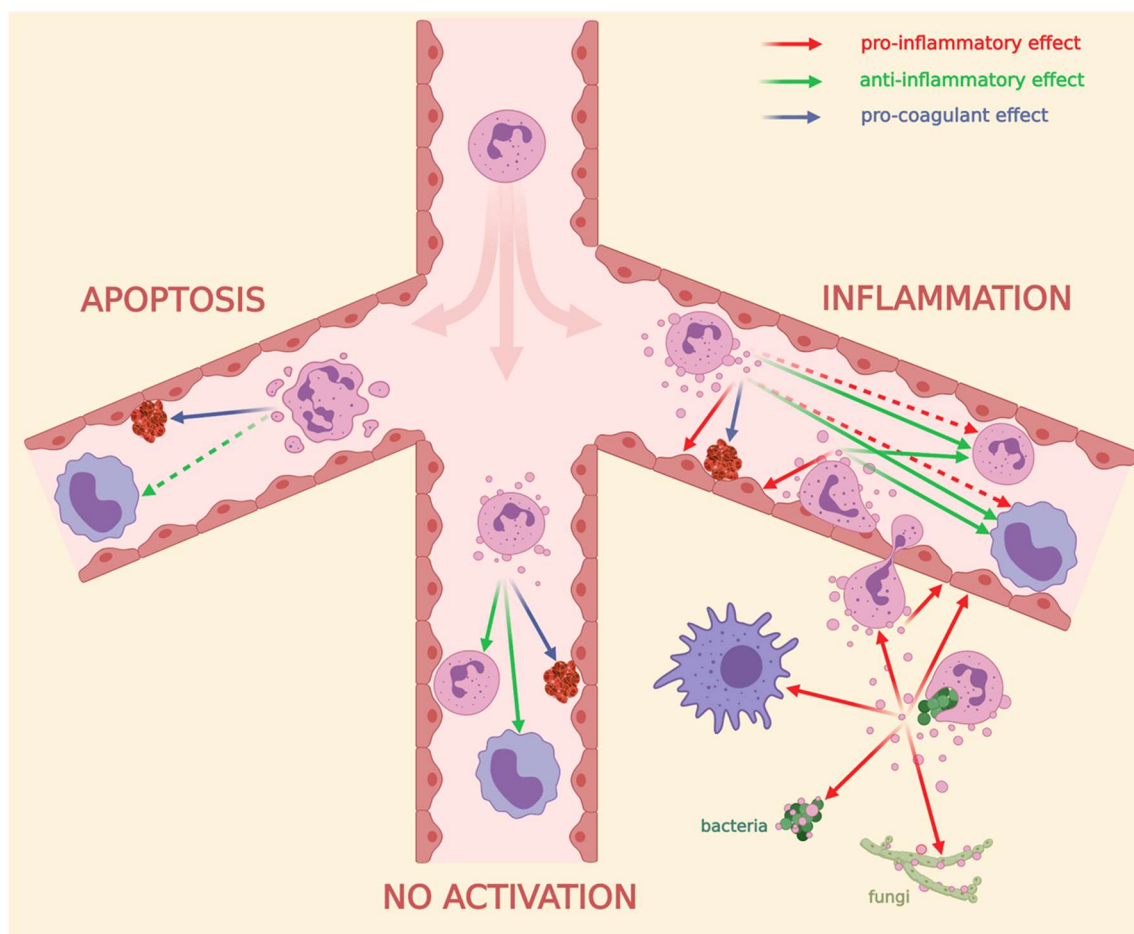
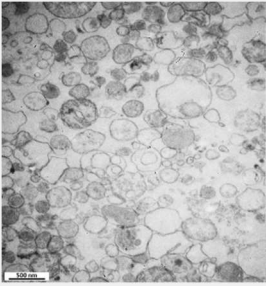
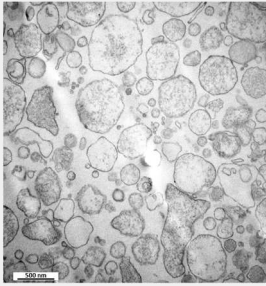
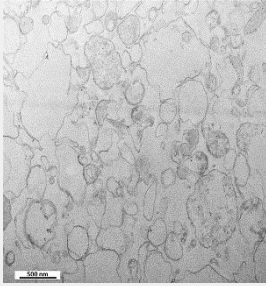


Figure 5. Overview of the neutrophilic granulocyte-derived EVs continuous spectrum model showing their role in intercellular communication, pathogen elimination, and coagulation. Broken arrows represent non-consensual effects. Source: (47)

Our group thoroughly investigated the characteristics of three types of neutrophil-derived EVs. We examined EVs produced by neutrophils without stimulation, spontaneously formed EVs (spEVs), and apoptotic vesicles (apoEVs) derived from 24 hours incubated neutrophils. We examined the characteristics and biological functions of opsonized particle (bacteria, zymosan) activation induced EVs (aEVs) from several perspectives. In our previous articles, and as a general term we applied the aEV abbreviation for this population. However, in our latest experiments, we solely applied zymosan particles to avoid interference of bacteria in the EV samples with our bacterial survival measurements. Therefore, in the thesis, I will use a more specific term for this population of opsonized zymosan-induced EVs (oZ-EVs). I summarized the characteristics and immunomodulatory effects that are observed so far in **Table 2**.

Previously, we started the investigation of the signaling pathway of oZ-EV biogenesis. We proved that the Mac-1 integrin complex plays a crucial role in the generation of the oZ-EVs (120). The process proved to be tyrosine kinase-dependent, and independent of phagocytosis. We found that PRR stimulation (e.g. with non-opsonized zymosan) enhances the EV production of the neutrophils, but these EVs do not show the characteristic antibacterial properties of oZ-EVs. The activation through Fc receptors (e.g. with only antibody opsonized zymosan) could not induce the EV production of the cells neither in the case of murine nor in the case of human neutrophils. We also found that spEV production is independent of extracellular Ca^{2+} supply or PLC γ 2 signaling, while oZ-EV production needs intact Ca^{2+} signaling (121). This differential requirement for extracellular Ca^{2+} supply and intracellular Ca^{2+} signaling indicates a distinct route of spEV and oZ-EV biogenesis. Interestingly, it revealed that the phagocytosis is independent of Ca^{2+} supply or PLC γ 2 signaling. Therefore we concluded that while both processes can be initiated by the same receptor, the phagocytosis and oZ-EV production are results of divergent signaling pathways after encountering the opsonized pathogen (121).

Table 2. Physical and biological properties of neutrophilic granulocyte-derived extracellular vesicles characterized by our group - based on our previous observations, published in (16, 47, 119, 126). Labels: - non-observed characteristics/effect, ✓ represents observed characteristics, arrows represent increasing (↑) or decreasing (↓) effects.

	spEV	aEV (oZ-EV)	apoEV
DIAMETER	50 – 800 nm	50 – 800 nm	200 – 1000 nm
MARKERS	PS ⁺ , CD11b ⁺ , CD18 ⁺	PS ⁺ , CD11b ⁺ , CD18 ⁺	PS ⁺ , PI ⁺ , CD11b ⁺ , CD18 ⁺
EM MORPHOLOGY	 dense, intact	 dense, intact	 empty, intact
LIPID : PROTEIN RATIO	1.28	0.82	1.07
DNA CONTENT	–	–	✓
RNA CONTENT	✓	✓	✓
ROS PRODUCTION	–	–	–
ANTIMICROBIAL EFFECT	–	✓	–
NEUTROPHIL IL-8 PRODUCTION	↓	↑	–
NEUTROPHIL MAXIMAL ROS PRODUCTION	↓	↑	–
NEUTROPHIL EARLY ROS PRODUCTION	↓	↑	↓
ENDOTHELIAL CELL IL-8 PRODUCTION	–	↑	–
ENDOTHELIAL CELL VCAM-1 EXPRESSION	–	↑	–
ENDOTHELIAL CELL E-SELECTIN EXPRESSION	–	↑	–
COAGULATION	–	–	↑

2. OBJECTIVES

In order to continue our investigations of neutrophil EVs, we had to optimize and develop our formerly used methods. The previously introduced methods for antibacterial effect assessment have drawbacks in the respect of time, throughput, and data conversion. We intended to develop a rapid flow cytometry-based and high-throughput method that is capable for the assessment of the antibacterial effect of cellular and subcellular samples, and suitable also for the examination of the dose-dependency of the oZ-EVs' antibacterial effect. Another methodological aim was to provide adequate quality control for our differential centrifugation and filtration-based EV separation technique by size exclusion chromatography (SEC) and examine whether the described antibacterial effect is due to protein contamination in our samples.

In our previous experiments, we were not able to rule out the possible auxiliary role of the PRRs in the process of oZ-EV generation when we stimulated the cells with opsonized particles. Therefore we planned to selectively examine the activation of the Mac-1 receptor *in vitro* by specific ligands and antibodies. Based on our observations the intact Ca^{2+} signal is crucial for the generation of the oZ-EVs, but we did not know whether the signal solely is sufficient for the oZ-EV formation.

Taken together, during my Ph.D. studies, I aimed to:

- 1) develop and validate a new, flow cytometry-based bacterial survival assessment assay in order to rapidly assess the antibacterial effect of biological samples, e.g. neutrophils and EVs,
- 2) perform a size exclusion chromatography based quality control of the differential centrifugation-based isolation of the neutrophil EVs,
- 3) investigate whether the specific activation of the Mac-1 integrin complex on its own is sufficient for the antibacterial, pro-inflammatory oZ-EV formation,
- 4) and examine whether the Ca^{2+} -signal on its own is sufficient for the initiation of the oZ-EV biogenesis from neutrophils.

3. METHODS

3.1. Materials

The composition and/or source of the applied solutions, buffers, and mediums are detailed in **Table 3**. The dextran was from Serva (Heidelberg, Germany). Zymosan A, bovine serum albumin (BSA), ovalbumin, lucigenin (N, N'-dimethyl-9,9'-biacridinium dinitrate), luminol, calcium ionophore A23187, glycine, Tween 20, and DMSO were from Sigma Aldrich (St. Louis, MO, USA). Acridine Orange was from Serva-Feinbiochemica (Heidelberg, Germany). DNase I was from Thermo Scientific (Waltham, MA, USA). Human complement iC3b and Factor H were from Merck Millipore (Darmstadt, Germany). Triton-X 100 was from Reanal (Budapest, Hungary) and the saponin was from Merck Millipore (Darmstadt, Germany). Isotype controls, AnnexinV-FITC were from BioLegend (San Diego, CA, USA), and the other applied specifications of the applied antibodies are detailed in **Table 4**. All other used reagents were research grade. Methicillin-sensitive *S. aureus* (ATCC: 29213) was used. Green fluorescent protein (GFP) expressing- and chloramphenicol resistant *S. aureus* (USA300) was a kind gift from Professor William Nauseef (University of Iowa, USA).

Table 3. Composition of applied buffers, solutions, and mediums

Buffer/solution	Composition	Source
Bradford reagent solution	0.24 g Coomassie Blue G 250, 125.5 ml 96% ethanol, 300 ml 85% orthophosphoric acid, 174.6 ml distilled water	own preparation
ECL reagent 1	5 ml 1 M Tris-HCl (pH=8.5), 500 µl luminol in DMSO, 220 µl p-coumaric acid in DMSO, 45 ml distilled water	own preparation
ECL reagent 2	5 ml 1 M Tris-HCl (pH=8.5), 30 µl 30% H ₂ O ₂ , 45 ml distilled water	own preparation
Electrophoresis buffer	3.03 g 0.025 M Tris, 14.41 g 0.192 glycine, 10 ml 10% SDS ad 1 L distilled water	own preparation
HBSS (1x)	0.14 g CaCl ₂ , 0.4 g KCl, 0.06 g KH ₂ PO ₄ , 0.0977 g MgSO ₄ , 8 g NaCl, 0.0477 g Na ₂ HPO ₄ , 0.35 g NaHCO ₃ , 1 g D-glucose in 1 L distilled water, pH adjusted between 7.0-7.4	GE Healthcare Life Sciences

Ficoll-Paque	5.7 g Ficoll PM400, 9 g diatrizoate Sodium, with edetate calcium disodium in 100 ml purified water	GE Healthcare Life Sciences
Laemmli sample buffer	4 ml 0.5 M Tris-HCl (pH=6.8), 4 ml 99% glycerol, 2 ml 2-mercaptoethanol, 200 µl 1% bromphenol blue, 0.8 g SDS ad 10 ml distilled water	own preparation
LB medium	10 g tryptone, 5 g yeast extract, 10 g NaCl in 1 L distilled water, pH was adjusted to 7.0	own preparation
PBS	8 g NaCl, 0.2 g KCl, 0.2 g KH ₂ PO ₄ , 1.44 g Na ₂ HPO ₄ *2H ₂ O in 1 L distilled water	own preparation
Semi-dry blot buffer	1.16 g Tris, 0.58 g glycine, 0.074 g SDS, 40 ml methanol ad 200 ml distilled water	own preparation

Table 4. List of the applied antibodies

Antibody specificity	Clone	Conjugated fluorophore	Source
β-actin, human	AC-74	-	Sigma Aldrich
CD11b, human concentration-dependent blocking (152)	M1/70	RPE or Alexa647	BioLegend
CD11b, human blocking	ICRF44	-	BioLegend
CD11b, human non-blocking	Bear-1	-	HycultBiotech
CD11b, human activation-specific epitope	CBRM1/5	RPE	ThermoFischer Scientific
CD11c, human blocking	3.9	-	BioLegend
CD18, human non-blocking	CBR LFA-1/2	Alexa647	BioLegend
lactoferrin, human	polyclonal	-	Sigma Aldrich

3.2. Isolation of human neutrophilic granulocytes

Venous blood samples were drawn from healthy adult volunteers approved by the National Ethical Committee (ETT-TUKEB No. IV/5448-5/EKU). Neutrophils were separated by dextran sedimentation followed by a 62.5 V/V% Ficoll gradient centrifugation (Beckman Coulter Allegra X-15R, 700 g, 20 min, 22 °C). The samples were prepared in non-pyrogen-free conditions generally. The isolates contained more than 95 % neutrophils and less than 0.5 % eosinophils. The viability of the cells was always above 99% (less than 1% propidium-iodide positivity). To control the activation of Mac-1 receptors after the cell preparation, we used conformation recognizing (clone: CBRM1/5) antibody labeling.

3.3. Opsonization of zymosan and bacteria

Zymosan A (5 mg/ml in HBSS) was opsonized with 200 µL pre-warmed, pooled (3 donors) human serum at 37 °C for 20 minutes with 600 rpm shaking in a dry block thermostat. After the opsonization, the zymosan was centrifuged (8,000 g, Hermle Z216MK 45° fixed angle rotor, 5 min, 4°C) and washed in HBSS. GFP-expressing USA300 bacteria (1,000 µl of OD_{600nm}=1.0) were opsonized with 200 µL pre-warmed, pooled (3 donors) human serum (600 rpm, 20 min, 37°C). After the opsonization, bacteria were centrifuged (8,000 g, Hermle Z216MK 45° fixed angle rotor, 5 min, 4°C) and washed in HBSS.

3.4. Isolation of extracellular vesicles

Immediately after isolation, the PMNs (in most cases, 10⁷ cells/ml HBSS) were freshly incubated with or without activating agent for 20 minutes at 37°C in a linear shaking water bath (120 rpm). Spontaneously formed EVs (spEV) were secreted without any activation; while stimulation triggered EV were secreted after PMN activation by: 0.5 mg/ml opsonized zymosan A (oZ-EV); 2 µM Ca²⁺ ionophore A23187 (Ca-i EV); 20 µg/ml BSA (BSA solub. EV); 50-150 µg/ml C3bi (C3bi solub. EV); 50-150 µg/ml FH (FH solub. EV). In indicated cases, we applied a combination of activators. We prepared indicated samples in a Ca²⁺-free environment (EV w/o Ca): commercial HBSS without Ca²⁺ and Mg²⁺ was supplemented with 1 mM Mg²⁺.

We also activated cells on surfaces coated with 20 µg/ml BSA (BSA surf. EV); or 50 µg/ml C3bi (C3bi surf. EV); or 50 µg/ml FH (FH surf. EV); or 150 µg/ml fibrinogen (fibrinogen surf. EV) overnight at 4°C. To avoid the interference of Ca²⁺ ionophore with the bacterial survival measurement, after the EV production period, we added BSA (2 mg/ml) to bind the free, rest Ca²⁺ ionophore in the samples. After preparation, EVs were analyzed immediately or processed for downstream application (27).

3.4.1. Differential centrifugation and gravitational filtration

After adequate activation, cells were sedimented (500 g, Hermle Z216MK 45° fixed angle rotor, 5 min, 4 °C). Upper 500 µl of the supernatant was filtered through a 5 µm pore sterile filter (Sterile Millex Filter Unit, Millipore, Billerica, MA, USA). The filtered fraction was sedimented (15 700 g, Hermle Z216MK 45° fixed angle rotor, 5 min, 4°C) and the pellet was carefully resuspended in HBSS in the original 500 µl volume for flow cytometry and functional tests. For the assessment of the protein content of EV fractions, we resuspended the EV pellet in distilled water and determined the protein concentration by Bradford protein assay using BSA as standard in a microplate reader (Labsystems iEMS Reader MF; Thermo Scientific, Waltham, MA, USA) at 595 nm.

3.4.2. Size exclusion chromatography (SEC)

Sepharose CL-2B (GE Healthcare; Uppsala, Sweden) was stacked in empty polypropylene columns that contained a 30 µm pore size polyethylene filter (ThermoFischer Scientific, USA). We prepared columns with 1.6 cm diameter, 6.5 cm height, and 13 ml total bed volume. Neutrophils (10⁷ cells/mL HBSS) were sedimented (500 g, Hermle Z216MK 45° fixed angle rotor, 5 min, 4 °C). We filtered the supernatant through a 5 µm pore sterile filter onto the top of the SEC column. A maximal volume of 1.5 ml was loaded on the column, followed by elution with HBSS (pH=7.4). The eluate was collected in 22 sequential fractions of 0.5 ml. Each fraction was analyzed by dynamic light scattering (DLS), flow cytometry, and western blotting. The collected fractions were centrifuged (15,700 g, Hermle Z216MK 45° fixed angle rotor, 5 min, 4 °C) and the pellet was carefully resuspended in 30 µL distilled water and 10 µl Laemmli sample buffer for western blotting, the indicated fractions were resuspended in 50 µl distilled water for Bradford protein measurements, and in 500 µl HBSS for bacterial survival assay and flow cytometry measurement.

After every separation, SEC columns were regenerated and were not used more than five times (153).

3.5. EV quantification by flow cytometry

We quantified the EVs by a Becton Dickinson FACSCalibur flow cytometer as we described previously (120). First, by HBSS buffer we set the threshold in order to eliminate the instrumental noise. With fluorescent polystyrene beads (3.8 μm SPHERO™ Ultra Rainbow Fluorescent Particles, Spherotech Inc., USA) we set the upper size limit of the EV detection range. We set the lower size limit with HBSS background measurement. EVs were labeled with RPE-conjugated monoclonal anti-CD11b (1 $\mu\text{g}/\text{ml}$, clone: M1/70) and FITC conjugated AnnexinV (1 $\mu\text{g}/\text{ml}$). After the measurement of an EV sample, the events of isotype control events (or 20 mM EDTA containing medium in case of AnnexinV labeling) and the 0.1 % TritonX-100 detergent non-sensitive events were subtracted to calculate the valid EV number. To avoid swarm detection, the flow rate was held below 1,000 events/s (3,750 events/ μl). To control the linearity of the measurements, we also re-measured the samples after a 2-fold dilution. We analyzed the data with Flowing 2.5 Software (Turku Center for Biotechnology, Finland).

3.6. Western blot analysis of EV samples

The EV fractions were lysed in Laemmli sample buffer and boiled at 100 °C for 5 minutes. We run the samples in 10 (w/V) % polyacrylamide gels and transferred them to nitrocellulose membranes by semi-dry blotting. The blocking was carried out for 1 hour in PBS containing 5 (w/V) % ovalbumin and 0.1% (w/V) Tween 20. Then blots were incubated with anti-lactoferrin polyclonal antibody in 1:5000 dilution or anti- β -actin monoclonal antibody in 1:1000 dilution in 5 (w/V) % ovalbumin for 1 hour. As secondary antibodies, we applied horseradish peroxidase linked whole anti-mouse-IgG or anti-rabbit-IgG (GE Healthcare) in 1:5000 dilution in PBS containing 5 (w/V) % ovalbumin for 40 minutes. Both after the primary and the secondary antibodies, we washed the membranes three times for 10 minutes with PBS containing 0.1% Tween 20. The bound antibodies were detected with enhanced chemiluminescence and the immunoblots were exposed to FUJI medical Super RX film.

3.7. Measurement of size distribution of EVs by Dynamic Light Scattering

These measurements were carried out with the help of Dániel Veres (Department of Biophysics and Radiation Biology, Semmelweis University). We performed the experiments at room temperature with equipment consisting of a goniometer system (ALV GmbH, Langen, Germany), a diode-pumped solid-state laser light source (Melles Griot 58-BLS-301, 457 nm, 150 mW), and a light detector (Hamamatsu H7155 PMT module). The evaluation software yielded the auto-correlation function of scattered light intensity that was analyzed by the maximum entropy method, and the different contributions of this function were determined. We calculated the radius of the particles by sphere approximation. We illustrated the results on size distribution graphs.

3.8. Measurement of size distribution of EVs by Nanoparticle Tracking Analysis

These measurements were assisted by Delaram Khamari (Department of Genetics, Cell- and Immunobiology, Semmelweis University). EV samples were resuspended in 1 ml PBS to reach the appropriate particle concentration range for the measurement. Particle size distribution and concentration were analyzed on the ZetaView PMX120 instrument (Particle Metrix, Inning am Ammersee, Germany). For each measurement, 11 cell positions were scanned in 2 cycles at 25 °C. The following camera settings were applied: shutter speed—100, sensitivity—75, frame rate—7.5, video quality—medium (30 frames). The videos were analyzed by the ZetaView Analyze software 8.05.10 with a minimum area of 5, a maximum area of 1,000, and minimum brightness of 20.

3.9. Bacterial survival assay based on optical density measurement

Opsonized GFP-expressing *Staphylococcus aureus* (USA300) bacteria (50 µl of OD_{600nm}=1.0) were added to 500 µl of EV (derived from 1*10⁷ PMNs, and normalized for protein content) suspended in HBSS containing 4V/V% LB. After a 40 minutes-long co-incubation at 37 °C in a linear shaking water bath (120 rpm), we stopped the measurement by adding 2 ml ice-cold stopping solution (0.5 mg/ml saponin in HBSS) that lyse EVs or cells. Then we froze the samples at -80 °C for 20 minutes and thawed them to room temperature. Then, the samples were inoculated to LB broth to follow the bacterial growth by the measurement of optical density (OD) in a microplate reader (Labsystems iEMS Reader MF; Thermo Scientific, Waltham, MA, USA).

We followed the OD changes for 8 hours, at 37 °C, at 600 nm. In the end, we calculated the initial bacterial counts indirectly using an equation similar to PCR calculation based on former calibration, as it was described previously (39).

3.10. Bacterial survival assay based on flow cytometry measurement

For parallel measurement with the OD-based method, in the case of this FC-based method, before their inoculation to LB broth, we proceeded with the samples by inoculation to HBSS buffer. Measurements were carried out by a BD FACSCalibur flow cytometer. As both the size and the refractive index of EV and bacteria are very similar, the gating procedure was similar to the EV detection and quantification. We used HBSS buffer and 3.8 µm fluorescent beads for thresholding. I present the applied gating strategy in **Figure 6**. Since the bacteria's size range (around 500–1000 nm) is near the detection limit of conventional flow cytometers, fluorescent labeling was used to improve FC detection of the bacteria. In the results presented in the thesis, we used endogenously fluorescent, GFP-expressing USA300. For fluorescent labeling of non-endogenously fluorescent bacteria, we stained methicillin-sensitive *S. aureus* (ATCC: 29213) with Acridine Orange (N,N,N',N'-tetramethylacridine-3,6-diamine) in 5 µg/ml final concentration (pH=3 adjusted by HCl) for 5 minutes, at room temperature. In each case, samples were very gently sonicated (Bandelin Sonopuls HD 2070, 10 % power) for 5 seconds to disrupt bacterial clumps and doublets. Our control measurements agreed with previous findings and indicated that weak sonication did not interfere with bacterial viability and Acridine Orange staining (154). The fluorescence gate was set above the autofluorescence of non-labeled bacteria detected by the 530/30 nm fluorescence detector. To avoid swarm detection, an optimal flow range was defined with a 10-fold dilution scale of fluorescent bacteria. The flow rate was held during measurements under 1,000 events/s (3,750 events/µL). As in the case of the EV samples, all samples were re-measured in a 2-fold dilution to control the linearity of measurements. We analyzed the FC data with Flowing 2.5 Software (Turku Centre for Biotechnology, Finland).

In the end, we expressed the bacterial survival (%) with the following quotient in both cases:

$$\frac{\textit{bacteria count in the examined sample}}{\textit{bacteria count in the control sample (0. time point)}}$$

Consequently, if the bacteria are inhibited from growing, the bacterial survival remains around 100 %, but it decreases if there is any direct bactericidal effect, and it increases above 100% if there is no growth-inhibiting action. Since our incubation media contains LB in 4V/V%, it provides the possibility to observe a bacteriostatic effect, not only a direct bactericidal effect. If there the bacterial survival is above 100%, but below the control conditions, we can consider the effect as growth inhibition or bacteriostatic effect.

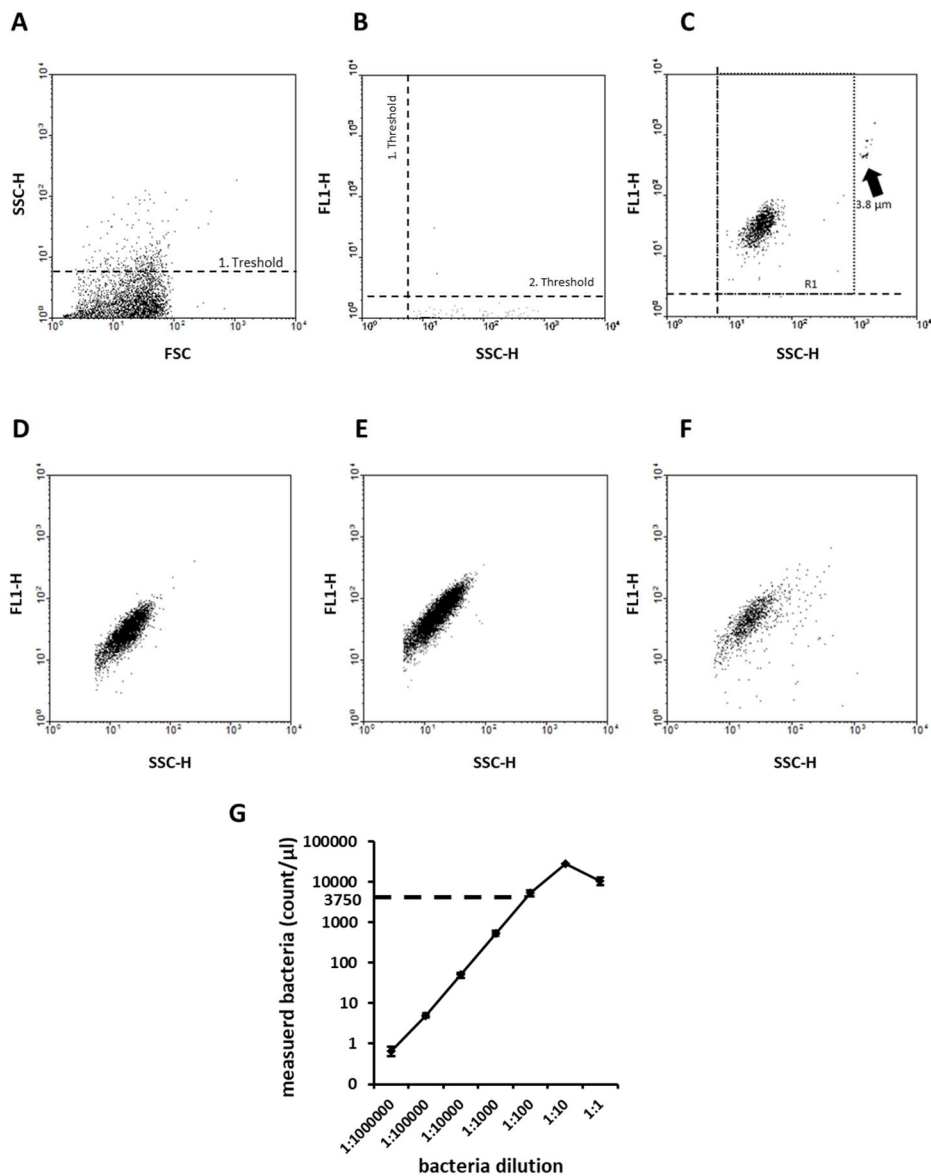


Figure 6. Gating strategy of the flow cytometric measurements presented with USA300 strain. On panel (A) side scatter (SSC) is presented against forward scatter (FSC), whereas in panels (B), (C) and (E)–(G) green fluorescence (FL-1) is presented against SSC. (A) and (B) panels show the threshold setting based on the HBSS background measurement. (C) panel shows the upper threshold setting by fluorescent, 3.8 μ m beads, where GFP-expressing USA300 is measured in the R1 gate. Panels (D)–(F) represents dot plots of USA300 bacteria killing assay: at the 0. minute (D), at the end of the co-incubation, in the 40. minute (E), and after 40 minutes co-incubation with neutrophils (F). (G) Adjusting the optimal flow rate based on the calibration with USA300 bacteria on BD FACSCalibur flow cytometer. The undiluted 1:1 sample had $OD_{600nm}=1.0$ ($n=5$, \pm SEM).

3.11. Measurement of cytokine production of neutrophils

PMNs (120 μ L of 2.5×10^7 /ml) were added to 480 μ l of EV samples at 37 °C in a linear shaker (120 rpm) for 3 hours. Cells were centrifuged (500 g, Hermle Z216MK 45° fixed angle rotor, 10 min, 4 °C) and supernatants were analyzed for IL-8 and TGF- β with a human IL-8 and TGF- β DuoSet sandwich ELISA kit according to the manufacturer's instructions (R&D Systems, Minneapolis, MN, USA) in a microplate reader (Labsystems iEMS Reader MF, Thermo Scientific).

For these measurements, we prepared a control sample for the oZ-EV samples that contained the same amount of zymosan as the oZ-EV isolates. To achieve this, in half of the oZ-EV batch EVs were lysed whereas zymosan particles were left intact (17). We refer to this control sample as “lysed oZ-EV”.

3.12. Measurement of reactive oxygen species production of PMNs

PMNs (200 μ l of 1×10^6 /ml) were placed onto fibrinogen surface (150 μ g/ml) in white flat-bottom 96-well plates. Lucigenin (5 mg/ml dissolved in DMSO) was added in a 1:100 volume ratio to the cells. As a negative control for the ROS production measurements, the inhibitor DPI (5 μ M) was used. We recorded the luminescence for 90 minutes, at 37°C with gentle shaking in a Varioskan CLARIOstar multi-mode microplate reader (BMG LabtechThermo Fisher Scientific) every minute.

3.13. TIRF imaging of clustering

The #1.5 coverslips (Thermo Scientific, Waltham, MA, USA) were overnight coated with C3bi (50 μ g/ml) or BSA (20 μ g/ml) at 4 °C. The PMNs were first labeled with Alexa647 conjugated monoclonal anti-CD11b (1 μ g/ml, clone: M1/70) antibodies for 20 minutes at 37 °C and washed in HBSS once. As we demonstrated with ROS measurements, this antibody does not interfere with Mac-1 activation in the used concentration. Then 10^5 cells were placed on BSA or C3bi coated coverslips. The imaging setup was supported by Pál Vági and László Barna (Nikon Center of Excellence, Institute of Experimental Medicine, Hungarian Academy of Science).

Images of the live cells were collected with a Nikon Eclipse Ti2 microscope, using HP Apo TIRF AC 100xH objective lens (numerical aperture=1.49), a HAMAMATSU C13440-20CU ORCA-Flash4.0 V3 camera (2048 (H) × 2048 (V) pixels, 6.5 μm × 6.5 μm pixel size), and a 647 nm, VFL-P-400-647-OEM2-B1 solid-state laser.

We collected the images in 4 x 4 fields every 30th seconds with an exposure time of 300 msec. The cells were followed for 20 minutes. It has to be noted, that we made “semi-TIRF images”, as we could not reach a flawless TIRF angle during the live experiments. We analyzed the images with ImageJ (155) by two different approaches.

First, we analyzed the Mac-1 intensities by fluorescence profile measurement along a 25 μm standard line placed on the equator of the cells (**Figure 7**). We ordered in descending sequence the measured intensity values of each cell and we compared the median of these ranked intensities.

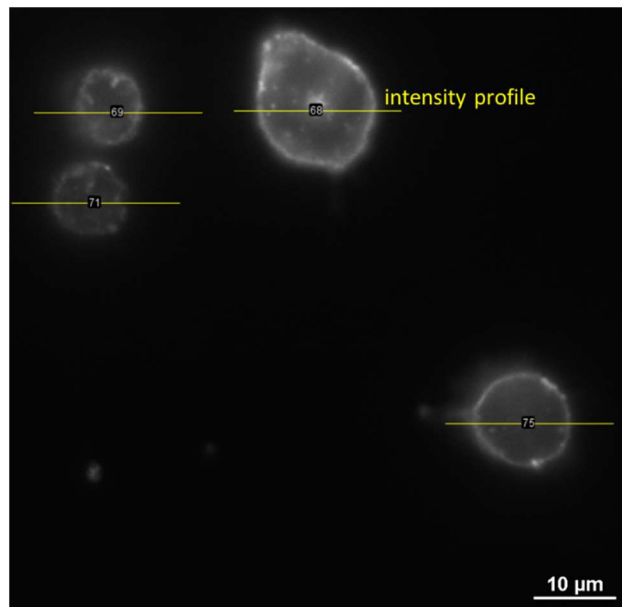


Figure 7. Evaluation of TIRF microscopic image - intensity profile measurement along a standard, 25 μm line placed on the equator of the cells placed on BSA- or C3bi-coated surfaces, after 20 minutes.

Second, we carried out a cluster outlining with particle analysis after subtracting the background with a 12 μm rolling ball radius and setting the threshold manually to 200 AU minimum intensity (**Figure 8**). We measured the maximal fluorescence intensities of all outlined clusters. The median of these peak fluorescence values was used for statistical comparison.

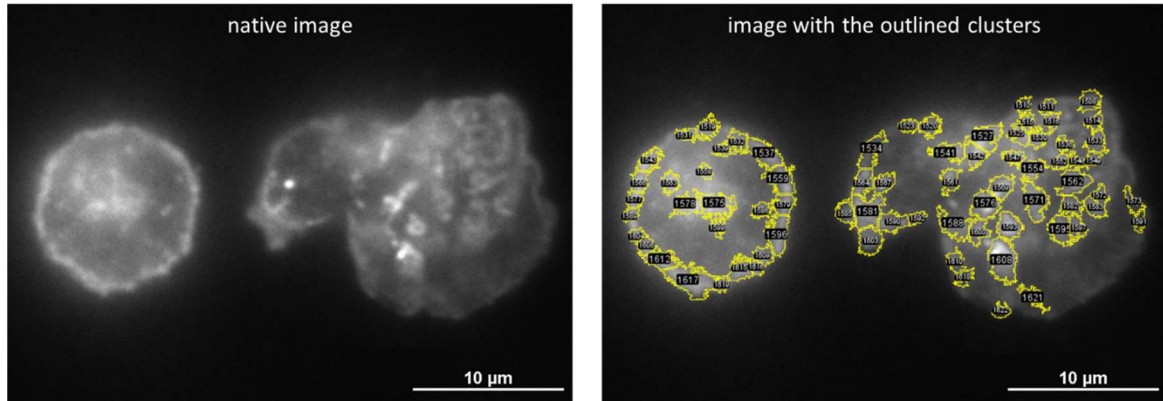


Figure 8. Evaluation of TIRF microscopic image – cluster outlining of the cells placed on BSA- or C3bi-coated surfaces, after 20 minutes.

3.14. Induction of cluster formation with antibodies

PMNs were incubated with 10 $\mu\text{g}/\text{ml}$ non-inhibitory anti-CD11b (clone: Bear-1) in PBS containing 1% BSA for 30 minutes at 37°C, followed by incubation with 10 $\mu\text{g}/\text{ml}$ mouse anti-human IgG1 for 30 minutes at 37°C. After the clustering induction, the cells were washed once in HBSS (500 g, Hermle Z216MK 45° fixed angle rotor, 10 min, 4°C) and further used for EV generation (Ab. clust. EV).

3.15. Statistics

All bar graphs show mean and \pm SEM. The difference was taken as significant if the P-value was <0.05 . * represents $P < 0.05$ and ** represents $P < 0.01$. In each experiment, “n” indicates the number of independent experiments from different donors, and “n.s.” indicates a non-significant difference. Statistical analysis was performed using GraphPad Prism 8 for Windows (La Jolla, California, USA).

4. RESULTS

4.1. Validation of the new, flow cytometry-based bacterial survival assay

Our aim was to develop a new method that is able to detect the antibacterial effect of cells, subcellular particles, and soluble agents in a fast, cost- and labor-effective way. I discussed in the Introduction the drawbacks of the available methods for bacterial survival assessment. The classical, gold-standard colony-forming unit (CFU) counting method is greatly time-(48 hours) and labor-consuming method. The optical density-based method developed earlier in our laboratory is also time-consuming (16 hours) and has limitations on the number of parallel samples (30, 39).

We compared our new FC-based method with the previously used OD-based method. The main difference between the techniques is that with the OD method we calculate indirectly the number of bacteria, while with the FC-based method we quantify them directly. Our incubating solution contains 4 V/V% LB in order to provide nutrients and gain the benefit of distinguishing bacteriostatic and bactericidal effects. In a non-inhibitory circumstance, where nutrients are present, the bacteria reach the logarithmic phase of growth during the incubation time, therefore we start the OD measurement with bacteria that are already started to divide, and in this way, the increase of the bacterial count is amplified. While, in an inhibitory circumstance, where the growth of the bacteria is inhibited and/or part of the bacteria killed or phagocytosed, the bacteria start the OD measurement in the lag phase and reach the log phase at a later time point that can reduce the number. On the contrary, our FC-based method is a direct quantification of the bacterial count at the endpoint of the co-incubation.

Within this project, we compared the killing capacity of human blood cells, wild type and NADPH oxidase-deficient murine neutrophils, and neutrophil-derived oZ-EVs in different dosages on Gram-positive and Gram-negative bacteria (30). In the frame of this thesis, I narrow down the results for the reproducibility of this new type of measurement.

Figure 9. summarizes all the data we gained for *S. aureus* (USA300 and Acridine Orange-labeled methicillin-sensitive *S. aureus*) survival from these above-mentioned measurements with cells and particles measured parallel with OD-based and FC-based methods.

The summary of the 37 experiments gave a regression coefficient of 0.8766 which indicates good comparability of the two techniques up to approximately 300 % growth rate. We observed however a higher deviation in the case of the OD measurement mainly in the higher range of bacterial survival. This higher deviation can be explained by the nature of the indirect measurement that can enlarge the differences. All together, we found that the FC-based method showed good correlation even in a narrow growth range when we examined the antibacterial effect of EVs. Therefore we could confidently use this method for further bacterial survival measurements.

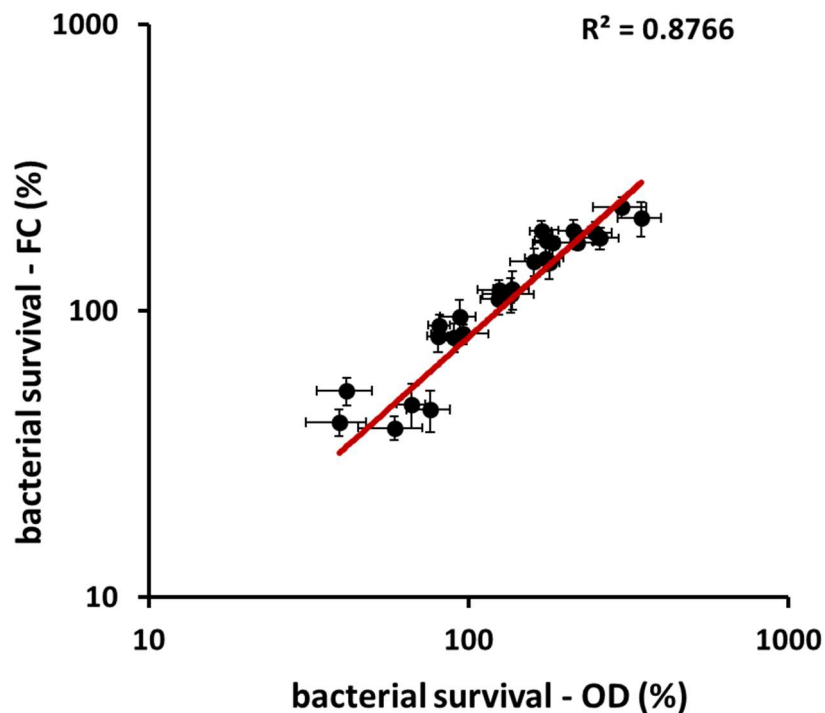


Figure 9. Comparison of the reproducibility of the new FC-based and OD-based methods. Linear regression of bacterial survival of *S. aureus* measured by OD- and FC-based methods ($n=37$, \pm SEM).

4.2. Quality control for the differential centrifugation, filtration based PMN EV isolation with size exclusion chromatography

Following the principles of MISEV2018 (1), we aimed to perform quality control measurements for our generally used EV isolation with differential centrifugation and filtration (DC+F). Previously, we did not detect intact granules in our samples based on the electron microscopic images, but we could not exclude the possibility that protein aggregates could be co-sedimented with the vesicles that may interfere with the observed antibacterial effect of oZ-EVs. For this reason, we planned to set up a size exclusion chromatography (SEC) platform to purify EVs from our samples and examine the size distribution, the EV quantity, protein content, and antibacterial effect of the collected fractions.

Both in the case of spEV, and oZ-EV preparations, fractions 8 to 12 contained EVs detectable by DLS, FC, and Bradford assay. This is in accordance with the literature in the case of SEC columns with similar technical properties (156). Compared to the DC+F isolation the size distribution of EVs isolated by SEC did not show significant alteration, the continuous shift of the peaks of the SEC samples is in accordance with the elution sequence of the fractions (**Figure 10**). Scattering intensity values were too low in the further fractions, therefore the SEC 8 to 11 fractions are represented in the figure.

I have to add that the DLS on its own provides information solely on the total light scatter of a suspension. The peaks indicate the size range of the detected particles, but the smaller particles scatter less light, thus the concentration of these particles can be underestimated by DLS. Therefore, for further experiments, we rather used nanoparticle tracking analysis (NTA) measurement.

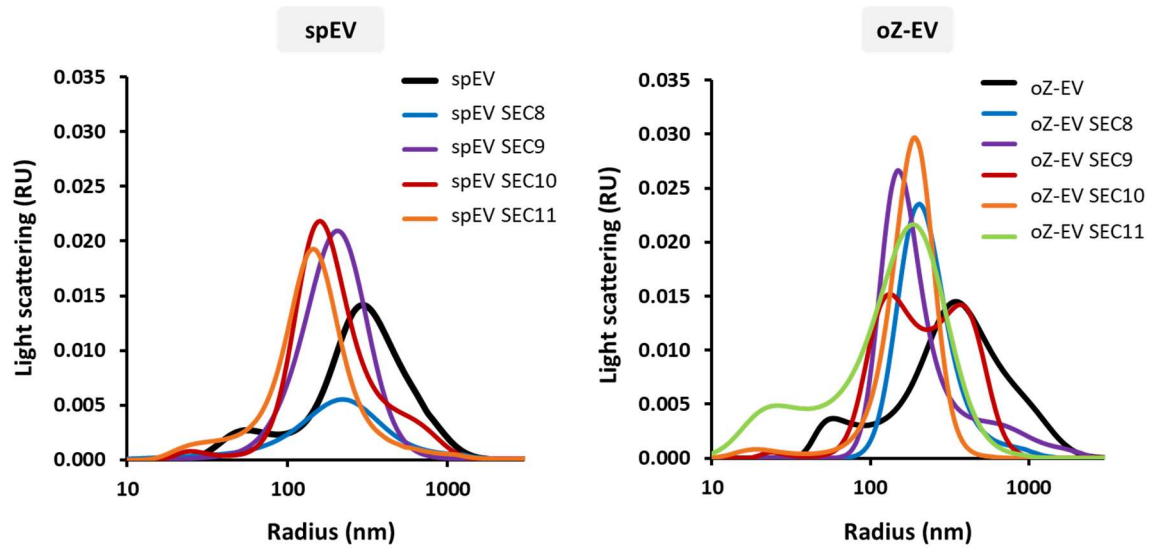


Figure 10. Representative size distribution spectra (out of $n=3$ DLS measurements) of spEVs and oZ-EVs isolated by DC+F (black lines) and SEC 8-11 fractions (colored, labeled accordingly).

In the same SEC fractions, EVs were detected also by flow cytometry and the proportion of the oZ-EVs versus spEVs was similar to the proportion gained with the DC+F method and to our previous observations as well (**Figure 11**). On the other hand, we obtained a lower yield of EVs by SEC in terms of EV number (**Figure 11**).

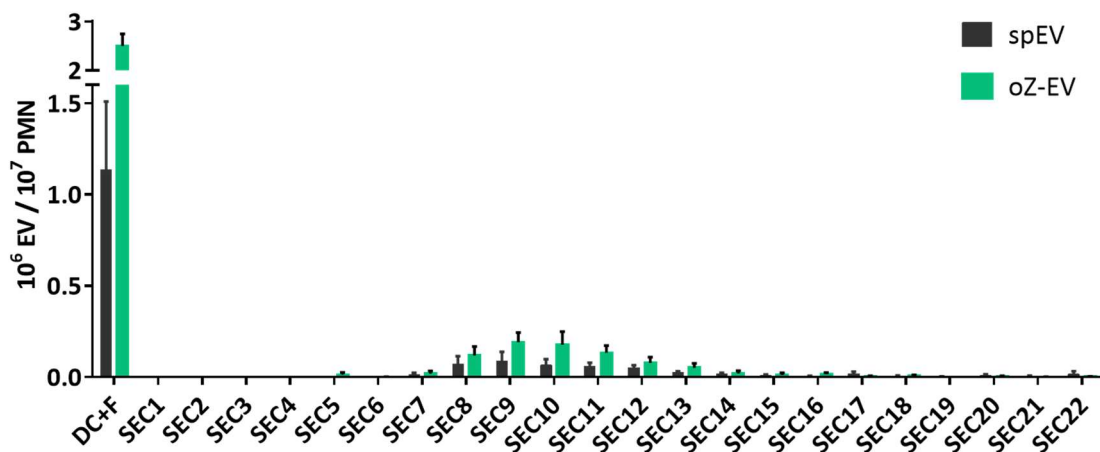


Figure 11. EV quantification of spEV and oZ-EV samples determined by flow cytometry as described in the Methods section. The first columns belong to the result of the DC+F isolation, the further columns belong to a particular SEC fraction ($n=3$, \pm SEM).

This observation would allow us to use this particular SEC preparation only to a limited extent, in selected experiments. Indubitably, the further optimization of this SEC isolation by changing technical parameters of the column (e.g. column height, diameter) could improve the separation and the recovery of the EVs. However, currently, our aim was to provide quality control for our generally used isolation, not to optimize the method in order to reach a higher yield.

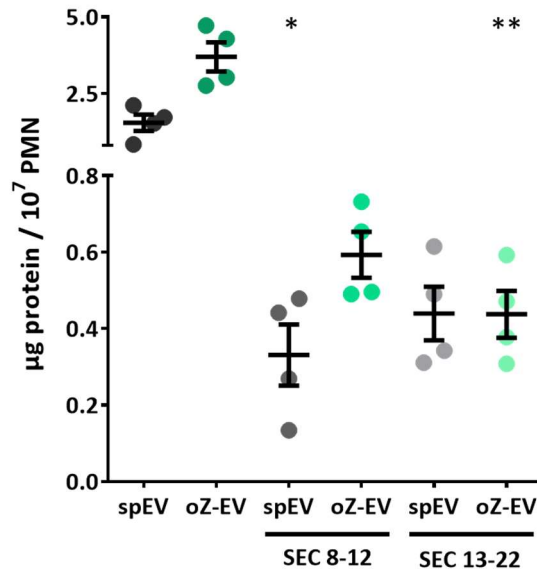


Figure 12. Protein content of pooled SEC fractions compared to DC+F isolated EV samples, measured by Bradford protein evaluation ($n=4$, \pm SEM). Data were compared to SEC 8-12 oZ-EV pool by RM one-way ANOVA with Dunnett's post hoc test.

The lower yield of the SEC preparation was evincible also in the case of the protein measurement. The increase of protein amount in oZ-EV preparation (compared to spEV) affected only the protein recovered in the vesicular (SEC 8-12) fractions, whereas the amount of co-sedimented protein recovered in fractions SEC 13-22 was not changed (**Figure 12**). Based on our previous findings, one of the major granule proteins that are present in the oZ-EVs is lactoferrin. Actin and actin-associated proteins are also present in EVs (119). We wanted to examine whether these proteins can be detected in those fractions where we identified EVs by FC, DLS, and Bradford measurement. In the fractions SEC 8-12 both lactoferrin and actin could be detected in the same fractions by western blotting (**Figure 13**).

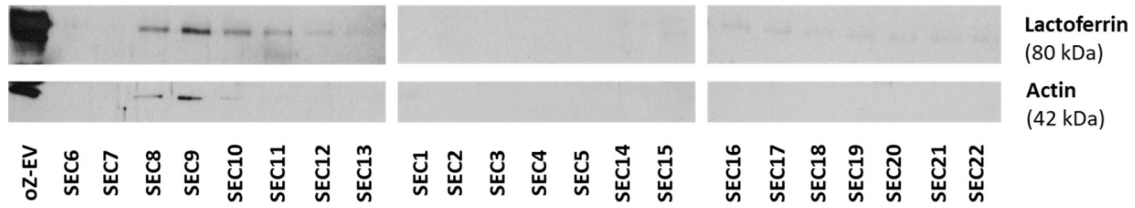


Figure 13. Representative ($n=3$) western blot for lactoferrin and actin content of the oZ-EV samples isolated by DC+F method (oZ-EV) and by SEC. The sequence of the SEC fractions was separated in order to demonstrate the relevant fractions on the same blot.

However, in the posterior SEC fractions (SEC 13-22) we can observe the presence of lactoferrin on the western blot. Also, the Bradford assay detected measurable protein content in those fractions (**Figure 12**). To reveal whether that protein content without EV structure expresses an antibacterial effect or not, we carried out USA300 bacterial survival measurement. We found that only the pool of vesicular EV fractions shared the same antibacterial property with the DC+F separated oZ-EVs, the SEC 13-22 fractions did not show a similar antibacterial effect to the DC+F oZ-EV sample (**Figure 14**).

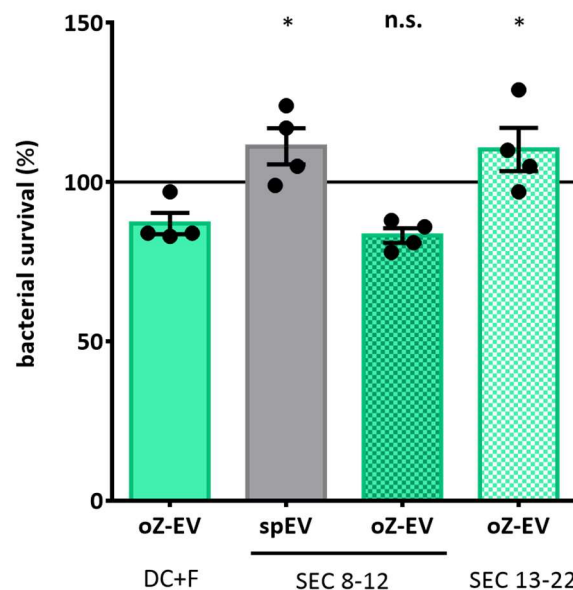


Figure 14. Bacterial survival of USA300 measured with OD-method in the presence of DC+F isolated oZ-EV sample, or pooled SEC fractions of spEV and oZ-EV ($n=4$, \pm SEM). Data were compared to oZ-EV isolated by DC+F by RM one-way ANOVA with Dunnett's post hoc test.

We performed a further quality control measurement for the possible DNA contamination of our samples. Previously, we did not detect DNA, and histone content in our oZ-EV samples, only in the case of apoEVs (16, 119)(**Table 2**). Nonetheless, we wanted to rule out the possibility that NETs could contribute to the observed antibacterial effect in our sample. It has been proved that DNase can disrupt NETs in *in vitro* and *in vivo* conditions (157, 158). Therefore, we treated our oZ-EV sample with DNase (100 U/ml) or with Triton X-100 (0.1%) and found that the detergent lysis of the EVs (disruption of the structure) diminished the antibacterial effect, but the DNase treatment did not change the effect compared to the control oZ-EV sample (**Figure 15, Panel A**). We checked that neither the DNase treatment nor the Triton X-100 treatment on their own did not affect the bacterial growth (**Figure 15, Panel B**).

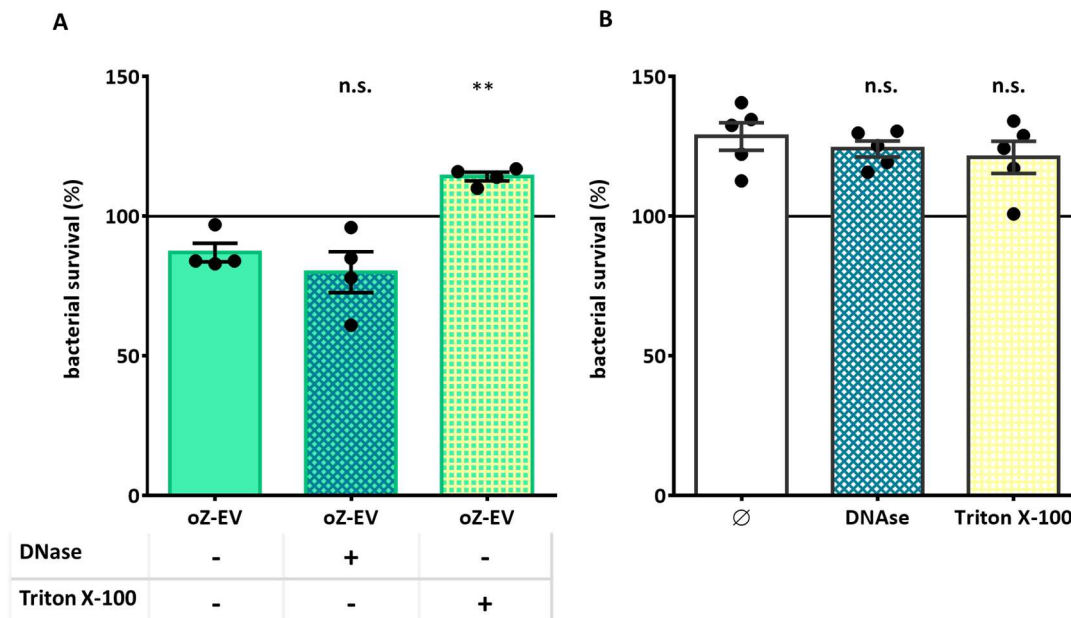


Figure 15. Bacterial survival of USA300 strain in the presence of oZ-EV (**A**) ($n=4$, \pm SEM) and without EVs (**B**) ($n=5$, \pm SEM). Data were compared to the according control sample by RM one-way ANOVA with Dunnett's post hoc test.

Altogether, we found that our EV pellets do contain detectable soluble proteins or protein aggregates, but the observed antibacterial effect of oZ-EVs is independent of the presence of these proteins and can be associated with the vesicular nature of the oZ-EVs.

4.3. Role of Mac-1 in the formation of neutrophil EVs

To examine the exclusive contribution of the Mac-1 for the antibacterial and pro-inflammatory type oZ-EV production, we selectively activated the Mac-1 receptors by different ligands. The receptor has over 40 ligands identified already (114). Complement receptors have been characterized for their preference for specific C3 opsonic fragments. Mac-1 specifically recognize C3bi (159, 160). The complement factor H (FH) was also discovered to specifically bind to neutrophils through the Mac-1 receptor (161, 162). It has been demonstrated that FH-coated surface activation can lead to induced ROS and IL-8 production of neutrophils (161, 163). Therefore, we decided to apply C3bi and FH as specific ligands of Mac-1.

We stimulated the neutrophils in suspension with increasing concentrations of FH and C3bi and compared the released EV numbers to the spontaneous EV release (spEV). There was no significant increase in the quantity of the EVs regardless of the concentration of the applied ligand (**Figure 16**). The question was raised, whether soluble C3bi or FH supports the high-affinity binding that induces the integrin activation. Therefore we primed the cells with TNF- α through inside-out activation of the integrin prior to the co-incubation with the ligand. The pre-treatment did not affect the number of formed EVs either (**Figure 16**).

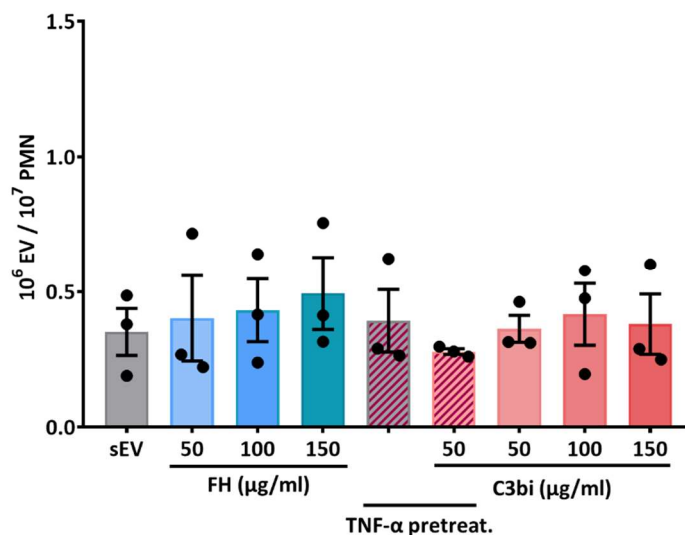


Figure 16. EV quantification determined by flow cytometry as described in the Methods section. TNF- α pretreatment (20 ng/ml) was applied for 20 minutes prior to secondary stimulation. Data were compared to spEV by RM one-way ANOVA with Dunnett's post hoc test ($n=3$, \pm SEM) and no significant difference was found.

Beyond that, we examined the proportion of the cells with high-affinity Mac-1 conformation immediately after the isolation of the cells. We examined whether this proportion can be further increased by TNF- α priming (20 ng/ml, 20 minutes stimulation). It was revealed that the dominant part of neutrophils carry Mac-1 receptors in high-affinity conformation and their activation could not be further increased by adding TNF- α . Neutrophils isolated with sterile preparation (pyrogen-free) had a lower percentage of activated Mac-1 receptors and TNF- α had a significant effect (**Figure 17**). These data suggest that the inability of soluble C3bi and FH to trigger increased EV formation is not due to the lack of Mac-1 in high-affinity conformation.

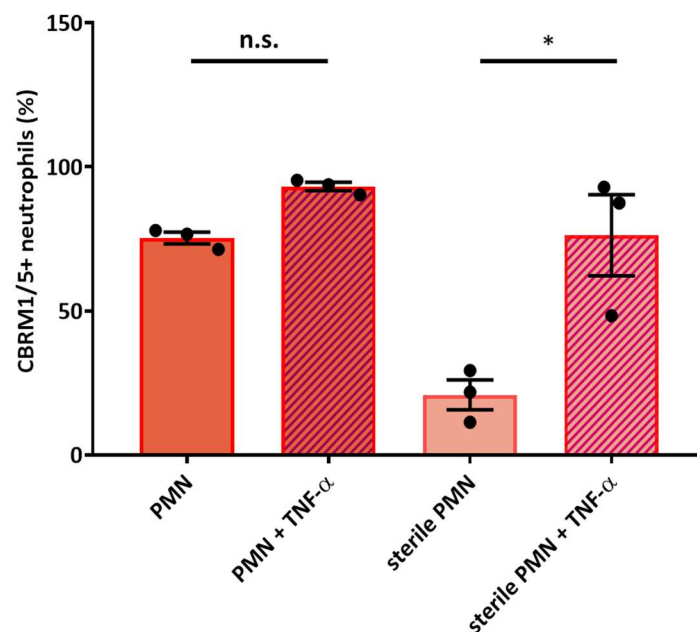


Figure 17. Percentage of the neutrophils with the active conformation of Mac-1 detected by conformation recognizing antibody (clone: CBRM1) with/without TNF- α pretreatment, measured after isolation of the cells in normal or sterile (pyrogen-free) circumstances. Data were compared to the non-pretreated control data by RM one-way ANOVA coupled with Sidak's multiple comparison test ($n=3$, \pm SEM).

4.3.1. Mac-1 ligand surface induces EV production from adherent PMNs

Surprisingly, when we applied the C3bi and FH in a surface-bound form, the cells placed on these ligand surfaces produced a significantly higher number of EVs compared to the albumin surface. The total protein content of the ligand surface-triggered EVs changed proportionally with to the quantity of the detected EVs (*Figure 18, Panel A*). These results are in agreement with our previous observation on the fibrinogen surface-induced EV release compared to resting neutrophils on the BSA surface (152). The flow cytometry has a limitation by detectable size. The nanoparticle tracking analysis (NTA) is also a gold standard method of EV research, because this approach is able to examine particles in suspension particle by particle, and determine their size based on their Brownian motion at the same time by scattering the laser beam. This method has no size limitation, it is possible to detect events around and below 100 nm size. We confirmed the observed difference between the surface and soluble stimulated EV production of the cells by NTA measurement of the EV concentration (*Figure 18, Panel B*). The size distribution of the EVs did not change by these means of activation (*Figure 18, Panel C*), the diameter of the EVs ranges between 100 and 700 nm with a modus around 200-300 nm.

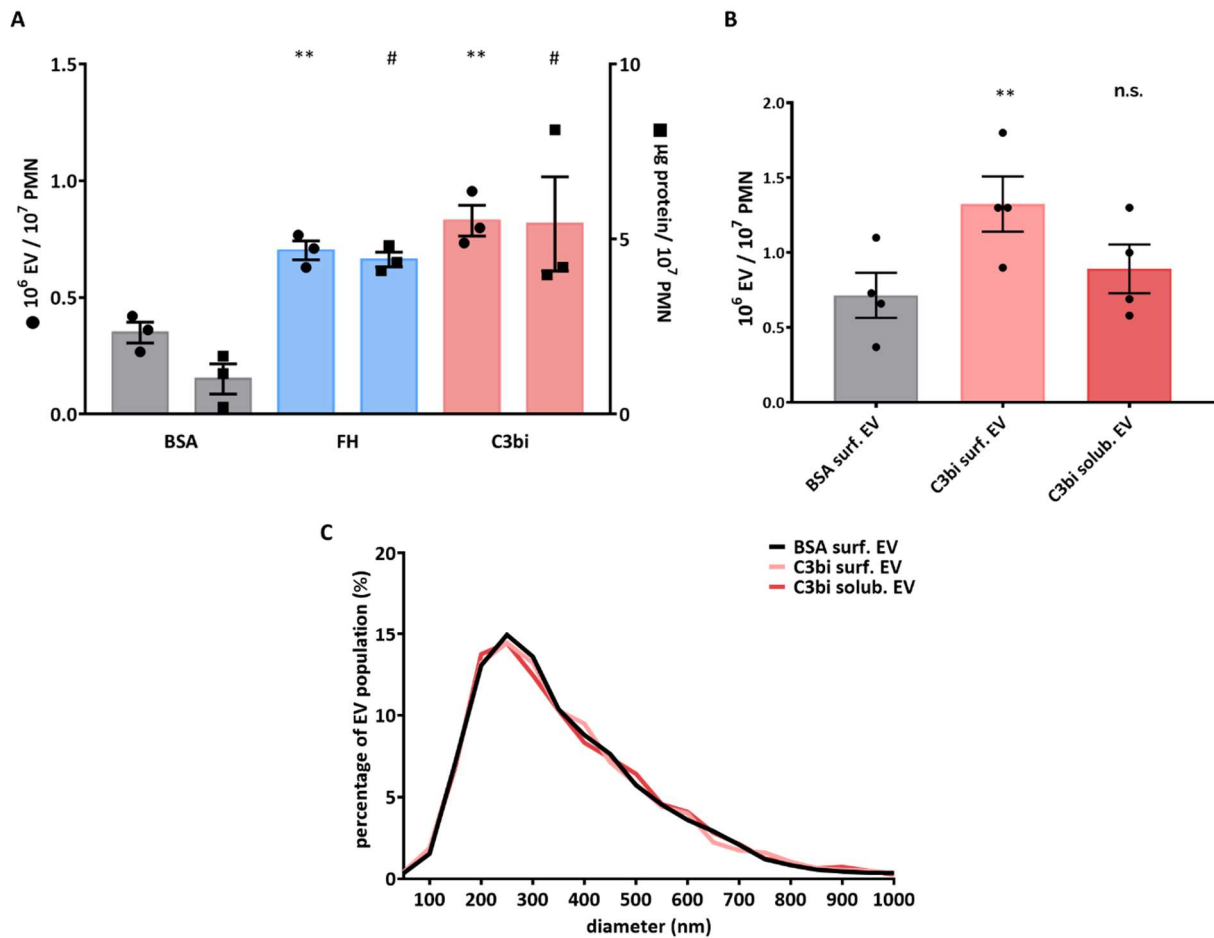


Figure 18. Adherent neutrophil EV production on Mac-1 ligand-coated surfaces. **(A)** Comparison of EV production on bovine serum albumin (BSA) and surface-bound Mac-1 ligands. Dot scatter bars represent the quantity of EVs determined by flow cytometry, square scatter bars represent the quantification based on total protein estimation measured by Bradford assay. The EV production was measured on BSA surface (20 $\mu\text{g/ml}$), on C3bi surface (50 $\mu\text{g/ml}$) and on FH surface (50 $\mu\text{g/ml}$) for 20 minutes. Data were compared to BSA by using RM one-way ANOVA coupled with Dunnett's post hoc test ($n=3$, \pm SEM). **(B)** Comparison of the concentration of EV samples released from adherent and soluble PMNs, measured by NTA. C3bi and BSA were used in the previously detailed concentration. Data were compared to BSA surface by using RM one-way ANOVA coupled with Dunnett's multiple comparisons test ($n=3$, \pm SEM). **(C)** Representative size distribution diagram of PMN EVs induced by soluble or surface-bound C3bi or BSA surface measured by NTA.

The C3bi and the FH are shown to be ligands of the complement receptor 4 (CR4, CD11c/CD18) as well (164). On neutrophils, the CR4 is far less abundant than Mac-1, and it has been also shown that in all human phagocytes (neutrophils, monocytes, macrophages, dendritic cells) solely Mac-1 takes part in the engulfment of C3bi-opsonized *S. aureus*, while CR4 is only responsible for the binding of the pathogen (165, 166). We wanted to confirm the dominant role of Mac-1 over CR4. We carried out EV production and ROS production measurements with specific, inhibitory antibodies of CD11b and CD11c. By the application of the inhibitory antibody against Mac-1, the oZ-EV production was significantly inhibited, and the ROS production was almost completely reduced (**Figure 19**). On the other hand, by the application of the CR4 inhibitory antibody, there was no significant change either in oZ-EV or in ROS production. Therefore, we concluded that anti-CR4 antibodies did not interfere with opsonin receptor-induced EV release of neutrophils.

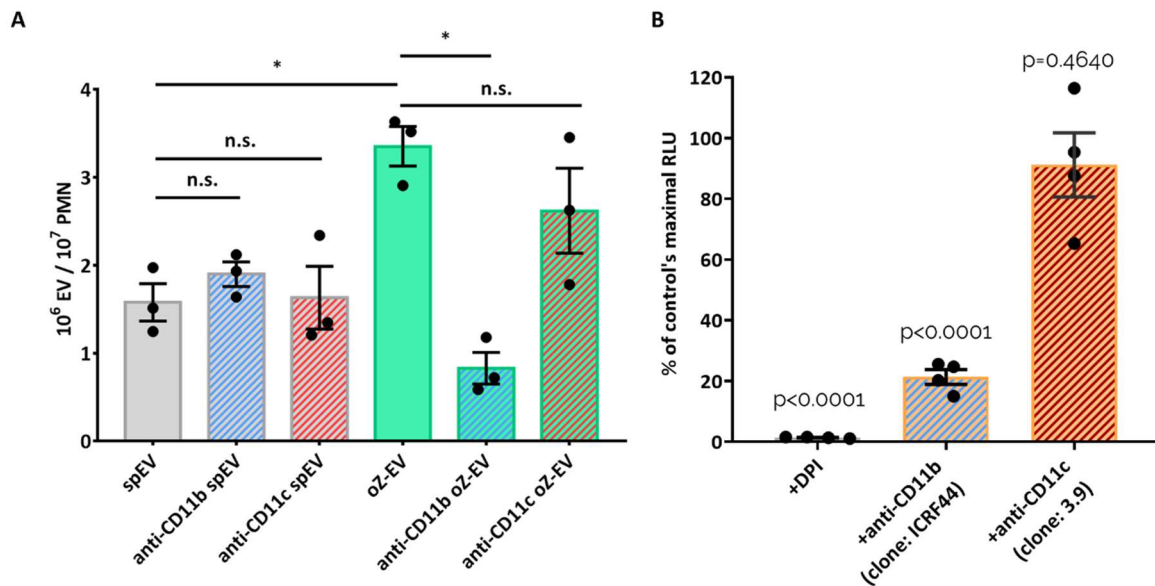


Figure 19. Examination of the possible contribution of CR4 in the oZ-EV formation and ROS production of neutrophils. **(A)** Spontaneous and opsonized zymosan-induced EV production of PMNs in the presence of anti-CD11b (clone: ICRF44) and anti-CD11c (clone: 3.9) inhibitory antibodies, measured by flow cytometry. EVs were labeled with FITC-Annexin V. Data were compared by using RM one-way ANOVA coupled with Sidak's multiple comparison test ($n=3$, \pm SEM). **(B)** Comparison of ROS production of PMNs placed on fibrinogen surface in the presence of anti-CD11b (clone: ICRF44) anti-CD11c (clone: 3.9) inhibitory antibodies, and in the presence of ROS inhibitor DPI applied as a negative control. The maximal ROS production was compared with the maximal ROS production of PMNs on the fibrinogen surface, and the percentages are presented. Data were analyzed by multiple one-sample t -tests ($n=4$, \pm SEM).

4.3.2. Mac-1 receptor clustering on BSA and C3bi surface

The discrepancy in the effect of Mac-1 activation on a surface or in suspension suggested the possibility that Mac-1 is not able to bind ligands in suspension or that the mere binding of a ligand is not able to initiate EV production. As we knew that Mac-1 receptors on the cells are mostly in an active state, the C3bi and FH could bind to Mac-1 on the surface of the neutrophils. Therefore, we aimed to investigate the possible importance of the Mac-1 receptor clustering in the vesicle formation of the PMNs. We carried out live total internal reflection fluorescence (TIRF) microscopy on cells undergoing surface activation in order to visualize the pattern of Mac-1 receptors during the process.

For this reason, we labeled the cells for CD11b with a non-inhibitory antibody (clone M1/70) and followed the adherence for 20 minutes (the time period we applied for EV generation). We could detect higher receptor concentrations in the membrane of the cells placed on the C3bi-coated surface compared to cells placed on the BSA-coated surface (*Figure 20*).

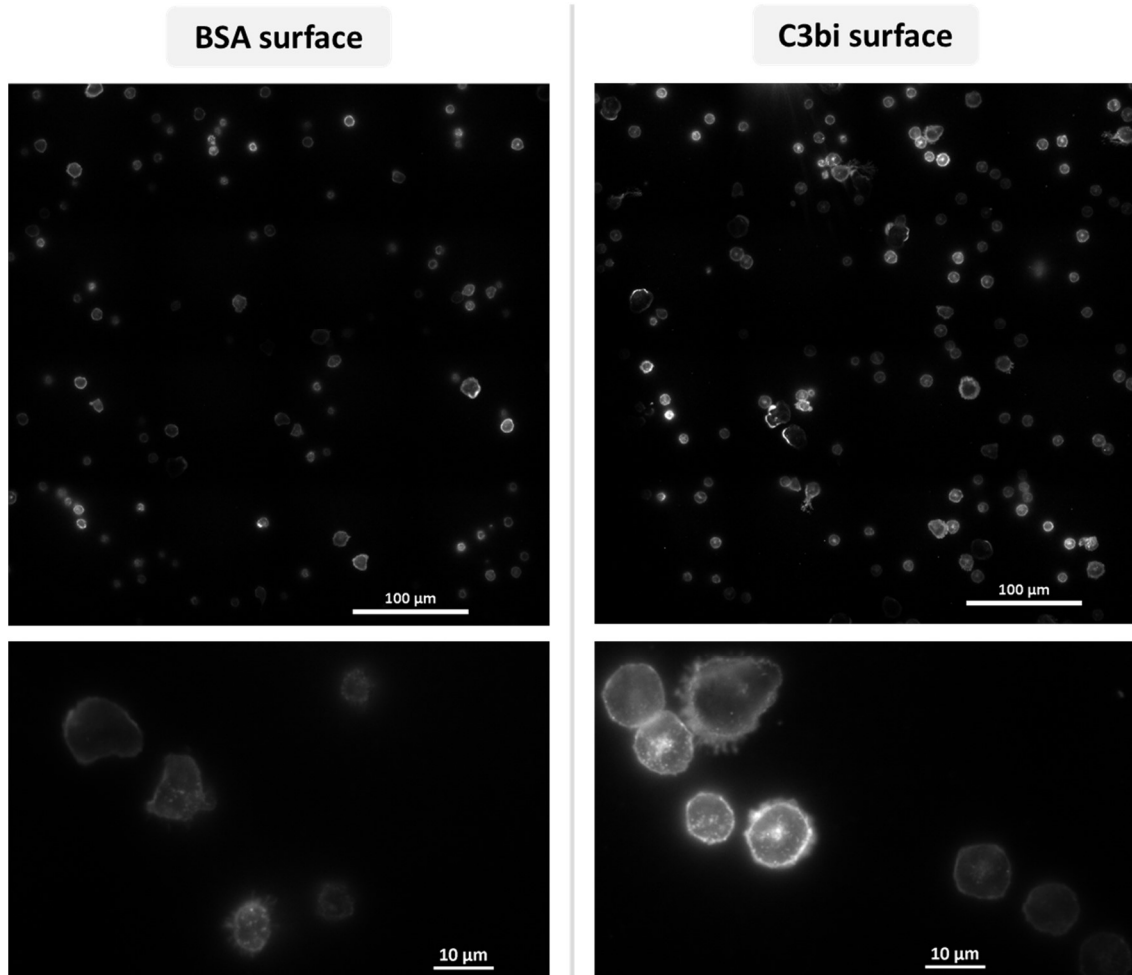


Figure 20. *Mac-1* receptor clustering on BSA and C3bi surface captured by TIRF microscopy at the 20th minute time point. Representative images of the cells on BSA and C3bi coated surfaces. Cells were labeled with Alexa647-conjugated anti-CD11b.

As further means of the comparison of the control and the ligand surface, we carried out two, different evaluations as it was detailed in the Methods section. We assessed the Mac-1 fluorescence intensity along the equator of each of the cells on the C3bi or BSA surface and ranked the values in descending order. We plotted the median values of the ranks of the samples and we got significantly different curves (**Figure 21, Panel A**). The intensity profile of C3bi surface-adherent cells demonstrates higher Mac-1 receptor concentration than BSA surface-adhered cells. When we outlined the clusters in the cells and measured the peak Mac-1 receptor density, we found that on the C3bi surface, the median values of the peak intensities were significantly higher compared to the control (**Figure 21, Panel B**).

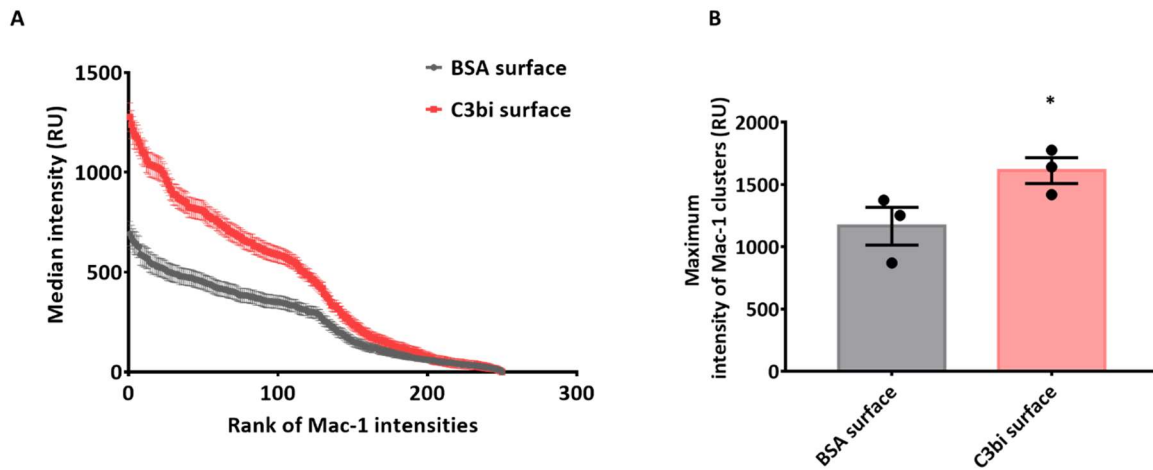


Figure 21. Evaluation of TIRF images of cells placed on BSA and C3bi surface. **(A)** Median fluorescence intensity values of the ranked intensities of all the cells measured along a standard 25 μm line. Data were compared by linear regression ($n=3$, \pm SEM). The two datasets are significantly different ($p<0.0001$). **(B)** Median of peak intensity values of the outlined clusters of the cells in the samples. Data were compared by using Student's *t*-test ($n=3$, \pm SEM).

4.3.3. Mac-1 ligand surface- and antibody-induced clustering initiates antibacterial and pro-inflammatory PMN EV production

We intended to examine the functional properties of the Mac-1 ligand-induced EVs. For that reason, we carried out different control measurements. First, we compared the bacterial survival of the USA300 strain in the presence of Mac-1 ligand surface-induced EVs and soluble ligand activation-derived EVs. We found that only those EVs expressed similar inhibition of bacterial growth as oZ-EV that were produced on ligand surface (**Figure 22, Panel A**). In parallel, we measured the antibacterial effect with our new flow cytometry-based method as well. However, we had to face technical difficulties at this time we could not conduct all the parallel measurements with the cytometer. Nevertheless, we were able to measure more samples with the new method, because we were not limited by the number of the wells on the plate as in the case of a spectrophotometry-based measurement. While the tendencies were similar to the results that we obtained with the OD-based measurement, in this case, we did not have the same significant differences among samples (**Figure 22, Panel B**). For further confirmation, we also tested the influence of inside-out activation of Mac-1 prior to ligand application on the antibacterial effect of the EVs. We observed no effect of the priming by TNF- α on the antibacterial capacity. However, we could confirm that fibrinogen surface-induced EVs are also potent inhibitors of bacterial growth (**Figure 22, Panel C**).

In order to substantiate the involvement of the Mac-1 clustering in the antibacterial type EV production of the cells, we performed antibody-induced receptor clustering, isolated the EVs thereafter, and examined the bacterial survival of USA300 after co-incubation with these EVs. For these experiments, we used a non-inhibitory CD11b primary antibody, and with a secondary antibody, we initiated the clustering. The measured antibacterial effect was significant but weaker than the effect of oZ-EV or C3bi surface-induced EVs (**Figure 22, Panel D**). Accordingly, this result suggests that clustered Mac-1 molecules can attract the signaling elements that are required for the initiation of the antibacterial oZ-EVs.

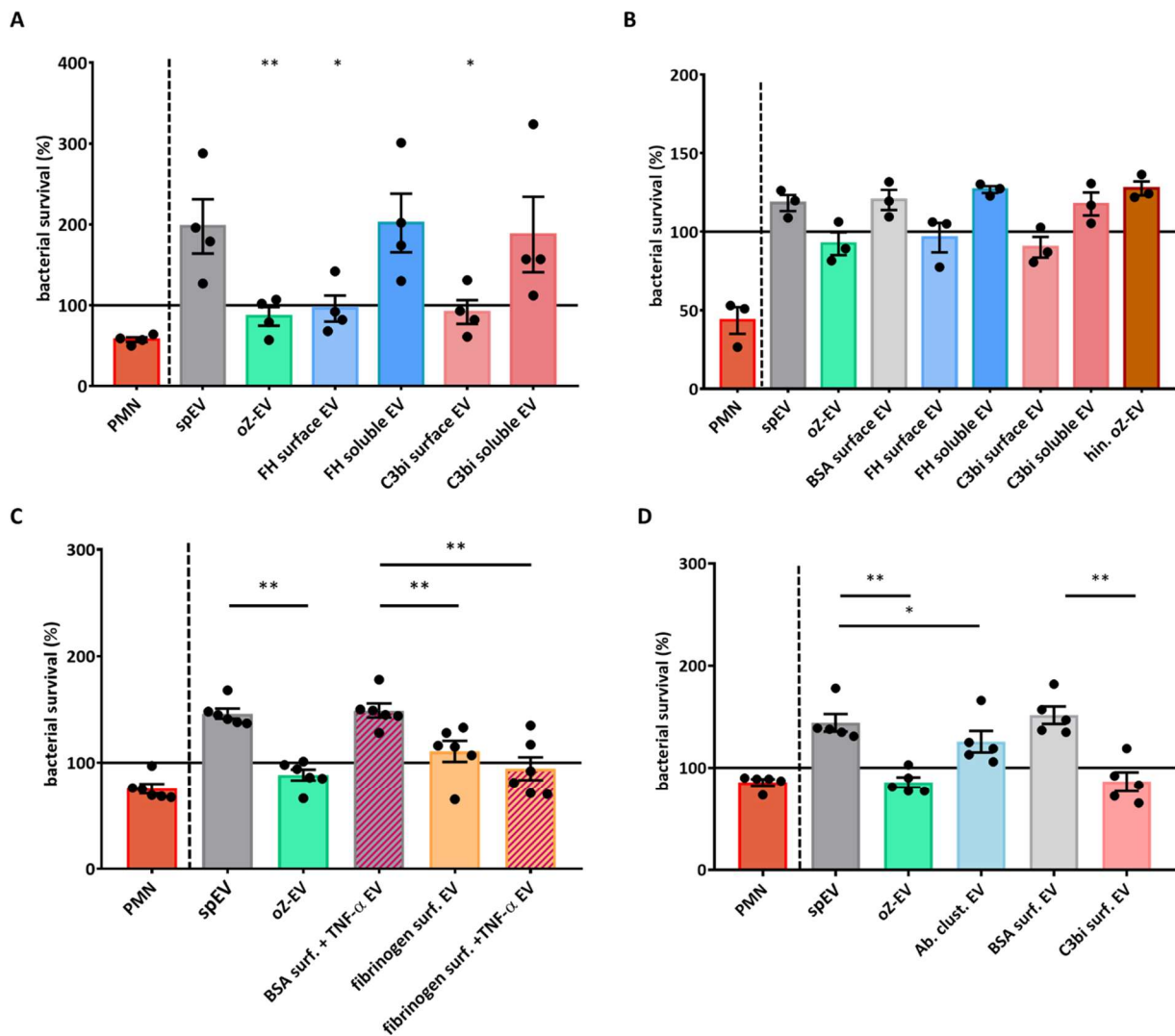


Figure 22. Bacterial survival of USA300 bacteria treated with differently induced neutrophil EVs. The amount of the applied EVs was normalized to protein content. **(A)** Bacterial survival measured by OD-based method in the presence of different types of neutrophil EVs. Data were compared to spEV by using RM one-way ANOVA coupled with Dunnett's post hoc test ($n=4$, \pm SEM). **(B)** Bacterial survival measured by FC-method in the presence of different types of neutrophil EVs. Data were compared to spEV by using RM one-way ANOVA coupled with Dunnett's post hoc test ($n=3$, \pm SEM), no significant difference was found. **(C)** Bacterial survival measured by OD-based method in the presence of fibrinogen surface induced PMN EVs. Data were compared by using RM one-way ANOVA coupled with Sidak's multiple comparison test ($n=6$, \pm SEM). **(D)** Bacterial survival measured by OD-based method in the presence of EVs produced after antibody triggered cluster formation (Ab clust. EV). Data were compared by using RM one-way ANOVA coupled with Sidak's multiple comparison test ($n=5$, \pm SEM).

We tested whether the C3bi surface-induced EVs possess the pro-inflammatory property of the oZ-EVs by inducing IL-8 production of resting neutrophils. We measured the cytokine production of the cells after 3 hours of co-incubation with the differently induced EV populations. As a control, we applied lysed oZ-EV samples to test the possible activating effect of remnant zymosan particles. In our preliminary experiments, we could not detect pro-inflammatory cytokines IL-1 α , IL-6, TNF- α , and anti-inflammatory IL-1RA from PMNs during 3 hours of co-incubation with opsonized zymosan (152). However, an interesting finding of these experiments, is that spontaneously released EVs increased the basal TGF- β production of the PMNs, but nothing else increased the TGF- β in the supernatant (**Figure 23, Panel B**). As we previously described, the oZ-EVs evoked a strong IL-8 answer from PMNs. While the EVs soluble C3bi treated cells did not increase the IL-8 production of resting PMNs, the EVs produced on the C3bi-coated surface resulted in a significantly higher IL-8 production compared to the BSA-coated surface-induced EVs (**Figure 23, Panel A**).

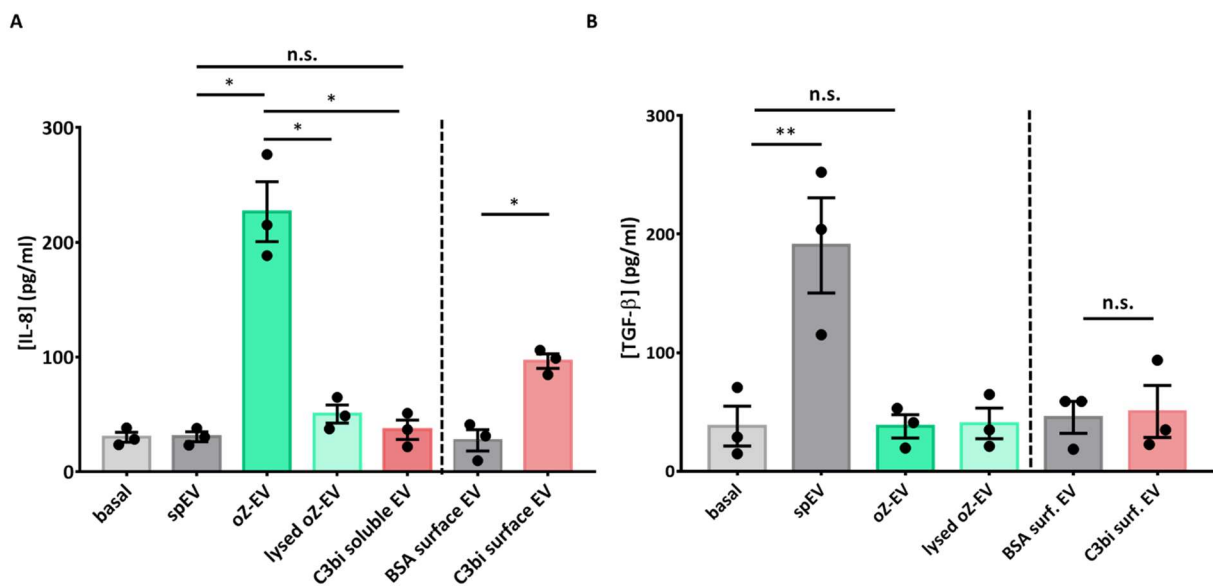


Figure 23. Cytokine production PMNs treated for 3 hours with different PMN EV populations. (A) IL-8 production was quantified with sandwich ELISA. Data were compared by using RM one-way ANOVA coupled with Sidak's multiple comparison test ($n=3$, \pm SEM). (B) TGF- β production was assessed with sandwich ELISA. Data were compared by using RM one-way ANOVA coupled with Sidak's multiple comparison test ($n=3$, \pm SEM).

4.4. Role of Ca²⁺ signal in the formation of neutrophil EVs

It has been shown that Ca²⁺ ionophores can initiate EV generation from cells, but the functional properties of these EVs are not investigated in detail yet (128, 167). In our earlier work, we showed that Ca²⁺ supply is important for the generation of oZ-EVs (121). To answer the question, of whether the Ca²⁺ signal itself is sufficient for the generation of oZ-EV, with the observed antibacterial and pro-inflammatory properties, we tested the effect of the Ca²⁺ ionophore A23187 and the absence of extracellular Ca²⁺.

4.4.1. Role of Ca²⁺ supply in the PMNs' EV production

When we quantified the number of the produced EVs, we found that the absence of extracellular Ca²⁺ does not affect the spontaneous EV release of the cells, but the oZ-EV production did decrease significantly in the lack of extracellular calcium (**Figure 24, Panel A**) A strong increase occurred in the EV number by the application of the Ca²⁺ ionophore in the presence of extracellular Ca²⁺. By the withdrawal of extracellular Ca²⁺ it was partially inhibited, but not fully diminished. We also tested the combination of stimuli to answer whether the Ca²⁺ ionophore has an additional, potentiating effect on the opsonized zymosan triggered EV generation, but the Ca²⁺ ionophore could not further potentiate the oZ-EV generation. The concentrations that we measured with NTA were in good agreement with the results of the flow cytometry quantification (**Figure 24, Panel B**). However, the NTA measurement showed an even more pronounced effect of the Ca²⁺ ionophore on the EV production enhancement of the neutrophils. The size distribution of the EVs was altered neither by the presence of the Ca²⁺ ionophore nor in the absence of extracellular calcium supply, the size of the EVs varied in the 100-700 nm range, with a peak around 200-300 nm (**Figure 24, Panel C**).

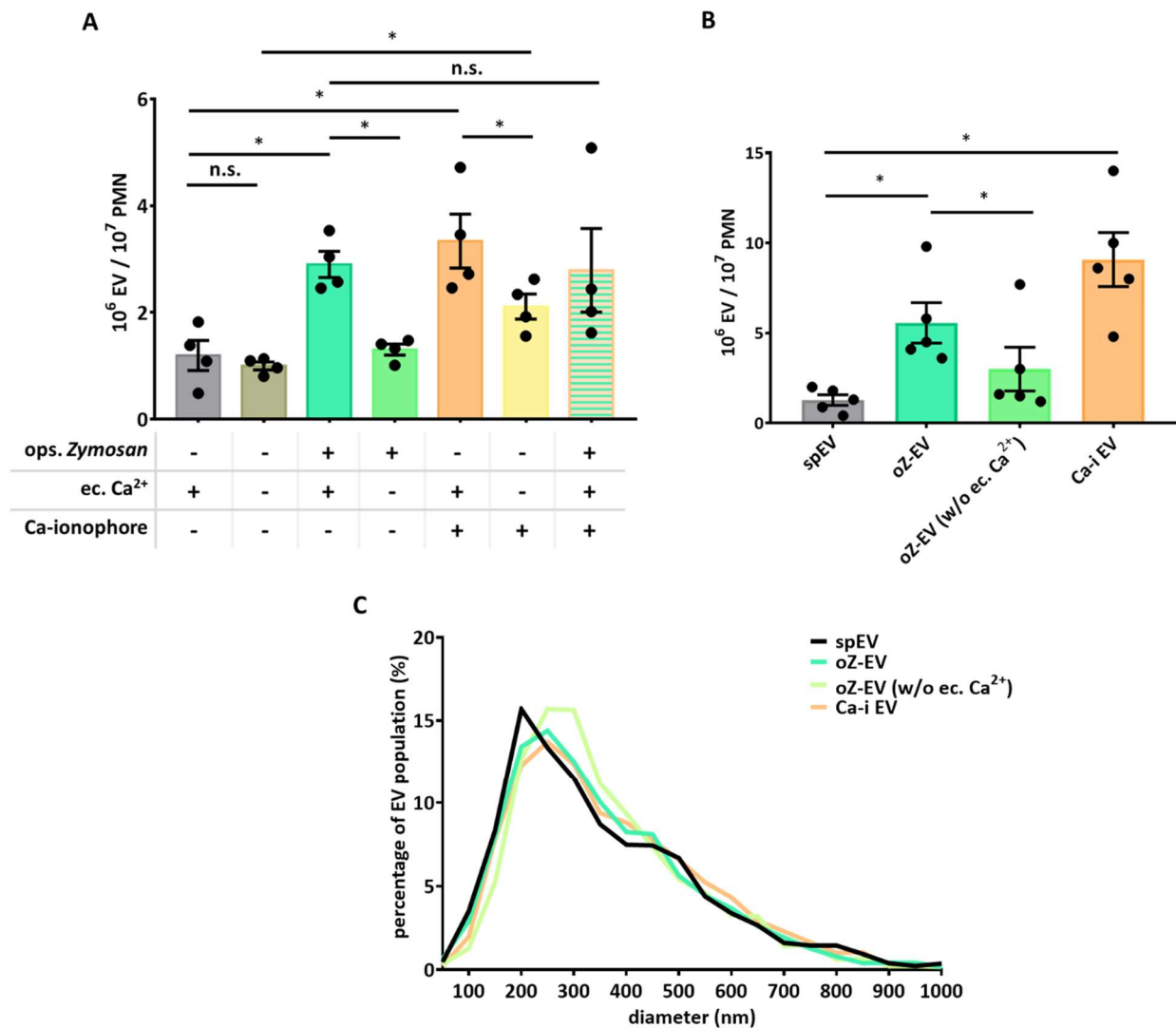


Figure 24. Role of the Ca^{2+} supply in the production of EVs from neutrophils. **(A)** EV production in different conditions, determined by flow cytometry. The Ca^{2+} supply dependence was tested by omitting Ca^{2+} from the incubation medium or by application of Ca^{2+} ionophore A23187. Data were compared by RM one-way ANOVA coupled with Sidak's post hoc test ($n=4$, \pm SEM). **(B)** NTA measurement of differently induced PMN EV concentration. Data were compared by using RM one-way ANOVA coupled with Sidak's multiple comparisons test ($n=3$, \pm SEM). Ca-i EV indicates sample is produced in the presence of Ca^{2+} ionophore and extracellular calcium. **(C)** Representative size distribution diagram of PMN EVs produced in different conditions, examined by NTA.

4.4.2. Role of Ca^{2+} supply in PMNs' antibacterial and pro-inflammatory EV production

We examined the functionality of the differently generated neutrophil EVs: produced in the absence of extracellular Ca^{2+} or in the presence of Ca^{2+} ionophore. In these experiments, the remaining Ca^{2+} ionophore in the samples was bound by BSA. The calcium ionophore induced-EVs could not decrease the survival of the *S. aureus*, except in the case when we stimulated the cells along with opsonized zymosan in the presence of extracellular calcium (**Figure 25**). However, the Ca^{2+} ionophore induction could not potentiate the effect of the oZ-EV against the bacteria. The other EV populations did not show any effect on the bacteria, similar to the spontaneously generated EVs.

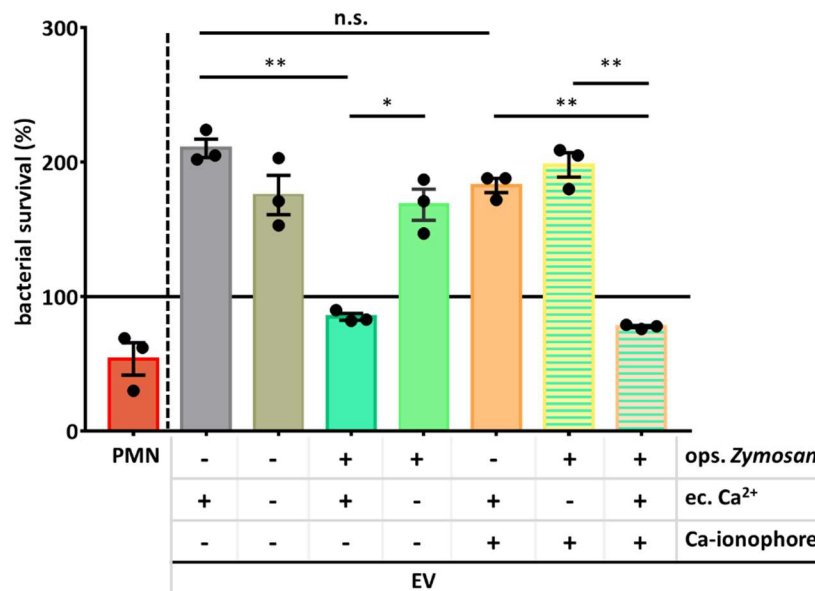


Figure 25. Extracellular Ca^{2+} is necessary for the PMNs' antibacterial EV production. Bacterial survival of USA300 measured with OD-method in the presence of different types of neutrophil EVs. The amount of the applied EVs was normalized to protein content. The bacterial survival was quantified by the optical density-based method. Data were compared by using RM one-way ANOVA coupled with Sidak's post hoc test ($n=3$, \pm SEM).

The observed differences in the amount of the resting neutrophils' released IL-8 were similar to the effect on bacterial survival. The Mac-1 stimulation (through opsonized zymosan particles) and the presence of extracellular Ca^{2+} together seem to be essential for the generation of pro-inflammatory EVs (**Figure 26**). These results support that the application of Ca^{2+} ionophore regardless of the extracellular Ca^{2+} supply cannot result in EVs with the same effect as the opsonized zymosan stimulation. The Ca^{2+} ionophore could not potentiate the IL-8 production increasing the effect of the oZ-EVs either.

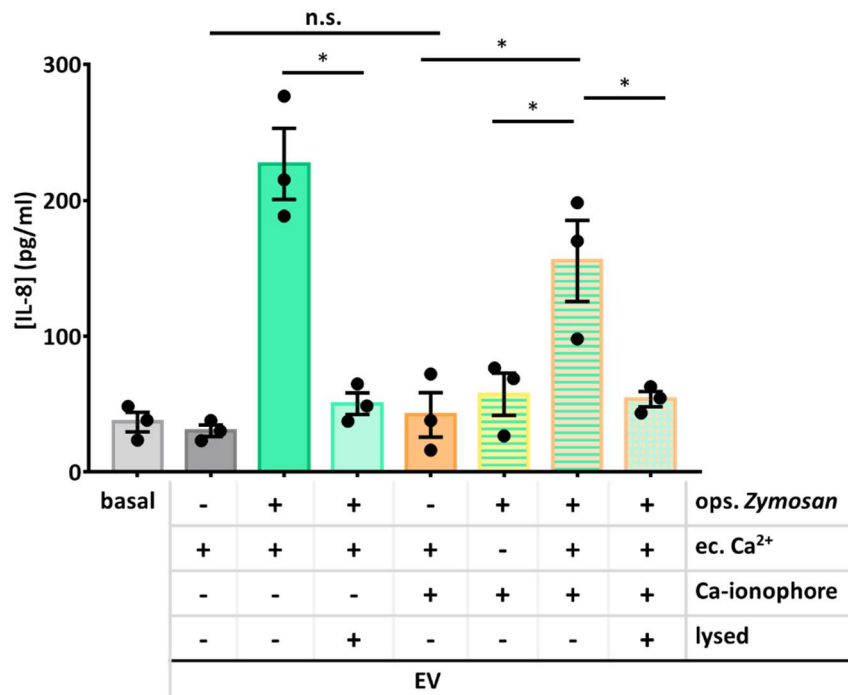


Figure 26. Extracellular Ca^{2+} is necessary for the PMNs' pro-inflammatory EV production. PMNs were treated for 3 h with different PMN EV populations or with controls. IL-8 production was quantified with sandwich ELISA. Data were compared by using RM one-way ANOVA coupled with Sidak's multiple comparison test ($n=3$, \pm SEM).

5. DISCUSSION

Extracellular vesicle research highly demands multiple parallel measurements of different modalities with adequate controls. Demonstration that the effect is associated with the EVs themselves and not to cell-cell contact or to soluble, non-vesicular components (1). Technical development is an inherent urge of the field. We aspired to develop a new, high throughput, fast, reliable, and reproducible flow cytometry-based bacterial survival assessment method. Our assay measures bacterial number directly, therefore no conversion or processing of the acquired data is needed for evaluation. We compared the new, FC-based method to an optical density-based measurement (**Figure 9**) (30). We got good comparability of the two techniques up to approximately 300 % growth rate. With the adequate selection of the incubation media, we can even distinguish the bactericidal and bacteriostatic effects of cellular and subcellular particles. Since then, a new antibiotic susceptibility testing method named MICy has been developed based on this work (168). We aimed to validate our EV isolation protocol in order to control the purity of our EV samples and ensure that neither DNA nor granule protein aggregates can be responsible for the observed antibacterial effect. The SEC isolation of neutrophil EVs resulted in lower EV yield compared to our regularly performed differential centrifugation and filtration-based EV isolation protocol (**Figure 11, Figure 12**). The bacterial survival assays carried out with the pooled SEC fractions of EVs revealed that the antibacterial effect is associated with the EVs themselves and not with soluble, non-vesicular structures (DNA or protein contamination) (**Figure 14, Figure 15**).

On the basis of these technical developments and findings, we proceeded to investigate the role of the Mac-1 in the neutrophilic granulocyte-derived EVs. The phenomenon of Mac-1 clustering both via inside-out and outside-in activation of the receptor has been shown to be important in the phagocytic function of the cells in several cases (169-171). Our previous observations confirmed the pivotal role of Mac-1 in the anti-bacterial and pro-inflammatory oZ-EV biogenesis accompanied by granule protein enrichment in these EVs (120). This suggests a connection between Mac-1 activation and sorting machinery that has not been revealed yet. However, the pathway seems to be divergent from the signaling pathway of the phagocytosis, independent of Syk and Src kinases, but depends on PLC γ 2 and intact calcium signaling (121).

Until now, we could not rule out the possible auxiliary role of the PRRs in the oZ-EV production as we applied serum opsonized zymosan particles as activators.

In the present work, I show evidence that specific activation of the receptor results in the oZ-EV formation, but only if the ligands are immobilized to a surface (**Figure 18**). This observation is in agreement with previous data concerning the differential impact of soluble and immobilized forms of FH on neutrophil activation (163). It has been shown that the soluble FH does not affect the neutrophil activation, except for the migration of the cells towards the FH gradient. We found that the EVs released on C3bi, FH, and fibrinogen surfaces possessed an antibacterial effect against *S. aureus*, and also C3bi surface-induced EVs increased the IL-8 production of neutrophils, but did not cause TGF- β release (**Figure 22, Figure 23**). This finding is in good agreement with the previous observation with opsonized zymosan that also serves as a ligand-coated surface for the neutrophils. We also show that a prominent portion of cells has Mac-1 receptors in high-affinity conformation on their surface prior to initiation of EV production by Mac-1 ligands, therefore the difference between soluble and surface activation cannot be explained by this (**Figure 17**). With blocking antibodies we showed the dominance of Mac-1 over CR4 not just in EV formation, but in ROS production as well (**Figure 19**). The TIRF microscopic images indicated also a higher Mac-1 concentration on the surface of neutrophils placed on the C3bi surface which strengthens the concept of receptor clustering (**Figure 21**). More explicit evidence for the role of Mac-1 clustering in the oZ-EV biogenesis is the experiment when antibody-induced receptor accumulation resulted in an EV population that did show inhibitory potential against *S. aureus* (**Figure 22, Panel C**). Therefore, we assume that the pathogen surface covered with opsonins that are ligands of Mac-1 induces the cluster formation of Mac-1 receptors that can attract the signaling components that are involved in the generation of the oZ-EVs (**Figure 27**).

In our earlier work, we found that oZ-EV release of neutrophils is strongly dependent on the presence of extracellular Ca^{2+} (121). In the current work, I show results that the strong pharmacologically induced Ca^{2+} signal can also lead to increased EV formation from neutrophils that can even exceed the EV triggering effect of Mac-1 stimulation (**Figure 24**). It should be noted that the application of the Ca^{2+} ionophore A23187 for the initiation of vesicle release is most likely accompanied by degranulation (172).

Nonetheless, the solely ionophore-induced EVs do not possess an antibacterial property and IL-8 production enhancing effect either (**Figure 25, Figure 26**). Moreover, the combined application of opsonized zymosan and Ca^{2+} ionophore does not result in further elevation of EV release or augmentation of the biological activity of oZ-EVs (**Figure 24, Figure 25, Figure 26**).

The lack of calcium from the extracellular space had no influence on the quantity and the examined biological functions of spontaneous EVs (**Figure 24**). Interestingly, the Ca^{2+} ionophore could increase the EV production of the resting neutrophils in the absence of extracellular Ca^{2+} , presumably by mobilizing Ca^{2+} from intracellular sources. This data supports that the machinery responsible for the formation of extracellular vesicles does depend on Ca^{2+} signaling but it is independent of the source of the calcium (173-175). Taken together, we can conclude that the extracellular Ca^{2+} and intact Ca^{2+} signaling is necessary for oZ-EV production, but by itself, it is not sufficient for oZ-EV formation. In contrast to the spontaneous EV release of neutrophils, the process of oZ-EV biogenesis has a different Ca^{2+} sensitivity or needs a store-operated refill of internal Ca^{2+} sources or a long-lasting Ca^{2+} signal.

Based on all the above-mentioned observations, we have to highlight that the extracellular environment determines the characteristics of the produced EVs.

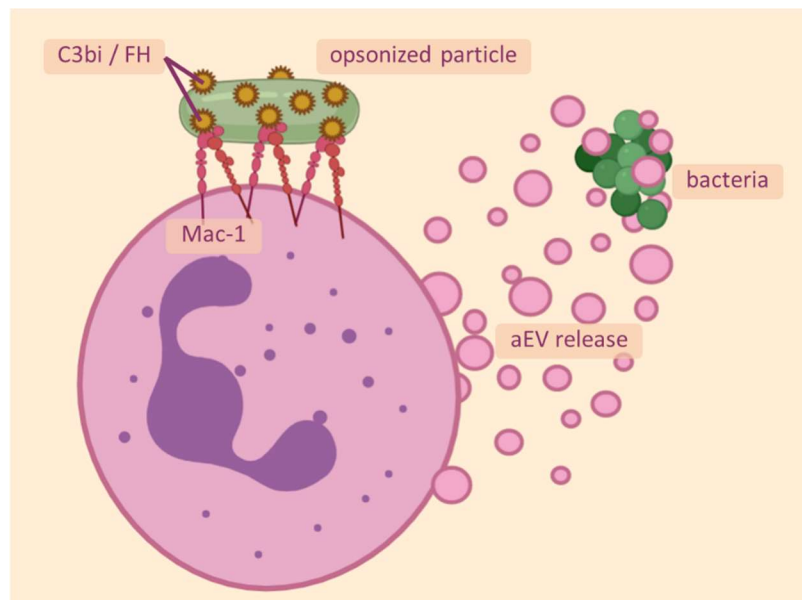


Figure 27. Neutrophilic granulocytes produce antibacterial and pro-inflammatory type extracellular vesicles upon encountering opsonized particles initiated by clustering of Mac-1 receptors

6. CONCLUSIONS

According to the objectives and based on the above-described results my conclusions are the following:

1. We developed a new, fast, reliable, and reproducible FC-based bacterial survival assessment method that is suitable for high throughput quantification of bacteriostatic or bactericidal effect of immune cells and subcellular particles.
2. The size exclusion chromatography-based isolation of neutrophils EVs revealed that the antibacterial effect of the oZ-EV preparation is associated with EVs themselves as neither soluble nor non-vesicular structures from other fractions showed the same property.
3. The selective Mac-1 activation and the clustering of the receptor are not just crucial, but sufficient in the initiation of the biogenesis of oZ-EVs that shows a completely different biological activity on other cells than spEV.
4. The CR4 activation is not sufficient for oZ-EV production from human neutrophils.
5. The spontaneously released spEVs increased the TGF- β production of resting neutrophils.
6. The Ca²⁺ signal is crucial, but not sufficient alone in the generation of oZ-EVs. The additionally applied Ca²⁺ ionophore could not potentiate the antibacterial effect of the oZ-EVs.

7. SUMMARY

The neutrophil granulocytes produce extracellular vesicles in response to several pharmacological, biological activators, and in various pathological conditions. These EVs as means of intercellular communication transmit a broad range of biological effects. Previously, our group characterized three distinct types of EVs released from neutrophils: EVs formed spontaneously (spEV), during apoptosis (apoEV), and upon activation with opsonized particles as zymosan (oZ-EV). The oZ-EVs have a pro-inflammatory effect on resting neutrophils and an antibacterial effect on bacteria and fungi.

In my Ph.D. work, I aimed to enrich the methodological arsenal in order to study the exclusive role of Mac-1 and Ca^{2+} signal in EV biogenesis under better-controlled conditions by developing a flow cytometry-based platform for the quick assessment of the antibacterial effect and by providing quality control for our EV isolation method with SEC. The FC-based bacterial survival assay correlated well with the reference OD-based method both in the case of cellular and subcellular samples. This allowed us to measure more samples in an efficient manner. We could confirm that the only intact oZ-EVs possess the antibacterial property in our samples. However, because of the lower EV yield we could not use the SEC method routinely.

On the basis of these technical developments, we proceeded to investigate the role of the Mac-1 in the oZ-EV biogenesis of neutrophils. We selectively activated the neutrophils with Mac-1 ligands (C3bi, FH) in soluble and surface-bound form. On C3bi-coated or FH-coated surface, we observed an increased EV production, and these EVs possessed antibacterial and pro-inflammatory capacity. However, in soluble conditions, neither C3bi nor FH did induce EV production. Live imaging and antibody-induced clustering experiments revealed that the clustering of Mac-1 is important in oZ-EV generation. The selective activation and clustering of Mac-1 are not just crucial, but sufficient for oZ-EV biogenesis. In contrast, we found that calcium ionophore enhanced EV release, but these EVs were ineffective in functional tests. Thus, intact Ca^{2+} signaling is crucial, but not sufficient on its own in the formation of oZ-EVs. We also demonstrated that spEVs increased the TGF- β production of resting neutrophils. We propose that the anti-inflammatory type spEV production is an inherent constitutive activity of resting neutrophils. Our observations support that neutrophils are able to change their EV production according to the environmental conditions detected by their receptors.

8. ÖSSZEFOGLALÁS

Neutrofil granulociták extracelluláris vezikulákat termelnek számos farmakológiai inger, biológiai aktiváció hatására és patológiás körülmények között is. Az EV-k az intercelluláris hírközlőként szerteágazó biológiai hatást közvetítenek. Munkacsoportunk korábban három különböző, neutrofilekből lefűződő EV populációt karakterizált: spontán termelt (spEV), apoptózis során termelt (apoEV) és opszonizált partikula, például opszonizált zimozán hatására lefűződő EV-t (oZ-EV). Az oZ-EV pro-inflammatórikus hatást gyakorol nyugvó neutrofilekre és antibakteriális hatást mutat baktérium törzseken és gombán is.

Doktori munkám során, célom volt módszertani fejlesztéseket végezni annak érdekében, hogy a Mac-1 és a Ca^{2+} jel kizárólagos szerepét vizsgálhassam jobban kontrollált körülmények között. Ennek érdekében fejlesztettünk áramlási citometria-alapú, gyors, a PMN EV-k antibakteriális hatásának meghatározására is alkalmas módszert, továbbá a korábban alkalmazott EV izolálásunknak minőségbiztosításaként SEC-kel izolált EV-eket vizsgáltunk. Az FC-alapú baktériumtúlélési esszé jó korrelációt mutatott a referencia OD-követésén alapuló módszerünkkel mind sejtes, mind szubcelluláris (EV) minták esetén. A módszer lehetővé tette, hogy hatékonyan vizsgálhassunk több, párhuzamos mintát. Igazolni tudtuk, hogy a korábban megfigyelt hatás kizárólag intakt oZ-EV mintákhoz köthető. Az alacsonyabb kinyerés miatt a SEC módszert nem használhattuk rutinszerűen.

Ezen technikai fejlesztések alapján folytattuk a Mac-1 kizárólagos szerepének vizsgálatát a neutrofilek oZ-EV termelésében. Szelektíven aktivációt Mac-1 ligandumokkal (C3bi, FH) szolubilis és felszínhez kötött formában végeztünk. C3bi és FH felszínen is emelkedett az EV termelés, ezek a vezikulák rendelkeztek a korábban megfigyelt antibakteriális és pro-inflammatórikus hatással. Azonban, szolubilis körülmények között sem a C3bi, sem a FH nem volt képes EV termelés emelésére. Mikroszkópos és antitest-indukált receptor clustering kísérleteink is arra utalnak, hogy a Mac-1 szelektív aktivációja és cluster-képzése nem csak alapvető, de önmagában elegendő is oZ-EV termeléshez. Ezzel szemben, Ca^{2+} ionofór emelte a sejtek EV termelését, de ezek az EV-k nem rendelkeztek a leírt hatásokkal. Úgy gondoljuk, hogy a Ca^{2+} jel szükséges, azonban nem elégséges oZ-EV lefűződés kiváltásához. Bemutattuk, hogy spEV-k emelték neutrofilek TGF- β termelését. Ez erősíti az elképzelésünket, hogy az anti-inflammatórikus spEV-k termelése egy permanens funkciója nyugvó neutrofileknek. Megfigyeléseink alátámasztják, hogy a neutrofilek környezetük változásaira eltérő típusú EV termeléssel reagálnak.

9. REFERENCES

1. Théry C, Witwer KW, Aikawa E, Alcaraz MJ, Anderson JD, Andriantsitohaina R, Antoniou A, Arab T, Archer F, Atkin-Smith GK, Ayre DC, Bach J-M, Bachurski D, Baharvand H, Balaj L, Baldacchino S, Bauer NN, Baxter AA, Bebawy M, Beckham C, Bedina Zavec A, Benmoussa A, Berardi AC, Bergese P, Bielska E, Blenkiron C, Bobis-Wozowicz S, Boilard E, Boireau W, Bongiovanni A, Borràs FE, Bosch S, Boulanger CM, Breakefield X, Breglio AM, Brennan MÁ, Brigstock DR, Brisson A, Broekman MLD, Bromberg JF, Bryl-Górecka P, Buch S, Buck AH, Burger D, Busatto S, Buschmann D, Bussolati B, Buzás EI, Byrd JB, Camussi G, Carter DRF, Caruso S, Chamley LW, Chang Y-T, Chen C, Chen S, Cheng L, Chin AR, Clayton A, Clerici SP, Cocks A, Cocucci E, Coffey RJ, Cordeiro-da-Silva A, Couch Y, Coumans FAW, Coyle B, Crescitelli R, Criado MF, D'Souza-Schorey C, Das S, Datta Chaudhuri A, de Candia P, De Santana EF, De Wever O, del Portillo HA, Demaret T, Deville S, Devitt A, Dhondt B, Di Vizio D, Dieterich LC, Dolo V, Dominguez Rubio AP, Dominici M, Dourado MR, Driedonks TAP, Duarte FV, Duncan HM, Eichenberger RM, Ekström K, El Andaloussi S, Elie-Caille C, Erdbrügger U, Falcón-Pérez JM, Fatima F, Fish JE, Flores-Bellver M, Försonits A, Frelet-Barrand A, Fricke F, Fuhrmann G, Gabrielsson S, Gámez-Valero A, Gardiner C, Gärtner K, Gaudin R, Gho YS, Giebel B, Gilbert C, Gimona M, Giusti I, Goberdhan DCI, Görgens A, Gorski SM, Greening DW, Gross JC, Gualerzi A, Gupta GN, Gustafson D, Handberg A, Haraszti RA, Harrison P, Hegyesi H, Hendrix A, Hill AF, Hochberg FH, Hoffmann KF, Holder B, Holthofer H, Hosseinkhani B, Hu G, Huang Y, Huber V, Hunt S, Ibrahim AG-E, Ikezu T, Inal JM, Isin M, Ivanova A, Jackson HK, Jacobsen S, Jay SM, Jayachandran M, Jenster G, Jiang L, Johnson SM, Jones JC, Jong A, Jovanovic-Talisman T, Jung S, Kalluri R, Kano S-i, Kaur S, Kawamura Y, Keller ET, Khamari D, Khomyakova E, Khvorova A, Kierulf P, Kim KP, Kislinger T, Klingeborn M, Klinké DJ, Kornek M, Kosanović MM, Kovács ÁF, Krämer-Albers E-M, Krasemann S, Krause M, Kurochkin IV, Kusuma GD, Kuypers S, Laitinen S, Langevin SM, Languino LR, Lannigan J, Lässer C, Laurent LC, Lavieu G, Lázaro-Ibáñez E, Le Lay S, Lee M-S, Lee YXF, Lemos DS, Lenassi M, Leszczynska A, Li ITS, Liao K, Libregts SF, Ligeti E, Lim R,

Lim SK, Linē A, Linnemannstōns K, Llorente A, Lombard CA, Lorenowicz MJ, Lőrincz ÁM, Lōtvall J, Lovett J, Lowry MC, Loyer X, Lu Q, Lukomska B, Lunavat TR, Maas SLN, Malhi H, Marcilla A, Mariani J, Mariscal J, Martens-Uzunova ES, Martin-Jaular L, Martinez MC, Martins VR, Mathieu M, Mathivanan S, Maugeri M, McGinnis LK, McVey MJ, Meckes DG, Meehan KL, Mertens I, Minciacchi VR, Möller A, Møller Jørgensen M, Morales-Kastresana A, Morhayim J, Mullier F, Muraca M, Musante L, Mussack V, Muth DC, Myburgh KH, Najrana T, Nawaz M, Nazarenko I, Nejsum P, Neri C, Neri T, Nieuwland R, Nimrichter L, Nolan JP, Nolte-'t Hoen ENM, Noren Hooten N, O'Driscoll L, O'Grady T, O'Loughlen A, Ochiya T, Olivier M, Ortiz A, Ortiz LA, Osteikoetxea X, Østergaard O, Ostrowski M, Park J, Pegtel DM, Peinado H, Perut F, Pfaffl MW, Phinney DG, Pieters BCH, Pink RC, Pisetsky DS, Pogge von Strandmann E, Polakovicova I, Poon IKH, Powell BH, Prada I, Pulliam L, Quesenberry P, Radeghieri A, Raffai RL, Raimondo S, Rak J, Ramirez MI, Raposo G, Rayyan MS, Regev-Rudzki N, Ricklefs FL, Robbins PD, Roberts DD, Rodrigues SC, Rohde E, Rome S, Rouschop KMA, Rughetti A, Russell AE, Saá P, Sahoo S, Salas-Huenuleo E, Sánchez C, Saugstad JA, Saul MJ, Schiffelers RM, Schneider R, Schøyen TH, Scott A, Shahaj E, Sharma S, Shatnyeva O, Shekari F, Shelke GV, Shetty AK, Shiba K, Siljander PRM, Silva AM, Skowronek A, Snyder OL, Soares RP, Sódar BW, Soekmadji C, Sotillo J, Stahl PD, Stoorvogel W, Stott SL, Strasser EF, Swift S, Tahara H, Tewari M, Timms K, Tiwari S, Tixeira R, Tkach M, Toh WS, Tomasini R, Torrecilhas AC, Tosar JP, Toxavidis V, Urbanelli L, Vader P, van Balkom BWM, van der Grein SG, Van Deun J, van Herwijnen MJC, Van Keuren-Jensen K, van Niel G, van Royen ME, van Wijnen AJ, Vasconcelos MH, Vechetti IJ, Veit TD, Vella LJ, Velot É, Verweij FJ, Vestad B, Viñas JL, Visnovitz T, Vukman KV, Wahlgren J, Watson DC, Wauben MHM, Weaver A, Webber JP, Weber V, Wehman AM, Weiss DJ, Welsh JA, Wendt S, Wheelock AM, Wiener Z, Witte L, Wolfram J, Xagorari A, Xander P, Xu J, Yan X, Yáñez-Mó M, Yin H, Yuana Y, Zappulli V, Zarubova J, Žėkas V, Zhang J-y, Zhao Z, Zheng L, Zheutlin AR, Zickler AM, Zimmermann P, Zivkovic AM, Zocco D, Zuba-Surma EK. (2018) Minimal information for studies of extracellular vesicles 2018 (MISEV2018): a position statement of the

- International Society for Extracellular Vesicles and update of the MISEV2014 guidelines. *Journal of Extracellular Vesicles*, 7: 1535750.
2. Colombo M, Raposo G, Théry C. (2014) Biogenesis, Secretion, and Intercellular Interactions of Exosomes and Other Extracellular Vesicles. *Annual Review of Cell and Developmental Biology*, 30: 255-289.
 3. van der Pol E, Böing AN, Harrison P, Sturk A, Nieuwland R. (2012) Classification, Functions, and Clinical Relevance of Extracellular Vesicles. *Pharmacological Reviews*, 64: 676-705.
 4. Yáñez-Mó M, Siljander PR, Andreu Z, Zavec AB, Borràs FE, Buzas EI, Buzas K, Casal E, Cappello F, Carvalho J, Colás E, Cordeiro-da Silva A, Fais S, Falcon-Perez JM, Ghobrial IM, Giebel B, Gimona M, Graner M, Gursel I, Gursel M, Heegaard NH, Hendrix A, Kierulf P, Kokubun K, Kosanovic M, Kralj-Iglic V, Krämer-Albers EM, Laitinen S, Lässer C, Lener T, Ligeti E, Linē A, Lipps G, Llorente A, Lötvall J, Manček-Keber M, Marcilla A, Mittelbrunn M, Nazarenko I, Nolte-'t Hoen EN, Nyman TA, O'Driscoll L, Olivan M, Oliveira C, Pállinger É, Del Portillo HA, Reventós J, Rigau M, Rohde E, Sammar M, Sánchez-Madrid F, Santarém N, Schallmoser K, Ostenfeld MS, Stoorvogel W, Stukelj R, Van der Grein SG, Vasconcelos MH, Wauben MH, De Wever O. (2015) Biological properties of extracellular vesicles and their physiological functions. *J Extracell Vesicles*, 4: 27066.
 5. Raposo G, Stoorvogel W. (2013) Extracellular vesicles: exosomes, microvesicles, and friends. *J Cell Biol*, 200: 373-383.
 6. Buzás EI, Tóth E, Sódar BW, Szabó-Taylor K. (2018) Molecular interactions at the surface of extracellular vesicles. *Semin Immunopathol*, 40: 453-464.
 7. van Niel G, D'Angelo G, Raposo G. (2018) Shedding light on the cell biology of extracellular vesicles. *Nat Rev Mol Cell Biol*, 19: 213-228.
 8. Hessvik NP, Llorente A. (2018) Current knowledge on exosome biogenesis and release. *Cell Mol Life Sci*, 75: 193-208.
 9. Kowal J, Arras G, Colombo M, Jouve M, Morath JP, Primdal-Bengtson B, Dingli F, Loew D, Tkach M, Théry C. (2016) Proteomic comparison defines novel markers to characterize heterogeneous populations of extracellular vesicle subtypes. *Proc Natl Acad Sci U S A*, 113: E968-977.

10. Trajkovic K, Hsu C, Chiantia S, Rajendran L, Wenzel D, Wieland F, Schwille P, Brügger B, Simons M. (2008) Ceramide triggers budding of exosome vesicles into multivesicular endosomes. *Science*, 319: 1244-1247.
11. Skotland T, Sandvig K, Llorente A. (2017) Lipids in exosomes: Current knowledge and the way forward. *Prog Lipid Res*, 66: 30-41.
12. Huotari J, Helenius A. (2011) Endosome maturation. *Embo j*, 30: 3481-3500.
13. Colombo M, Moita C, van Niel G, Kowal J, Vigneron J, Benaroch P, Manel N, Moita LF, Théry C, Raposo G. (2013) Analysis of ESCRT functions in exosome biogenesis, composition and secretion highlights the heterogeneity of extracellular vesicles. *J Cell Sci*, 126: 5553-5565.
14. Ståhl A-I, Johansson K, Mossberg M, Kahn R, Karpman D. (2019) Exosomes and microvesicles in normal physiology, pathophysiology, and renal diseases. *Pediatric Nephrology*, 34: 11-30.
15. Colombo M, Raposo G, Théry C. (2014) Biogenesis, secretion, and intercellular interactions of exosomes and other extracellular vesicles. *Annu Rev Cell Dev Biol*, 30: 255-289.
16. Lorincz AM, Schutte M, Timar CI, Veres DS, Kittel A, McLeish KR, Merchant ML, Ligeti E. (2015) Functionally and morphologically distinct populations of extracellular vesicles produced by human neutrophilic granulocytes. *J Leukoc Biol*, 98: 583-589.
17. Crescitelli R, Lässer C, Szabó TG, Kittel A, Eldh M, Dianzani I, Buzás EI, Lötvall J. (2013) Distinct RNA profiles in subpopulations of extracellular vesicles: apoptotic bodies, microvesicles and exosomes. *J Extracell Vesicles*, 2.
18. Van Deun J, Mestdagh P, Sormunen R, Cocquyt V, Vermaelen K, Vandesompele J, Bracke M, De Wever O, Hendrix A. (2014) The impact of disparate isolation methods for extracellular vesicles on downstream RNA profiling. *J Extracell Vesicles*, 3.
19. Nordin JZ, Lee Y, Vader P, Mäger I, Johansson HJ, Heusermann W, Wiklander OP, Hällbrink M, Seow Y, Bultema JJ, Gilthorpe J, Davies T, Fairchild PJ, Gabrielsson S, Meisner-Kober NC, Lehtiö J, Smith CI, Wood MJ, El Andaloussi S. (2015) Ultrafiltration with size-exclusion liquid chromatography for high yield

- isolation of extracellular vesicles preserving intact biophysical and functional properties. *Nanomedicine*, 11: 879-883.
20. Vergauwen G, Dhondt B, Van Deun J, De Smedt E, Berx G, Timmerman E, Gevaert K, Miinalainen I, Cocquyt V, Braems G, Van den Broecke R, Denys H, De Wever O, Hendrix A. (2017) Confounding factors of ultrafiltration and protein analysis in extracellular vesicle research. *Scientific Reports*, 7: 2704.
 21. Abramowicz A, Widlak P, Pietrowska M. (2016) Proteomic analysis of exosomal cargo: the challenge of high purity vesicle isolation. *Mol Biosyst*, 12: 1407-1419.
 22. Gámez-Valero A, Monguió-Tortajada M, Carreras-Planella L, Franquesa M, Beyer K, Borràs FE. (2016) Size-Exclusion Chromatography-based isolation minimally alters Extracellular Vesicles' characteristics compared to precipitating agents. *Sci Rep*, 6: 33641.
 23. Németh A, Orgovan N, Sódar BW, Osteikoetxea X, Pálóczi K, Szabó-Taylor K, Vukman KV, Kittel Á, Turiák L, Wiener Z, Tóth S, Drahos L, Vékey K, Horvath R, Buzás EI. (2017) Antibiotic-induced release of small extracellular vesicles (exosomes) with surface-associated DNA. *Sci Rep*, 7: 8202.
 24. Sódar BW, Kittel Á, Pálóczi K, Vukman KV, Osteikoetxea X, Szabó-Taylor K, Németh A, Sperlágh B, Baranyai T, Giricz Z, Wiener Z, Turiák L, Drahos L, Pállinger É, Vékey K, Ferdinandy P, Falus A, Buzás EI. (2016) Low-density lipoprotein mimics blood plasma-derived exosomes and microvesicles during isolation and detection. *Sci Rep*, 6: 24316.
 25. György B, Módos K, Pállinger E, Pálóczi K, Pásztói M, Misják P, Deli MA, Sipos A, Szalai A, Voszka I, Polgár A, Tóth K, Csete M, Nagy G, Gay S, Falus A, Kittel A, Buzás EI. (2011) Detection and isolation of cell-derived microparticles are compromised by protein complexes resulting from shared biophysical parameters. *Blood*, 117: e39-48.
 26. Tóth E, Turiák L, Visnovitz T, Cserép C, Mázló A, Sódar BW, Försönits AI, Petővári G, Sebestyén A, Komlósi Z, Drahos L, Kittel Á, Nagy G, Bácsi A, Dénes Á, Gho YS, Szabó-Taylor K, Buzás EI. (2021) Formation of a protein corona on the surface of extracellular vesicles in blood plasma. *J Extracell Vesicles*, 10: e12140.

27. Lorincz AM, Timar CI, Marosvari KA, Veres DS, Otrókocsi L, Kittel A, Ligeti E. (2014) Effect of storage on physical and functional properties of extracellular vesicles derived from neutrophilic granulocytes. *J Extracell Vesicles*, 3: 25465.
28. Jeyaram A, Jay SM. (2017) Preservation and Storage Stability of Extracellular Vesicles for Therapeutic Applications. *The AAPS journal*, 20: 1-1.
29. Osteikoetxea X, Sódar B, Németh A, Szabó-Taylor K, Pálóczi K, Vukman KV, Tamási V, Balogh A, Kittel Á, Pállinger É, Buzás EI. (2015) Differential detergent sensitivity of extracellular vesicle subpopulations. *Org Biomol Chem*, 13: 9775-9782.
30. Lőrincz Á M, Szeifert V, Bartos B, Ligeti E. (2018) New flow cytometry-based method for the assessment of the antibacterial effect of immune cells and subcellular particles. *J Leukoc Biol*, 103: 955-963.
31. Breed RS, Dotterer WD. (1916) The Number of Colonies Allowable on Satisfactory Agar Plates. *J Bacteriol*, 1: 321-331.
32. Hamers MN, Bot AA, Weening RS, Sips HJ, Roos D. (1984) Kinetics and mechanism of the bactericidal action of human neutrophils against *Escherichia coli*. *Blood*, 64: 635-641.
33. Atosuo JT, Lilius EM. (2011) The real-time-based assessment of the microbial killing by the antimicrobial compounds of neutrophils. *ScientificWorldJournal*, 11: 2382-2390.
34. Atosuo J, Lehtinen J, Vojtek L, Lilius EM. (2013) *Escherichia coli* K-12 (pEGFP_{lux}ABCDEamp): a tool for analysis of bacterial killing by antibacterial agents and human complement activities on a real-time basis. *Luminescence*, 28: 771-779.
35. Aellen S, Que YA, Guignard B, Haenni M, Moreillon P. (2006) Detection of live and antibiotic-killed bacteria by quantitative real-time PCR of specific fragments of rRNA. *Antimicrob Agents Chemother*, 50: 1913-1920.
36. Nocker A, Cheung CY, Camper AK. (2006) Comparison of propidium monoazide with ethidium monoazide for differentiation of live vs. dead bacteria by selective removal of DNA from dead cells. *J Microbiol Methods*, 67: 310-320.

37. Schwartz J, Leidal KG, Femling JK, Weiss JP, Nauseef WM. (2009) Neutrophil bleaching of GFP-expressing staphylococci: probing the intraphagosomal fate of individual bacteria. *J Immunol*, 183: 2632-2641.
38. Pang YY, Schwartz J, Thoendel M, Ackermann LW, Horswill AR, Nauseef WM. (2010) agr-Dependent interactions of *Staphylococcus aureus* USA300 with human polymorphonuclear neutrophils. *J Innate Immun*, 2: 546-559.
39. Rada BK, Geiszt M, Káldi K, Timár C, Ligeti E. (2004) Dual role of phagocytic NADPH oxidase in bacterial killing. *Blood*, 104: 2947-2953.
40. Wimmer JL, Long SW, Cernoch P, Land GA, Davis JR, Musser JM, Olsen RJ. (2012) Strategy for rapid identification and antibiotic susceptibility testing of gram-negative bacteria directly recovered from positive blood cultures using the Bruker MALDI Biotyper and the BD Phoenix system. *J Clin Microbiol*, 50: 2452-2454.
41. Kostrzewa M, Sparbier K, Maier T, Schubert S. (2013) MALDI-TOF MS: an upcoming tool for rapid detection of antibiotic resistance in microorganisms. *Proteomics Clin Appl*, 7: 767-778.
42. Comas J, Vives-Rego J. (1997) Assessment of the effects of gramicidin, formaldehyde, and surfactants on *Escherichia coli* by flow cytometry using nucleic acid and membrane potential dyes. *Cytometry*, 29: 58-64.
43. Diaper JP, Tither K, Edwards C. (1992) Rapid assessment of bacterial viability by flow cytometry. *Appl Microbiol Biotechnol*, 38: 268-272.
44. Mason DJ, Gant VA. (1995) The application of flow cytometry to the estimation of bacterial antibiotic susceptibility. *J Antimicrob Chemother*, 36: 441-443.
45. Takahashi A, Okada R, Nagao K, Kawamata Y, Hanyu A, Yoshimoto S, Takasugi M, Watanabe S, Kanemaki MT, Obuse C, Hara E. (2017) Exosomes maintain cellular homeostasis by excreting harmful DNA from cells. *Nature Communications*, 8: 15287.
46. van der Pol E, Böing AN, Harrison P, Sturk A, Nieuwland R. (2012) Classification, functions, and clinical relevance of extracellular vesicles. *Pharmacol Rev*, 64: 676-705.

47. Kolonics F, Szeifert V, Timar CI, Ligeti E, Lorincz AM. (2020) The Functional Heterogeneity of Neutrophil-Derived Extracellular Vesicles Reflects the Status of the Parent Cell. *Cells*, 9.
48. Raposo G, Nijman HW, Stoorvogel W, Liejendekker R, Harding CV, Melief CJ, Geuze HJ. (1996) B lymphocytes secrete antigen-presenting vesicles. *J Exp Med*, 183: 1161-1172.
49. Théry C, Ostrowski M, Segura E. (2009) Membrane vesicles as conveyors of immune responses. *Nature Reviews Immunology*, 9: 581-593.
50. Valadi H, Ekström K, Bossios A, Sjöstrand M, Lee JJ, Lötvall JO. (2007) Exosome-mediated transfer of mRNAs and microRNAs is a novel mechanism of genetic exchange between cells. *Nature Cell Biology*, 9: 654-659.
51. Yáñez-Mó M, Siljander PRM, Andreu Z, Zavec AB, Borràs FE, Buzas EI, Buzas K, Casal E, Cappello F, Carvalho J, Colás E, Cordeiro-da Silva A, Fais S, Falcon-Perez JM, Ghobrial IM, Giebel B, Gimona M, Graner M, Gursel I, Gursel M, Heegaard NHH, Hendrix A, Kierulf P, Kokubun K, Kosanovic M, Kralj-Iglic V, Krämer-Albers E-M, Laitinen S, Lässer C, Lener T, Ligeti E, Linē A, Lipps G, Llorente A, Lötvall J, Manček-Keber M, Marcilla A, Mittelbrunn M, Nazarenko I, Nolte-'t Hoen ENM, Nyman TA, O'Driscoll L, Olivan M, Oliveira C, Pállinger É, Del Portillo HA, Reventós J, Rigau M, Rohde E, Sammar M, Sánchez-Madrid F, Santarém N, Schallmoser K, Ostenfeld MS, Stoorvogel W, Stukelj R, Van der Grein SG, Vasconcelos MH, Wauben MHM, De Wever O. (2015) Biological properties of extracellular vesicles and their physiological functions. *Journal of extracellular vesicles*, 4: 27066-27066.
52. Fais S. (2013) NK cell-released exosomes: Natural nanobullets against tumors. *Oncoimmunology*, 2: e22337.
53. Lugini L, Cecchetti S, Huber V, Luciani F, Macchia G, Spadaro F, Paris L, Abalsamo L, Colone M, Molinari A, Podo F, Rivoltini L, Ramoni C, Fais S. (2012) Immune surveillance properties of human NK cell-derived exosomes. *J Immunol*, 189: 2833-2842.
54. Bardelli C, Amoruso A, Federici Canova D, Fresu L, Balbo P, Neri T, Celi A, Brunelleschi S. (2012) Autocrine activation of human monocyte/macrophages by

- monocyte-derived microparticles and modulation by PPAR γ ligands. *Br J Pharmacol*, 165: 716-728.
55. Eyre J, Burton JO, Saleem MA, Mathieson PW, Topham PS, Brunskill NJ. (2011) Monocyte- and endothelial-derived microparticles induce an inflammatory phenotype in human podocytes. *Nephron Exp Nephrol*, 119: e58-66.
 56. Cerri C, Chimenti D, Conti I, Neri T, Paggiaro P, Celi A. (2006) Monocyte/macrophage-derived microparticles up-regulate inflammatory mediator synthesis by human airway epithelial cells. *J Immunol*, 177: 1975-1980.
 57. Skokos D, Botros HG, Demeure C, Morin J, Peronet R, Birkenmeier G, Boudaly S, Mécheri S. (2003) Mast cell-derived exosomes induce phenotypic and functional maturation of dendritic cells and elicit specific immune responses in vivo. *J Immunol*, 170: 3037-3045.
 58. Cañas JA, Sastre B, Mazzeo C, Fernández-Nieto M, Rodrigo-Muñoz JM, González-Guerra A, Izquierdo M, Barranco P, Quirce S, Sastre J, Del Pozo V. (2017) Exosomes from eosinophils autoregulate and promote eosinophil functions. *J Leukoc Biol*, 101: 1191-1199.
 59. Laughlin RC, Mickum M, Rowin K, Adams LG, Alaniz RC. (2015) Altered host immune responses to membrane vesicles from *Salmonella* and Gram-negative pathogens. *Vaccine*, 33: 5012-5019.
 60. Ismail S, Hampton MB, Keenan JJ. (2003) *Helicobacter pylori* outer membrane vesicles modulate proliferation and interleukin-8 production by gastric epithelial cells. *Infection and immunity*, 71: 5670-5675.
 61. Hong SW, Kim MR, Lee EY, Kim JH, Kim YS, Jeon SG, Yang JM, Lee BJ, Pyun BY, Gho YS, Kim YK. (2011) Extracellular vesicles derived from *Staphylococcus aureus* induce atopic dermatitis-like skin inflammation. *Allergy*, 66: 351-359.
 62. Mashburn-Warren LM, Whiteley M. (2006) Special delivery: vesicle trafficking in prokaryotes. *Mol Microbiol*, 61: 839-846.
 63. Kerris EWJ, Hoptay C, Calderon T, Freishtat RJ. (2020) Platelets and platelet extracellular vesicles in hemostasis and sepsis. *J Investig Med*, 68: 813-820.
 64. Karasu E, Eisenhardt SU, Harant J, Huber-Lang M. (2018) Extracellular Vesicles: Packages Sent With Complement. *Front Immunol*, 9: 721.

65. Owens AP, 3rd, Mackman N. (2011) Microparticles in hemostasis and thrombosis. *Circ Res*, 108: 1284-1297.
66. Van Der Meijden PE, Van Schilfgaarde M, Van Oerle R, Renné T, ten Cate H, Spronk HM. (2012) Platelet- and erythrocyte-derived microparticles trigger thrombin generation via factor XIIa. *J Thromb Haemost*, 10: 1355-1362.
67. Zecher D, Cumpelik A, Schifferli JA. (2014) Erythrocyte-derived microvesicles amplify systemic inflammation by thrombin-dependent activation of complement. *Arterioscler Thromb Vasc Biol*, 34: 313-320.
68. Koshiar RL, Somajo S, Norström E, Dahlbäck B. (2014) Erythrocyte-derived microparticles supporting activated protein C-mediated regulation of blood coagulation. *PLoS One*, 9: e104200.
69. Somajo S, Koshiar RL, Norström E, Dahlbäck B. (2014) Protein S and factor V in regulation of coagulation on platelet microparticles by activated protein C. *Thromb Res*, 134: 144-152.
70. Clayton A, Harris CL, Court J, Mason MD, Morgan BP. (2003) Antigen-presenting cell exosomes are protected from complement-mediated lysis by expression of CD55 and CD59. *Eur J Immunol*, 33: 522-531.
71. Sadallah S, Eken C, Schifferli JA. (2008) Erythrocyte-derived ectosomes have immunosuppressive properties. *J Leukoc Biol*, 84: 1316-1325.
72. Gasser O, Schifferli JA. (2005) Microparticles released by human neutrophils adhere to erythrocytes in the presence of complement. *Exp Cell Res*, 307: 381-387.
73. Iida K, Whitlow MB, Nussenzweig V. (1991) Membrane vesiculation protects erythrocytes from destruction by complement. *J Immunol*, 147: 2638-2642.
74. Ståhl AL, Sartz L, Karpman D. (2011) Complement activation on platelet-leukocyte complexes and microparticles in enterohemorrhagic *Escherichia coli*-induced hemolytic uremic syndrome. *Blood*, 117: 5503-5513.
75. Nielsen CT, Østergaard O, Stener L, Iversen LV, Truedsson L, Gullstrand B, Jacobsen S, Heegaard NH. (2012) Increased IgG on cell-derived plasma microparticles in systemic lupus erythematosus is associated with autoantibodies and complement activation. *Arthritis Rheum*, 64: 1227-1236.

76. van Eijk IC, Tushuizen ME, Sturk A, Dijkmans BA, Boers M, Voskuyl AE, Diamant M, Wolbink GJ, Nieuwland R, Nurmohamed MT. (2010) Circulating microparticles remain associated with complement activation despite intensive anti-inflammatory therapy in early rheumatoid arthritis. *Ann Rheum Dis*, 69: 1378-1382.
77. Biró E, Nieuwland R, Tak PP, Pronk LM, Schaap MC, Sturk A, Hack CE. (2007) Activated complement components and complement activator molecules on the surface of cell-derived microparticles in patients with rheumatoid arthritis and healthy individuals. *Ann Rheum Dis*, 66: 1085-1092.
78. Mócsai A. (2013) Diverse novel functions of neutrophils in immunity, inflammation, and beyond. *J Exp Med*, 210: 1283-1299.
79. Németh T, Mócsai A. (2012) The role of neutrophils in autoimmune diseases. *Immunol Lett*, 143: 9-19.
80. Granot Z. (2019) Neutrophils as a Therapeutic Target in Cancer. *Front Immunol*, 10: 1710.
81. Hidalgo A, Chilvers ER, Summers C, Koenderman L. (2019) The Neutrophil Life Cycle. *Trends in Immunology*, 40: 584-597.
82. Ella K, Csépanyi-Kömi R, Káldi K. (2016) Circadian regulation of human peripheral neutrophils. *Brain Behav Immun*, 57: 209-221.
83. Lawrence SM, Corriden R, Nizet V. (2018) The Ontogeny of a Neutrophil: Mechanisms of Granulopoiesis and Homeostasis. *Microbiology and Molecular Biology Reviews*, 82: e00057-00017.
84. Granfeldt D, Harbecke O, Björstad A, Karlsson A, Dahlgren C. (2006) Neutrophil secretion induced by an intracellular Ca²⁺ rise and followed by whole-cell patch-clamp recordings occurs without any selective mobilization of different granule populations. *J Biomed Biotechnol*, 2006: 97803.
85. Lew PD, Monod A, Waldvogel FA, Dewald B, Baggiolini M, Pozzan T. (1986) Quantitative analysis of the cytosolic free calcium dependency of exocytosis from three subcellular compartments in intact human neutrophils. *J Cell Biol*, 102: 2197-2204.
86. Nordenfelt P, Tapper H. (2010) The role of calcium in neutrophil granule-phagosome fusion. *Commun Integr Biol*, 3: 224-226.

87. Pham CT. (2008) Neutrophil serine proteases fine-tune the inflammatory response. *Int J Biochem Cell Biol*, 40: 1317-1333.
88. Faurschou M, Borregaard N. (2003) Neutrophil granules and secretory vesicles in inflammation. *Microbes Infect*, 5: 1317-1327.
89. Ley K, Laudanna C, Cybulsky MI, Nourshargh S. (2007) Getting to the site of inflammation: the leukocyte adhesion cascade updated. *Nature Reviews Immunology*, 7: 678-689.
90. Schnoor M, Vadillo E, Guerrero-Fonseca IM. (2021) The extravasation cascade revisited from a neutrophil perspective. *Current Opinion in Physiology*, 19: 119-128.
91. Futosi K, Fodor S, Mócsai A. (2013) Neutrophil cell surface receptors and their intracellular signal transduction pathways. *International Immunopharmacology*, 17: 638-650.
92. Belaouaj A, McCarthy R, Baumann M, Gao Z, Ley TJ, Abraham SN, Shapiro SD. (1998) Mice lacking neutrophil elastase reveal impaired host defense against gram negative bacterial sepsis. *Nature Medicine*, 4: 615-618.
93. Reeves EP, Lu H, Jacobs HL, Messina CGM, Bolsover S, Gabella G, Potma EO, Warley A, Roes J, Segal AW. (2002) Killing activity of neutrophils is mediated through activation of proteases by K⁺ flux. *Nature*, 416: 291-297.
94. Rada B, Leto TL. (2008) Oxidative innate immune defenses by Nox/Duox family NADPH oxidases. *Contributions to microbiology*, 15: 164-187.
95. Nathan C, Cunningham-Bussel A. (2013) Beyond oxidative stress: an immunologist's guide to reactive oxygen species. *Nature Reviews Immunology*, 13: 349-361.
96. Rada B, Hably C, Meczner A, Timár C, Lakatos G, Enyedi P, Ligeti E. (2008) Role of Nox2 in elimination of microorganisms. *Semin Immunopathol*, 30: 237-253.
97. Gray MJ, Wholey WY, Jakob U. (2013) Bacterial responses to reactive chlorine species. *Annu Rev Microbiol*, 67: 141-160.
98. Cassatella MA. (1995) The production of cytokines by polymorphonuclear neutrophils. *Immunology Today*, 16: 21-26.

99. Tamassia N, Bianchetto-Aguilera F, Arruda-Silva F, Gardiman E, Gasperini S, Calzetti F, Cassatella MA. (2018) Cytokine production by human neutrophils: Revisiting the "dark side of the moon". *Eur J Clin Invest*, 48 Suppl 2: e12952.
100. Tecchio C, Micheletti A, Cassatella MA. (2014) Neutrophil-derived cytokines: facts beyond expression. *Front Immunol*, 5: 508.
101. Scapini P, Lapinet-Vera JA, Gasperini S, Calzetti F, Bazzoni F, Cassatella MA. (2000) The neutrophil as a cellular source of chemokines. *Immunol Rev*, 177: 195-203.
102. Chen F, Yang W, Huang X, Cao AT, Bilotta AJ, Xiao Y, Sun M, Chen L, Ma C, Liu X, Liu CG, Yao S, Dann SM, Liu Z, Cong Y. (2018) Neutrophils Promote Amphiregulin Production in Intestinal Epithelial Cells through TGF- β and Contribute to Intestinal Homeostasis. *J Immunol*, 201: 2492-2501.
103. Haddad A, Gaudet M, Plesa M, Allakhverdi Z, Mogas AK, Audusseau S, Baglote CJ, Eidelman DH, Olivenstein R, Ludwig MS, Hamid Q. (2019) Neutrophils from severe asthmatic patients induce epithelial to mesenchymal transition in healthy bronchial epithelial cells. *Respiratory Research*, 20: 234.
104. Brinkmann V, Reichard U, Goosmann C, Fauler B, Uhlemann Y, Weiss DS, Weinrauch Y, Zychlinsky A. (2004) Neutrophil Extracellular Traps Kill Bacteria. *Science*, 303: 1532-1535.
105. Papayannopoulos V. (2018) Neutrophil extracellular traps in immunity and disease. *Nature Reviews Immunology*, 18: 134-147.
106. Fuchs TA, Abed U, Goosmann C, Hurwitz R, Schulze I, Wahn V, Weinrauch Y, Brinkmann V, Zychlinsky A. (2007) Novel cell death program leads to neutrophil extracellular traps. *J Cell Biol*, 176: 231-241.
107. Yipp BG, Kubes P. (2013) NETosis: how vital is it? *Blood*, 122: 2784-2794.
108. Pérez-Figueroa E, Álvarez-Carrasco P, Ortega E, Maldonado-Bernal C. (2021) Neutrophils: Many Ways to Die. *Frontiers in Immunology*, 12.
109. Arnaout MA. (1990) Leukocyte adhesion molecules deficiency: its structural basis, pathophysiology and implications for modulating the inflammatory response. *Immunol Rev*, 114: 145-180.
110. Plow EF, Zhang L. (1997) A MAC-1 attack: integrin functions directly challenged in knockout mice. *J Clin Invest*, 99: 1145-1146.

111. Bouti P, Webbers SDS, Fagerholm SC, Alon R, Moser M, Matlung HL, Kuijpers TW. (2021) β 2 Integrin Signaling Cascade in Neutrophils: More Than a Single Function. *Frontiers in Immunology*, 11.
112. Preedy VR. *Adhesion Molecules*, doi:10.1201/b10167. CRC Press, Boca Raton, 2010: 5-10.
113. Futosi K, Fodor S, Mócsai A. (2013) Neutrophil cell surface receptors and their intracellular signal transduction pathways. *Int Immunopharmacol*, 17: 638-650.
114. Simon DI. (2011) Opening the field of integrin biology to "biased agonism". *Circ Res*, 109: 1199-1201.
115. Ustinov VA, Plow EF. (2002) Delineation of the key amino acids involved in neutrophil inhibitory factor binding to the I-domain supports a mosaic model for the capacity of integrin α M β 2 to recognize multiple ligands. *J Biol Chem*, 277: 18769-18776.
116. Mócsai A, Ruland J, Tybulewicz VL. (2010) The SYK tyrosine kinase: a crucial player in diverse biological functions. *Nat Rev Immunol*, 10: 387-402.
117. Moser M, Legate KR, Zent R, Fässler R. (2009) The tail of integrins, talin, and kindlins. *Science*, 324: 895-899.
118. Stein JM, Luzio JP. (1991) Ectocytosis caused by sublytic autologous complement attack on human neutrophils. The sorting of endogenous plasma-membrane proteins and lipids into shed vesicles. *Biochem J*, 274 (Pt 2): 381-386.
119. Timar CI, Lorincz AM, Csepanyi-Komi R, Valyi-Nagy A, Nagy G, Buzas EI, Ivanyi Z, Kittel A, Powell DW, McLeish KR, Ligeti E. (2013) Antibacterial effect of microvesicles released from human neutrophilic granulocytes. *Blood*, 121: 510-518.
120. Lorincz AM, Bartos B, Szombath D, Szeifert V, Timar CI, Turiak L, Drahos L, Kittel A, Veres DS, Kolonics F, Mocsai A, Ligeti E. (2020) Role of Mac-1 integrin in generation of extracellular vesicles with antibacterial capacity from neutrophilic granulocytes. *J Extracell Vesicles*, 9: 1698889.
121. Lorincz AM, Szeifert V, Bartos B, Szombath D, Mocsai A, Ligeti E. (2019) Different Calcium and Src Family Kinase Signaling in Mac-1 Dependent Phagocytosis and Extracellular Vesicle Generation. *Front Immunol*, 10: 2942.

122. Shopova IA, Belyaev I, Dasari P, Jahreis S, Stroe MC, Cseresnyes Z, Zimmermann AK, Medyukhina A, Svensson CM, Kruger T, Szeifert V, Nietzsche S, Conrad T, Blango MG, Kniemeyer O, von Lilienfeld-Toal M, Zipfel PF, Ligeti E, Figge MT, Brakhage AA. (2020) Human Neutrophils Produce Antifungal Extracellular Vesicles against *Aspergillus fumigatus*. *mBio*, 11.
123. Genschmer KR, Russell DW, Lal C, Szul T, Bratcher PE, Noerager BD, Abdul Roda M, Xu X, Rezonzew G, Viera L, Dobosh BS, Margaroli C, Abdalla TH, King RW, McNicholas CM, Wells JM, Dransfield MT, Tirouvanziam R, Gaggari A, Blalock JE. (2019) Activated PMN Exosomes: Pathogenic Entities Causing Matrix Destruction and Disease in the Lung. *Cell*, 176: 113-126.e115.
124. Gasser O, Hess C, Miot S, Deon C, Sanchez JC, Schifferli JA. (2003) Characterisation and properties of ectosomes released by human polymorphonuclear neutrophils. *Exp Cell Res*, 285: 243-257.
125. Dalli J, Montero-Melendez T, Norling LV, Yin X, Hinds C, Haskard D, Mayr M, Perretti M. (2013) Heterogeneity in neutrophil microparticles reveals distinct proteome and functional properties. *Mol Cell Proteomics*, 12: 2205-2219.
126. Kolonics F, Kajdacs E, Farkas VJ, Veres DS, Khamari D, Kittel A, Merchant ML, McLeish KR, Lorincz AM, Ligeti E. (2021) Neutrophils produce proinflammatory or anti-inflammatory extracellular vesicles depending on the environmental conditions. *J Leukoc Biol*, 109: 793-806.
127. Turbica I, Gallais Y, Gueguen C, Tharinger H, Al Sabbagh C, Gorges R, Gary-Gouy H, Kerdine-Römer S, Pallardy M, Mascarell L, Gleizes A, Chollet-Martin S. (2015) Ectosomes from neutrophil-like cells down-regulate nickel-induced dendritic cell maturation and promote Th2 polarization. *J Leukoc Biol*, 97: 737-749.
128. Pitanga TN, de Aragão França L, Rocha VC, Meirelles T, Borges VM, Gonçalves MS, Pontes-de-Carvalho LC, Noronha-Dutra AA, dos-Santos WL. (2014) Neutrophil-derived microparticles induce myeloperoxidase-mediated damage of vascular endothelial cells. *BMC Cell Biol*, 15: 21.
129. Hong Y, Eleftheriou D, Hussain AAK, Price-Kuehne FE, Savage CO, Jayne D, Little MA, Salama AD, Klein NJ, Brogan PA. (2012) Anti-neutrophil cytoplasmic

- antibodies stimulate release of neutrophil microparticles. *Journal of the American Society of Nephrology : JASN*, 23: 49-62.
130. Rhys HI, Dell'Accio F, Pitzalis C, Moore A, Norling LV, Perretti M. (2018) Neutrophil Microvesicles from Healthy Control and Rheumatoid Arthritis Patients Prevent the Inflammatory Activation of Macrophages. *EBioMedicine*, 29: 60-69.
 131. Gasser O, Schifferli JA. (2004) Activated polymorphonuclear neutrophils disseminate anti-inflammatory microparticles by ectocytosis. *Blood*, 104: 2543-2548.
 132. Karasu E, Demmelmaier J, Kellermann S, Holzmann K, Köhl J, Schmidt CQ, Kalbitz M, Gebhard F, Huber-Lang MS, Halbgebauer R. (2020) Complement C5a Induces Pro-inflammatory Microvesicle Shedding in Severely Injured Patients. *Front Immunol*, 11: 1789.
 133. Eken C, Gasser O, Zenhausern G, Oehri I, Hess C, Schifferli JA. (2008) Polymorphonuclear neutrophil-derived ectosomes interfere with the maturation of monocyte-derived dendritic cells. *J Immunol*, 180: 817-824.
 134. Eken C, Martin PJ, Sadallah S, Treves S, Schaller M, Schifferli JA. (2010) Ectosomes released by polymorphonuclear neutrophils induce a MerTK-dependent anti-inflammatory pathway in macrophages. *J Biol Chem*, 285: 39914-39921.
 135. Cumpelik A, Ankli B, Zecher D, Schifferli JA. (2016) Neutrophil microvesicles resolve gout by inhibiting C5a-mediated priming of the inflammasome. *Ann Rheum Dis*, 75: 1236-1245.
 136. Pliyev BK, Kalintseva MV, Abdulaeva SV, Yarygin KN, Savchenko VG. (2014) Neutrophil microparticles modulate cytokine production by natural killer cells. *Cytokine*, 65: 126-129.
 137. Dalli J, Norling LV, Renshaw D, Cooper D, Leung KY, Perretti M. (2008) Annexin 1 mediates the rapid anti-inflammatory effects of neutrophil-derived microparticles. *Blood*, 112: 2512-2519.
 138. Mesri M, Altieri DC. (1999) Leukocyte microparticles stimulate endothelial cell cytokine release and tissue factor induction in a JNK1 signaling pathway. *J Biol Chem*, 274: 23111-23118.

139. Mesri M, Altieri DC. (1998) Endothelial cell activation by leukocyte microparticles. *J Immunol*, 161: 4382-4387.
140. Ajikumar A, Long MB, Heath PR, Wharton SB, Ince PG, Ridger VC, Simpson JE. (2019) Neutrophil-Derived Microvesicle Induced Dysfunction of Brain Microvascular Endothelial Cells In Vitro. *International journal of molecular sciences*, 20: 5227.
141. Lim K, Sumagin R, Hyun Y-M. (2013) Extravasating Neutrophil-derived Microparticles Preserve Vascular Barrier Function in Inflamed Tissue. *Immune network*, 13: 102-106.
142. Vargas A, Roux-Dalvai F, Droit A, Lavoie JP. (2016) Neutrophil-Derived Exosomes: A New Mechanism Contributing to Airway Smooth Muscle Remodeling. *Am J Respir Cell Mol Biol*, 55: 450-461.
143. El Habhab A, Altamimy R, Abbas M, Kassem M, Amoura L, Qureshi AW, El Itawi H, Kreutter G, Khemais-Benkhiat S, Zobairi F, Schini-Kerth VB, Kessler L, Toti F. (2020) Significance of neutrophil microparticles in ischaemia-reperfusion: Pro-inflammatory effectors of endothelial senescence and vascular dysfunction. *J Cell Mol Med*, 24: 7266-7281.
144. Moraes JA, Frony AC, Barcellos-de-Souza P, Menezes da Cunha M, Brasil Barbosa Calcia T, Benjamim CF, Boisson-Vidal C, Barja-Fidalgo C. (2019) Downregulation of Microparticle Release and Pro-Inflammatory Properties of Activated Human Polymorphonuclear Neutrophils by LMW Fucoidan. *Journal of Innate Immunity*, 11: 330-346.
145. Herrmann IK, Bertazzo S, O'Callaghan DJP, Schlegel AA, Kallepitis C, Antcliffe DB, Gordon AC, Stevens MM. (2015) Differentiating sepsis from non-infectious systemic inflammation based on microvesicle-bacteria aggregation. *Nanoscale*, 7: 13511-13520.
146. Allen ER, Lempke SL, Miller MM, Bush DM, Braswell BG, Estes CL, Benedict EL, Mahon AR, Sabo SL, Greenlee-Wacker MC. (2020) Effect of extracellular vesicles from *S. aureus*-challenged human neutrophils on macrophages. *J Leukoc Biol*, 108: 1841-1850.
147. Alvarez-Jiménez VD, Leyva-Paredes K, García-Martínez M, Vázquez-Flores L, García-Paredes VG, Campillo-Navarro M, Romo-Cruz I, Rosales-García VH,

- Castañeda-Casimiro J, González-Pozos S, Hernández JM, Wong-Baeza C, García-Pérez BE, Ortiz-Navarrete V, Estrada-Parra S, Serafín-López J, Wong-Baeza I, Chacón-Salinas R, Estrada-García I. (2018) Extracellular Vesicles Released from *Mycobacterium tuberculosis*-Infected Neutrophils Promote Macrophage Autophagy and Decrease Intracellular Mycobacterial Survival. *Frontiers in immunology*, 9: 272-272.
148. Duarte TA, Noronha-Dutra AA, Nery JS, Ribeiro SB, Pitanga TN, Lapa ESJR, Arruda S, Boéchat N. (2012) *Mycobacterium tuberculosis*-induced neutrophil ectosomes decrease macrophage activation. *Tuberculosis (Edinb)*, 92: 218-225.
149. Salei N, Hellberg L, Köhl J, Laskay T. (2017) Enhanced survival of *Leishmania major* in neutrophil granulocytes in the presence of apoptotic cells. *PLoS One*, 12: e0171850.
150. Ren Y, Xie Y, Jiang G, Fan J, Yeung J, Li W, Tam PK, Savill J. (2008) Apoptotic cells protect mice against lipopolysaccharide-induced shock. *J Immunol*, 180: 4978-4985.
151. Shen G, Krienke S, Schiller P, Nießen A, Neu S, Eckstein V, Schiller M, Lorenz HM, Tykocinski LO. (2017) Microvesicles released by apoptotic human neutrophils suppress proliferation and IL-2/IL-2 receptor expression of resting T helper cells. *Eur J Immunol*, 47: 900-910.
152. Szeifert V, Kolonics F, Bartos B, Khamari D, Vagi P, Barna L, Ligeti E, Lorincz AM. (2021) Mac-1 Receptor Clustering Initiates Production of Pro-Inflammatory, Antibacterial Extracellular Vesicles From Neutrophils. *Front Immunol*, 12: 671995.
153. Monguió-Tortajada M, Morón-Font M, Gámez-Valero A, Carreras-Planella L, Borràs FE, Franquesa M. (2019) Extracellular-Vesicle Isolation from Different Biological Fluids by Size-Exclusion Chromatography. *Curr Protoc Stem Cell Biol*, 49: e82.
154. Kerstens M, Boulet G, Van Kerckhoven M, Clais S, Lanckacker E, Delputte P, Maes L, Cos P. (2015) A flow cytometric approach to quantify biofilms. *Folia Microbiol (Praha)*, 60: 335-342.
155. Schneider CA, Rasband WS, Eliceiri KW. (2012) NIH Image to ImageJ: 25 years of image analysis. *Nature Methods*, 9: 671-675.

156. Böing AN, van der Pol E, Grootemaat AE, Coumans FA, Sturk A, Nieuwland R. (2014) Single-step isolation of extracellular vesicles by size-exclusion chromatography. *J Extracell Vesicles*, 3.
157. Hakkim A, Fürnrohr BG, Amann K, Laube B, Abed UA, Brinkmann V, Herrmann M, Voll RE, Zychlinsky A. (2010) Impairment of neutrophil extracellular trap degradation is associated with lupus nephritis. *Proc Natl Acad Sci U S A*, 107: 9813-9818.
158. Agarwal S, Loder SJ, Cholok D, Li J, Bian G, Yalavarthi S, Li S, Carson WF, Hwang C, Marini S, Pagani C, Edwards N, Delano MJ, Standiford TJ, Knight JS, Kunkel SL, Mishina Y, Ward PA, Levi B. (2019) Disruption of Neutrophil Extracellular Traps (NETs) Links Mechanical Strain to Post-traumatic Inflammation. *Frontiers in Immunology*, 10.
159. Bilsland CA, Diamond MS, Springer TA. (1994) The leukocyte integrin p150,95 (CD11c/CD18) as a receptor for iC3b. Activation by a heterologous beta subunit and localization of a ligand recognition site to the I domain. *J Immunol*, 152: 4582-4589.
160. Micklem KJ, Sim RB. (1985) Isolation of complement-fragment-iC3b-binding proteins by affinity chromatography. The identification of p150,95 as an iC3b-binding protein. *Biochem J*, 231: 233-236.
161. Losse J, Zipfel PF, Józsi M. (2010) Factor H and factor H-related protein 1 bind to human neutrophils via complement receptor 3, mediate attachment to *Candida albicans*, and enhance neutrophil antimicrobial activity. *J Immunol*, 184: 912-921.
162. DiScipio RG, Daffern PJ, Schraufstatter IU, Sriramarao P. (1998) Human polymorphonuclear leukocytes adhere to complement factor H through an interaction that involves alphaMbeta2 (CD11b/CD18). *J Immunol*, 160: 4057-4066.
163. Schneider AE, Sándor N, Kárpáti É, Józsi M. (2016) Complement factor H modulates the activation of human neutrophil granulocytes and the generation of neutrophil extracellular traps. *Molecular Immunology*, 72: 37-48.
164. Svoboda E, Schneider AE, Sándor N, Lermann U, Staib P, Kremlitzka M, Bajtay Z, Barz D, Erdei A, Józsi M. (2015) Secreted aspartic protease 2 of *Candida*

- albicans inactivates factor H and the macrophage factor H-receptors CR3 (CD11b/CD18) and CR4 (CD11c/CD18). *Immunol Lett*, 168: 13-21.
165. Erdei A, Lukácsi S, Mácsik-Valent B, Nagy-Baló Z, Kurucz I, Bajtay Z. (2019) Non-identical twins: Different faces of CR3 and CR4 in myeloid and lymphoid cells of mice and men. *Semin Cell Dev Biol*, 85: 110-121.
166. Bajtay Z. (2021) *Biologia Futura*: stories about the functions of $\beta(2)$ -integrins in human phagocytes. *Biol Futur*, 72: 7-13.
167. Aatonen MT, Ohman T, Nyman TA, Laitinen S, Grönholm M, Siljander PR. (2014) Isolation and characterization of platelet-derived extracellular vesicles. *J Extracell Vesicles*, 3.
168. Kállai A, Kelemen M, Molnár N, Tropotei A, Hauser B, Iványi Z, Gál J, Ligeti E, Kristóf K, Lőrincz ÁM, Asempa TE. (2021) MICy: a Novel Flow Cytometric Method for Rapid Determination of Minimal Inhibitory Concentration. *Microbiology Spectrum*, 9: e00901-00921.
169. Detmers PA, Wright SD, Olsen E, Kimball B, Cohn ZA. (1987) Aggregation of complement receptors on human neutrophils in the absence of ligand. *J Cell Biol*, 105: 1137-1145.
170. Lishko VK, Yakubenko VP, Ugarova TP, Podolnikova NP. (2018) Leukocyte integrin Mac-1 (CD11b/CD18, $\alpha(M)\beta(2)$, CR3) acts as a functional receptor for platelet factor 4. *J Biol Chem*, 293: 6869-6882.
171. Jongstra-Bilen J, Harrison R, Grinstein S. (2003) Fc γ receptors induce Mac-1 (CD11b/CD18) mobilization and accumulation in the phagocytic cup for optimal phagocytosis. *J Biol Chem*, 278: 45720-45729.
172. Lacy P. (2006) Mechanisms of Degranulation in Neutrophils. *Allergy, Asthma & Clinical Immunology*, 2: 98.
173. Ambattu LA, Ramesan S, Dekiwadia C, Hanssen E, Li H, Yeo LY. (2020) High frequency acoustic cell stimulation promotes exosome generation regulated by a calcium-dependent mechanism. *Commun Biol*, 3: 553.
174. Savina A, Furlán M, Vidal M, Colombo MI. (2003) Exosome release is regulated by a calcium-dependent mechanism in K562 cells. *J Biol Chem*, 278: 20083-20090.

175. Taylor J, Azimi I, Monteith G, Bebawy M. (2020) Ca(2+) mediates extracellular vesicle biogenesis through alternate pathways in malignancy. *J Extracell Vesicles*, 9: 1734326.

10. BIBLIOGRAPHY OF CANDIDATE'S PUBLICATIONS

Candidate's publications related to the work discussed in this thesis:

Szeifert, Viktória; Kolonics, Ferenc; Bartos, Balázs; Khamari, Delaram; Vági, Pál; Barna, László; Ligeti, Erzsébet; Lőrincz, Ákos M. Mac-1 Receptor Clustering Initiates Production of Pro-Inflammatory, Antibacterial Extracellular Vesicles From Neutrophils. FRONTIERS IN IMMUNOLOGY 12 Paper: 671995, 12 p. (2021)

SJR indicator: Q1, IF (expected): 7.561

DOI: 10.3389/fimmu.2021.671995

Lőrincz, Ákos M.; Bartos, Balázs*; Szombath, Dávid; **Szeifert, Viktória**; Timár, Csaba I.; Turiák, Lilla; Drahos, László; Kittel, Ágnes; Veres, Dániel S.; Kolonics, Ferenc; Mócsai, Attila; Ligeti, Erzsébet. Role of Mac-1 integrin in generation of extracellular vesicles with antibacterial capacity from neutrophilic granulocytes. JOURNAL OF EXTRACELLULAR VESICLES 9: 1 Paper: 1698889, 17 p. (2020)

SJR indicator: D1, IF: 25.841

DOI: 10.1080/20013078.2019.1698889

Lőrincz, Ákos M.; **Szeifert, Viktória**; Bartos, Balázs; Szombath, Dávid; Mócsai, Attila; Ligeti, Erzsébet. Different Calcium and Src Family Kinase Signaling in Mac-1 Dependent Phagocytosis and Extracellular Vesicle Generation. FRONTIERS IN IMMUNOLOGY 10 Paper: 2942, 11 p. (2019)

SJR indicator: Q1, IF: 5.085

DOI: 10.3389/fimmu.2019.02942

Lőrincz, Ákos M.; **Szeifert, Viktória***; Bartos, Balázs; Ligeti, Erzsébet. New flow cytometry-based method for the assessment of the antibacterial effect of immune cells and subcellular particles. JOURNAL OF LEUKOCYTE BIOLOGY 103: 5 pp. 955-963., 9 p. (2018) (*shared first authors)

SJR indicator: Q1, IF: 4.012

DOI: 10.1002/JLB.4TA0817-317R

Candidate's publications unrelated to the work discussed in this thesis:

Kolonics, Ferenc; **Szeifert, Viktória***; Timár, Csaba I.; Ligeti, Erzsébet; Lőrincz, Ákos M. The Functional Heterogeneity of Neutrophil-Derived Extracellular Vesicles Reflects the Status of the Parent Cell. CELLS 9: 12 Paper: 2718, 27 p. (2020) (*shared first authors)

SJR indicator: Q1, IF: 6.600

DOI: 10.3390/cells9122718

Shopova, Iordana A; Belyaev, Ivan; Dasari, Prasad; Jahreis, Susanne; Stroe, Maria C ; Cseresnyés, Zoltán; Zimmermann, Ann-Kathrin; Medyukhina, Anna; Svensson, Carl-Magnus; Krüger, Thomas; **Szeifert, Viktória**; Nietzsche, Sandor; Conrad, Theresia; Blango, Matthew G.; Kniemeyer, Olaf; von Lilienfeld-Toal, Marie; Zipfel, Peter F.; Ligeti, Erzsébet; Figge, Marc Thilo; Brakhage, Axel A. Human Neutrophils Produce Antifungal Extracellular Vesicles against *Aspergillus fumigatus*. MBIO 11:2 Paper: 00596-20 (2020)

JR indicator: D1, IF: 7.867

DOI: 10.1128/mBio.00596-20

11. DIVISION OF RESULTS BETWEEN CO-AUTHORS

Szeifert, V. et al. FRONTIERS IN IMMUNOLOGY 12 Paper: 671995, 12 p. (2021)

There are no shared results between co-authors. The experiments were implemented by myself, in the case of NTA and TIRF measurements with technical help, and support as indicated in the methods section.

Lőrincz, Á.M.; Bartos, B.* et al. JOURNAL OF EXTRACELLULAR VESICLES 9: 1 Paper: 1698889, 17 p. (2020)

I was responsible for the size exclusion chromatography-based validation experiments of the extracellular vesicle isolation protocol: SEC isolation followed by FC, Bradford, Western blot analysis, bacterial survival experiments, and DLS with the help of Dániel Veres as indicated in the methods section. The first results of my C3bi surface-induced EV production are also presented in this article.

Lőrincz, Á.M. et al. FRONTIERS IN IMMUNOLOGY 10 Paper: 2942, 11 p. (2019)

I was responsible for the bacterial survival assay with different neutrophil EVs in the presence and absence of extracellular calcium. These data were reproduced and presented in this thesis.

Lőrincz, Á.M.; Szeifert, V.* et al. JOURNAL OF LEUKOCYTE BIOLOGY 103: 5 pp. 955-963., 9 p. (2018)

There are no shared results between co-authors. Balázs Bartos carried out KO murine experiments. I performed all other experiments with the supervision of Ákos M. Lőrincz. The thesis contains one figure from this article.

12. ACKNOWLEDGEMENTS

In the first place, I would like to thank my supervisor Dr. Ákos Márton Lőrincz for the last nine years of mentorship. His researcher perspective, attitude, and passion for work, science, and life always impressed me. His faith in me and in my work has always been an incredible motivation during my work, even in the hardest times.

I would like to express my sincere gratitude to Professor Erzsébet Ligeti who gave me the opportunity to work in her laboratory as a Research Student in 2013, and after that as a Ph.D. Student in 2018. She built up a research group where I could happily conduct research and grow. But most importantly, I am grateful for her advices, critical thinking, scientific and personal support. She has always been a role model for me.

I would like to thank Professors Attila Mócsai and László Hunyady, the current and former head of the Department of Physiology for creating such a good, inspiring scientific and working environment in the institute.

I also would like to thank former and current colleagues in the Department of Physiology, who have always been ready to help with various questions regarding my research. I especially thank my laboratory co-workers Dr. Roland Csépanyi-Kömi, Domonkos Czárán, Dr. Ferenc Kolonics, Dr. Péter Sasvári, Dr. Csaba Tímár and Dr. Éva Wisniewski. Their scientific expertise and friendship made my days in our laboratory memorable, and enjoyable. I am incredibly thankful to Mrs. Regina Tóth-Kun for her precise technical assistance and maintenance of the everyday work. Her aid and the fun times together helped me through many of the hardships during my experiments from the beginning.

I thank Dr. Dániel Veres for his help with the dynamic light scattering measurement; Ms. Delaram Khamari for her help with the nanoparticle tracking analysis; Dr. Pál Vági and Dr. László Barna for their great support with the TIRF imaging experiments.

I am greatly thankful to all the volunteers who contributed to the results of this thesis with their generous blood donations.

Finally, I would like to express my thankfulness to the best husband, my family, and my friends for their enormous encouragement during the years of my doctoral studies. This thesis is dedicated to my parents for their unconditional love and support from day 1.